THE EFFECT OF 5'-AMINOIMIDAZOLE-4-CARBOXAMIDE RIBONUCLEOSIDE (AICAR) AND 5'-AMINOIMIDAZOLE-4-CARBOXAMIDE-RIBONUCLEOSIDE- PHOSPHATE (ZMP) ON MYOCARDIAL GLUCOSE UPTAKE

Ingrid Webster

Thesis presented in complete fulfillment of the requirements for the degree

Master of Science in Medical Sciences

Department of Medical Physiology and Biochemistry

University of Stellenbosch

Supervisor: Dr Barbara Huisamen

Co-Supervisor: Prof Amanda Lochner

April 2005

Declaration

I, the undersigned, hereby declare that the work in this thesis is my own original work and that I have not previously in its entirety or in part submitted it at any university for a degree.

Signature:

Date:

ABSTRACT

Introduction: Exercise increases skeletal muscle glucose uptake via AMP-activated protein kinase (AMPK) activation and GLUT4 translocation from cytosol to cell membrane. It also promotes glucose utilisation in type 2 diabetic patients via increased insulin sensitivity. Insulin stimulates GLUT4 translocation by activating PI3-kinase and protein kinase B (PKB/Akt). We therefore postulated that a connection exists between these two pathways upstream of GLUT4 translocation. Understanding this connection is important in the development of treatment strategies for type 2 diabetes. This exercise-induced increase in AMP-activated protein kinase (AMPK) activation can be mimicked by a pharmacological agent, 5'-aminoimidazole-4-carboxamide ribonucleoside (AICAR), which is converted intracellularly into 5'-aminoimidazole-4-carboxamide-ribonucleosidephosphate (ZMP), an AMP analogue.

Aim: To investigate the effect of two pharmacological AMPK-activating compounds, ZMP and AICAR, on the phosphorylation of AMPK, the phosphorylation of PKB/Akt as well as possible feedback on insulin-stimulated glucose uptake and GLUT4 translocation.

Materials and Methods: Adult ventricular cardiomyocytes were isolated from male Wistar rats by collagenase perfusion and treated with 1 mM AICAR or 1 mM ZMP in the presence or absence of 100 nM insulin or 100 nM wortmannin, an inhibitor of PI3-kinase. Glucose uptake was measured via [^{3}H]-2-deoxyglucose (2DG) accumulation. PKB/Akt and AMPK phosphorylation and GLUT4 translocation was detected by Western blotting. Purinergic receptors were blocked with 8-cyclopentyl-1,3-

dipropylxanthine (8CPT) and the effect on AMPK phosphorylation noted. Certain results were confirmed or refuted by repeating experiments using the isolated rat heart model.

Results: AICAR and ZMP promoted AMPK phosphorylation. Neither drug increased glucose uptake but in fact inhibited basal glucose uptake, although GLUT4 translocation from cytosol to membrane occurred. Both compounds also attenuated insulin stimulated glucose uptake. Wortmannin abolished glucose uptake and PKB/Akt phosphorylation elicited by insulin while, in the presence of wortmannin, AICAR and ZMP increased levels of PKB/Akt phosphorylation. Although AICAR and ZMP increased glucose uptake in skeletal muscle, this was not seen in cardiomyocytes. However both compounds increased GLUT4 translocation, clearly demonstrating that translocation and activation of GLUT4 are separate processes. 8CPT had no effect on the phosphorylation of AMPK by either AICAR or ZMP indicating that there was no involvement of the purinergic receptors.

Conclusion: Although AICAR and ZMP increase glucose uptake in skeletal muscle, this was not seen in cardiomyocytes. Conversely, both compounds inhibited both basal and insulin stimulated glucose uptake despite increasing GLUT4 translocation. Inhibition of PI3-kinase in presence or absence of insulin unmasked hitherto unknown effects of AICAR and ZMP on PKB phosphorylation.

UITTREKSEL

Agtergrond: Oefening verhoog skeletspier glukose opname via AMP-geaktiveerde protein kinase (AMPK) aktivering en GLUT4 translokering vanaf die sitosol na die selmembraan. Dit verbeter ook glukose verbruik in tipe 2 diabetes pasiënte via verhoogde insulien sensitiwiteit. Insulien stimuleer GLUT4 translokering deur PI3-kinase en protein kinase B (PKB/Akt) te aktiveer. Dit word dus gepostuleer dat daar 'n verbinding tussen hierdie twee paaie, wat beide betrokke is by GLUT4 translokering, bestaan. Dit is belangrik om hierdie verbinding te verstaan aangesien dit in behandelingstrategieë van tipe 2 diabetes geteiken kan word. Die oefening geïnduseerde verhoging in AMPK aktivering, kan deur 'n farmakologiese middel 5'-aminoimidasool-4-karboksamied ribonukleosied (AICAR), wat intrasellulêr omgesit word na 5'-aminoimidasool-4-karboksamied-ribonukleosiedfosfaat (ZMP), 'n AMP analoog, nageboots word.

Doel: Om die effek van twee farmakologiese AMPK-aktiveringsmiddels, AICAR en ZMP, op die fosforilering van AMPK en PKB/Akt, sowel as moontlike effekte daarvan op insulien-gestimuleerde glukose opname en GLUT4 translokering, te ondersoek.

Materiale en Metodes: Volwasse ventrikulêre kardiomiosiete is uit manlike Wistar rotharte geÏsoleer d.m.v kollagenase perfusies en behandel met 1 mM AICAR of 1 mM ZMP in die teenwoordigheid of afwesigheid van 100 nM insulien of 100 nM wortmannin. Glukose opname is gemeet via intrasellulêre [^{3}H]-2-deoksiglukose akkumulasie; PKB/Akt en AMPK fosforilering sowel as GLUT4 translokering is bepaal deur Western blot analises. Purinergiese reseptore is geblokkeer met 8-siklopentiel-1,3-dipropielxanthien (8CPT) en die effek daarvan op AMPK fosforilering genoteer.

Ten einde resultate wat in die geïsoleerde kardiomiosiet-model verkry is, te bevestig, is sekere eksperimente in die geïsoleerde rothart herhaal.

Resultate: Beide AICAR en ZMP stimuleer AMPK fosforilering. Die middels kan nie glukose opname verhoog nie, inteendeel, basale glukose opname is onderdruk alhoewel GLUT4 translokering vanaf die sitosol na die selmembraan wel plaasgevind het. Wortmannin kon insulien gemedieerde glukose opname en PKB/Akt fosforilering onderdruk. In die teenwoordigheid van wortmannin het beide AICAR en ZMP PKB/Akt fosforilering verhoog. Alhoewel beide AICAR en ZMP glukose opname in skeletspier verhoog, was dit nie die geval in kardiomiosiete nie. Beide middels het wel GLUT4 translokering verhoog, wat duidelik demonstreer dat die translokering en aktivering van GLUT4, verskillende prosesse is. 8CPT het geen effek gehad op die fosforilering van AMPK deur AICAR of ZMP nie, wat bewys dat daar geen betrokkenheid van die purinergiese reseptore was nie.

Gevolgtrekking: Alhoewel AICAR en ZMP glukose opname in skeletspier verhoog is dit nie die geval in kardiomiosiete nie. Beide middels inhibeer basale en insulien-gestimuleerde glukose opname maar stimuleer GLUT4 translokeering. Inhibisie van PI3-kinase in die teenwoordigheid of afwesigheid van insulien, ontmasker voorheen onbekende effekte van AICAR en ZMP op PKB/Akt fosforilering.

ACKNOWLEDGEMENTS

I would like to thank my supervisors, Dr Barbara Huisamen and Professor Amanda Lochner, for their patience, guidance, assistance and motivation throughout this study.

For financial support I would like to thank the National Research Foundation and Department of Medical Physiology.

Thank you to lab F530 for the smiles and laughter and many helping hands.

And most importantly I would like to thank my Heavenly Father and my parents. You are the wind beneath my wings.

TABLE OF CONTENTS

LIST OF ILLUSTRATIONS

TABLES

ABBREVIATIONS

Units of measurements

%	percentage
µ	micro
µm	micro meter
µl	micro liter
°C	degrees celcius
Ci	Curie
cm	centimeter
g	gram
mm	millimeter
m	milli
min	minutes
mol	mole
n	nano
M	molar

Chemical Compounds

8-CPT	8-cyclopentyl-1,3-dipropylxanthine
2DG	[^{3}H]-2-deoxyglucose

AC	adenylyl cyclase
ACC	acetyl-CoA carboxylase
ADP	adenosine diphosphate
AICAR	5'-aminoimidazole-4-carboxamide-ribonucleoside
AMP	adenosine monophosphate
AMPK	AMP-activated protein kinase
AMPKK	AMP-activated protein kinase kinase
APS	ammonium peroxodisulphate
ATP	adenosine triphosphate
BAD	I-2 pro-apoptotic family member
BDM	2-3,butane-dione monoxime
BRCA-1	breast cancer susceptibility gene product 1
BSA	Bovine Serum Albumin
Ca^{2+}	calcium
$CaCl_2$	calcium chloride
CaMKK	calcium/calmodulin dependant kinase kinase
CK	creatine kinase
CO_2	carbon dioxide
CP	creatine phosphate
CPT-1	carnitine palmitoyltransferase 1
CPT-II	carnitine palmitoyltransferase 2
Cr	creatine
CREB	cAMP responsive element binding protein

ECL	electro-chemiluminescence
eNOS	endothelial nitric oxide synthase
FACS	fatty acyl CoA synthase
FAT/CD36	fatty acid translocase/CD36
FAD	flavine adenine nucleotide
FFA	free fatty acids
FKHRL1	forkhead transcription factor family member 1
G-6-P	glucose-6-phosphate
G-6-Pase	glucose-6-phosphatase
GAPDH	glyceraldehyde 3-phosphate dehydrogenase
GBD	glycogen binding domain
GLUT1	glucose transporter 1
GLUT4	glucose transporter 4
GSK-3	glycogen synthase kinase-3
GTP	guanine triphosphate
GTPase	guanine triphosphatase enzyme
H	hydrogen
HCl	Hydrogen chloride
H_2O	water
hTERT	human telomerase catalytic subunit gene
I-κB	inhibitor of NFκB
IGF	insulin-like growth factor
ILK	integrin-linked kinase

IRS-1	insulin receptor substrate 1
JNK	jun-N-terminal kinase
K^+	potassium
KCl	potassium chloride
KH_2PO_4	potassium dihydrogenphosphate
MAPK	mitogen-activated protein kinase
MCD	malonyl-CoA decarboxylase
$MgSO_4$	magnesium sulphate
MTOR	mammalian target of rapamycin
NaCl	sodium chloride
NADH	nicotinamide adenine dinucleotide
NADPH	nicotinamide adenine dinucleotide phosphate-reduced form
$NaHCO_3$	sodium hydrogen carbonate
Na^+K^+ATPase	sodium potassium ATPase enzyme
NaOH	sodium hydroxide
NFκB	nuclear factor κB
NO	nitric oxide
NOS	nitric oxide synthase
Nur77	orphan nuclear receptor/transcription factor
O_2	oxygen
OH^-	hydroxide ion
p21CIP	inhibitor of cell cycle progression
p38 MAPK	p38 mitogen activated protein kinase

PCR	polymerase chain reaction
PCr	phosphocreatine
PDE	phosphodiesterase
PDH	pyruvate dehydrogenase
PDHK	pyruvate dehydrogenase kinase
PDK	phosphoinositide-dependant protein kinase
PFK	phosphofructokinase
PH	pleckstrin homology
P_i	phosphate
PIP_2	phosphatidylinositol (3,4) bisphosphate
PIP_3	phosphatidylinositol (3,4,5) triphosphate
PI3-K	phosphatidylinositol 3-kinase
PKA	protein kinase A
PKB/Akt	protein kinase B
PKC	protein kinase C
PLC	phospholipase C
PMSF	phenylmethyl sulphonyl fluoride
p-NPP	p-nitrophenylphosphate
Ponseau-S	3-hydroxy- 4-[2-sulfo-4-(4-sulfo-phenylazo)phenylazo]-2.7-naphthalene disulphonic acid
PTB	phosphotyrosine binding domain
PTEN	phosphatase and tensin homologue deleted on chromosome ten

PVDF	poly vinylidene fluoride
PYPase	phosphotyrosine phosphatase
SDS	sodium dodecyl sulphate
Ser	Serine
SH-2	Src homology-2
Shc	Shc, an adaptor molecule involved in Ras activation
SNARE	soluble N-ethylmaleimide sensitive factor attachment protein Receptor
TBE	trypan blue exclusion
TBS	Tris-buffered saline
TBST	TBS 0.1% Tween
TCA	tricarboxylic acid
Temed	N,N,N',N'-Tetramethyl ethylene diamine ammonium
Thr	Threonine
TRIS	tris(hydromethyl) aminomethane hydrochloride
ZMP	5'-Aminoimidazole-4-carboxamide-ribonucleoside phosphate

CHAPTER 1

INTRODUCTION

The energy that the heart requires for maintenance of normal contraction is supplied by adenosine triphosphate (ATP), and this high-energy phosphate is primarily produced in the heart by the metabolism of carbohydrates and fatty acids (Lopaschuk & Stanley, 1997). Substrate metabolism varies between carbohydrates as fuel in the fed state, of which glucose and lactate are the major contributors, and fatty acids in the fasting state (Wang *et al*, 1999; Sakamoto *et al*, 2000). This is due to the fact that in the fed state there are more carbohydrates available in the blood, and in the fasting state there are more free fatty acids (FFA) available. In the latter case, fatty acid oxidation occurs predominantly, and glucose oxidation is inhibited (Opie, 1991). The glucose that is taken up is converted to glycogen and stored instead of undergoing glycolysis (Randle *et al*, 1963). Conversely, in the carbohydrate-fed-state, when glucose levels are high in the blood, the uptake of fatty acids decreases while glucose uptake and glycolysis increases (Opie, 1998).

1.1 Randle's Principle and Pasteur Effect

The variation in the roles of glucose and fatty acid between the fasting and the fed states forms the basis of the glucose-fatty acid cycle first described by Randle *et al* (1963). The basic trigger in the cycle is the cyclic production of FFA by the adipose tissue (see Figure 1.1). In the fasting state, adipose tissue is

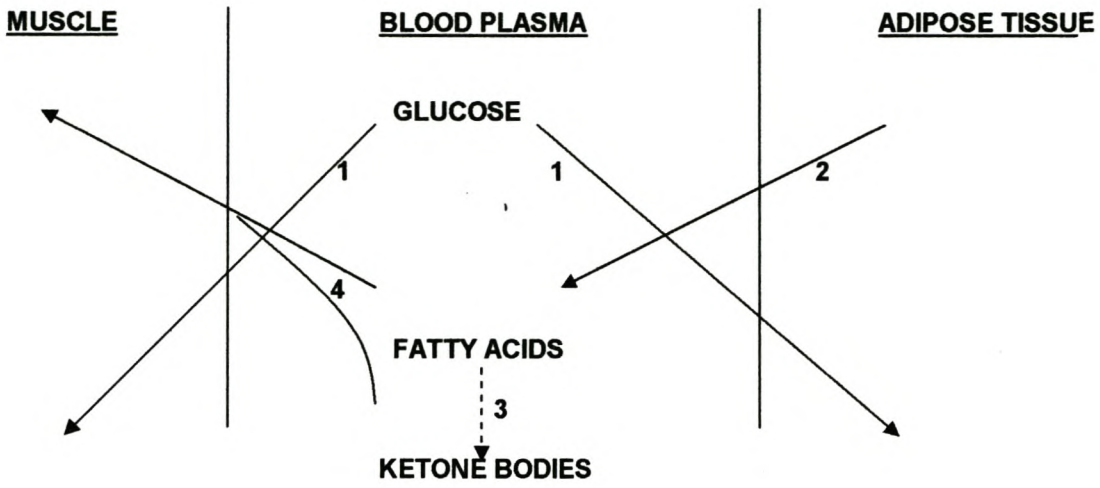

Figure 1.1. **Glucose-fatty acid cycle, blood phase. 1. Glucose uptake by muscle and adipose tissue. 2. Release of fatty acids from adipose tissue into plasma. 3. Formation of ketone bodies from fatty acids by liver and 4. Fatty acid uptake and ketone body uptake by muscle tissue. (Figure adapted from Randle *et al*, 1963).**

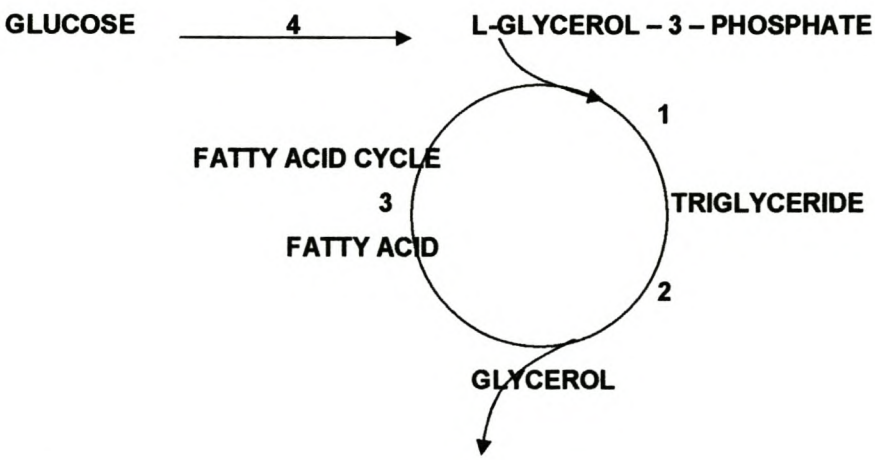

Figure 1.2 **Glucose fatty-acid cycle, tissue phase. 1. Esterification, 2. Lypolysis, 3. Fatty acid activation and 4. Glycerol phosphate synthesis. (From Randle et al, 1963)**

broken down to release FFA and this inhibits the metabolism of glucose by the heart. In the fed state the abundance of glucose and insulin inhibits this release of FFA and therefore glucose becomes the major fuel (see Figure 1.2).

These events require complex control mechanisms, as will be discussed later in Chapter 2.1.2 and 2.2.

Although glucose is not the major fuel for either the normal beating heart (Bing *et al*, 1954) or during mild to moderate exercise (Zierler *et al*, 1999), it is an important metabolic fuel in cardiomyocytes. It is stored as glycogen, and becomes the primary fuel of these cells during fasting or hypoxic conditions (Opie 1991, 1998). This is because, when the oxygen supply to the heart is normal the rate of glycolysis is inhibited by high levels of citrate and ATP formed by oxidative metabolism in the citrate cycle (Randle & Morgan, 1962). When the oxygen supply is inhibited or decreased this oxidative metabolism is inhibited, citrate and ATP levels fall and glycolysis is stimulated (see Fig 1.3). This feedback mechanism is known as the Pasteur Effect.

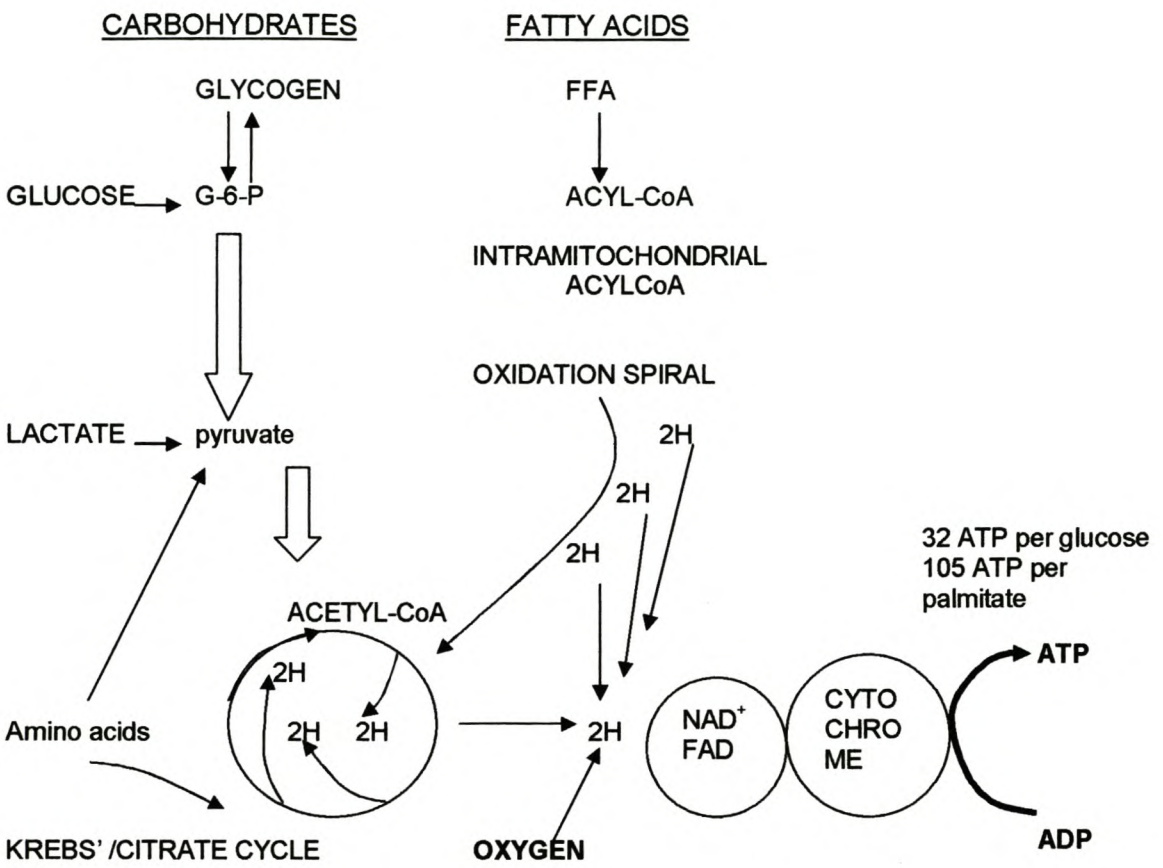

Figure 1.3 Major fuels of the heart are carbohydrates (glucose and lactate) and non-esterified fatty acids (FFA). All fuels are ultimately broken down to acetyl-CoA, which produces hydrogen atoms (H^+) by various dehydrogenase enzymes to produce $NADH_2$ (NADH + H^+), which enters the respiratory chain to produce ATP. Fatty acids also produce $FADH_2$ from the oxidation spiral which enters the cytochrome chain and produces ATP. (Adapted from Depré *et al*, 1998 and Opie 2004).

CHAPTER 2

LITERATURE REVIEW

2.1 Glucose Uptake and Metabolism

2.1.1 Glucose Uptake

Glucose uptake into muscle cells is accomplished through a series of steps and signaling pathways, from the delivery of blood to the interstitial space to the trans-membrane transport of glucose into the cell (Richter *et al* 2001). The cell cannot absorb glucose by simple diffusion, since the cell membrane is hydrophobic and glucose is hydrophilic. It must instead use a special carrier protein, the glucose transporter molecule, for this purpose. (Lienhard *et al*, 1992). This carrier requires no energy for transport of glucose since the extracellular glucose concentration is so much greater than the intracellular concentration (Opie, 1991).

2.1.2 Glucose transporters (GLUTs)

As stated above, the uptake of glucose from the blood stream across the sarcolemma and into the heart cells is regulated and carried out by the glucose transporters or GLUTs (Pessin & Bell, 1992; Lopaschuk & Stanley, 1997). The specific glucose transporters in the heart all belong to the GLUT family and are encoded by different nuclear genes. They are transmembrane proteins containing

about 500 amino acid residues and 12 membrane-spanning β-helices, five of which could form a hydrophilic channel responsible for glucose transport (Meukler, 1994).

The glucose transporter that is predominantly expressed in cardiomyocytes is the insulin-sensitive GLUT4-isotype which is also expressed in adipose tissue and skeletal muscle. GLUT4 is largely confined to an intracellular vesicle storage site in the basal, non-stimulated state (Meukler, 1994; Holman & Kasuga, 1997). It becomes recruited to the cell surface under the influence of insulin (Fischer *et al*, 1997; Calera *et al*, 1998; Becker *et al*, 2001) or other stimuli such as contraction and hypoxia or anoxia. GLUT4 vesicles respond to insulin in a marked and dramatic way, increasing GLUT4 in the membrane up to nine times that of basal (Holloszy, 2003). When blood insulin and glucose levels decrease, then the transporter recruitment is reversed (Lienhard *et al*, 1992).

The GLUT1-transporter, which is present in most tissues and is also a characteristic feature of fetal tissues (Depre *et al,* 1998), is also present in cardiomyocytes although it is about 5 times less abundant than GLUT4 (Meukler, 1994). It is thought to be a specialized "house-keeping" protein to provide the steady basal flow of glucose into cells for homeostasis in their inactive state.

While there is substantial evidence that the GLUT4 transporter exists in specialized vesicles within the cell (Saltiel & Pessin, 2003), the precise intracellular location and trafficking pathways of these vesicles are unclear. GLUT4 is localized in

tubulovesicular and vesicular structures that are biochemically distinct from the recycling endosomal network. Furthermore the GLUT4 compartment is enriched in the v-SNARE (soluble N-ethylmaleimide sensitive factor attachment protein receptor) protein VAMP2 (Pessin *et al*, 1999). There is also evidence to suggest that the plasma membrane target for the GLUT4 vesicle is the t-SNARE syntaxin 4 (Syn4) (Cheatham *et al*, 1996; Volchuk *et al*, 1996; Rea & James 1997; Olson *et al*, 1997). Thus the docking of vesicles may be mediated by the interaction of the Syn4 with the GLUT4 vesicle v-SNARE protein, VAMP2 (Saltiel & Pessin, 2003).

In 2001 Somwar and colleagues found that there was a delay of 2 minutes between the arrival of GLUT4 at the membrane and the observation of any increase in glucose uptake. This suggested that an intermediate existed which activated GLUT4 before glucose uptake could occur. Evidence has been presented by Konrad *et al* (2001) and Somwar *et al* (2001, 2002) that suggests a role for p38 mitogen-activated protein kinase (p38 MAPK) in the activation of GLUT4 by insulin. Konrad and colleagues showed that SB203580, an inhibitor of p38 MAPK, attenuated insulin-stimulated glucose uptake without altering GLUT4 translocation. These results suggested that insulin might activate GLUT4 via a p38 MAPK-dependent pathway, and that GLUT4 translocation and GLUT4 activation to take up glucose may be two independent events.

2.1.3 Glucose Metabolism

Glucose metabolism has two main components, glycolysis and glucose oxidation. (See fig 2.1)

Glycolysis

Glycolysis ('lysis of glucose') is the first part of the glucose metabolic pathway and produces ATP from either exogenous glucose or from glycogen without requiring oxygen (Depre *et al*, 1998). It is the biochemical process that produces lactate in anaerobic conditions (Opie, 1991). During normal oxidative metabolism, glycolysis yields pyruvate, which is then broken down aerobically in the citrate cycle (under adequate mitochondrial capacity). This process is also called aerobic glycolysis. Thus ATP is produced not only during aerobic conditions, but anaerobically too (Opie, 1991).

Intracellular glucose is rapidly converted into glucose-6-phosphate by hexokinase, and glycolysis then converts this into a compound containing two phosphate groups, fructose-1,6-bisphosphate. After this, each 6-carbon hexose phosphate is converted into two three-carbon triose phosphates, eventually forming pyruvate. In the first stage, two molecules of ATP are used per glucose molecule converted to two triose phosphate molecules. In the second stage four molecules of ATP are made, independently of oxygen, for each glucose 6-phosphate converted to pyruvate,

resulting in a net production of 2 molecules of ATP per molecule of glucose metabolized.

The role of the enzyme phosphofructokinase (PFK) is of great importance. When its activity increases, as in hypoxia, glucose-6-phosphate is converted to fructose-6-phosphate at an increased rate and this reaction, which uses ATP, is irreversible, since the enzyme which catalyses the reverse reaction is not present in the heart (Opie, 1998). Thus PFK's activity serves as a one directional valve to regulate the rate of glycolysis. Increased PFK activity causes decreased glucose-6-phosphate levels in the cell, therefore the inhibition of hexokinase which is normally caused by glucose-6-phosphate is decreased, and more glucose can be phosphorylated. In contrast, the activity of PFK can be inhibited when the oxidation of alternate fuels like fatty acid or lactate produces citrate, and the opposite then occurs. This is therefore a coordinated intracellular control. (Opie, 1991; Opie, 1998)

Glycolysis is increased during hypoxia and ischemia and this is controlled by the activity of two enzymes, PFK and glyceraldehyde 3-phosphate dehydrogenase (GAPDH). The PFK reaction is sensitive to the energy status of the myocardial cells, and is therefore ideally suited for metabolic control. As ATP levels fall, and those of ADP, AMP and Pi rise, the activity of this enzyme is enhanced resulting in increased anaerobic glycolysis (Morgan *et al*, 1961).

At maximal work oads under the same conditions, glyceraldehyde 3-phosphate dehydrogenase becomes rate-limiting because of the accumulation of nicotinamide adenine dinucleotide (NADH). Pyruvate oxidation is regulated by pyruvate dehydrogenase (PDH) activity, and the active enzyme converts pyruvate to acetyl-CoA (Marks, 1990). In the maximally working heart perfused with insulin and glucose, pyruvate dehydrogenase is fully active, and the rate-limiting step in glucose metabolism is NADH oxidation. This is dependent on the transport of reducing equivalents into the mitochondria (Hue *et al*, 1988).

When glucose is the source of glycolysis, the entire glycolytic pathway uses 2 ATP and produces 4 ATP, so the net production is 2 molecules of ATP. When glycogen is the source, ATP production is 3 (Opie, 1991).

Glucose oxidation

The other component of glucose metabolism is glucose oxidation and this involves the pyruvate derived from glycolysis being taken up by the mitochondria and its further metabolism in the citric acid cycle. Glucose is metabolized in the cytosol to pyruvate while oxidation occurs entirely in the mitochondria (see Fig 2.1). Pyruvate is converted to acetyl-CoA by pyruvate dehydrogenase (PDH), which is active when the concentration of its substrates is high, and relatively inactive when its substrates are of low concentration. Pyruvate is also formed from lactate in the healthy human heart (Lopaschuk & Stanley, 1997).

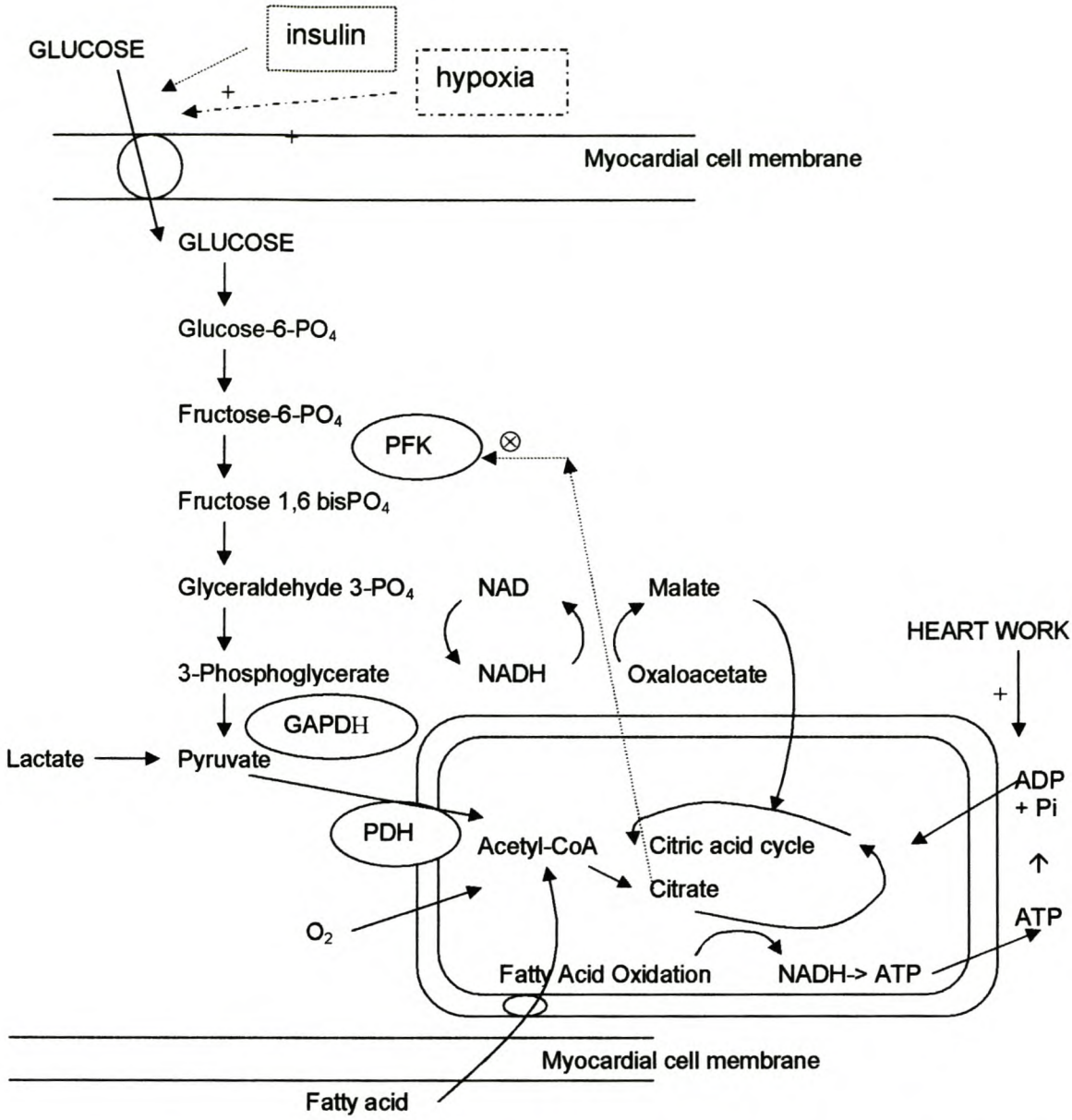

Figure 2.1. Glucose and fatty acid oxidation with the rate limiting steps shown. Glucose transport is regulated by insulin and the energy state of the cell. In the well-oxygenated heart, glucose uptake and glycolysis can be accelerated by heart work and substrate glucose, and partially inhibited by fatty acid oxidation. PFK phosphofructokinase, PDH pyruvate dehydrogenase, FFA free fatty acids. (Modified from Opie 1991 and McDaniel *et al*, 1988)

2.2 Fatty Acid Uptake and Metabolism

2.2.1 Fatty Acid Uptake

Free fatty acids (FFA's) in circulation are bound to albumin, Dissociation from albumin represents the first step of the cellular uptake process, involving membrane proteins with high affinity for fatty acids, e.g., fatty acid translocase (FAT/CD 36) or the membrane fatty acid-binding protein (FABPpm). (Rauch *et al*, 1987; Stremmel *et al*, 2001). The higher the circulating FFA/ albumin ratio the greater the uptake into the myocardium. According to the thus created transmembrane concentration gradient, uncharged fatty acids can flip-flop from the outer leaflet across the phospholipid bilayer. Eventually feedback systems will limit the uptake i.e. increased tissue acyl-CoA.

Fatty Acid Translocase (FAT)/CD36

Fatty acid uptake seems to be regulated by translocation of fatty acid translocase/CD36 (FAT/CD36) from intracellular, presumably endosomal, stores to the sarcolemma (Luiken *et al*, 2003). Insulin and cellular contractions are two important physiological factors which are able to contribute to this process (Bonen *et al*, 2000; Luiken *et al,* 2002). Wortmannin completely blocked insulin-inducable fatty acid uptake but had no effect on contraction induced fatty acid uptake. Luiken and co-workers recently published work (2003) that showed contraction induced FAT/CD36 translocation in rat cardiomyocytes is mediated though AMP-activated

protein kinase (AMPK) signaling. Channeling fatty acids to the different metabolic pathways requires activation to acyl-CoA. For this process, the family of fatty acid transport proteins (FATP 1-5/6) might be relevant because they have been shown to possess acyl-CoA synthetase activity (Stremmel *et al*, 2001).

Fatty Acid Oxidation

The first step in fatty acid oxidation is the activation of fatty acids so that acetyl CoA is formed and used to generate fatty acyl-CoA. Acyl-CoA molecules are then transferred from the cytosol to within the mitochondria by a transfer system that requires carnitine.

Carnitine palmitoyltransferase (CPT) 1, a key enzyme involved in fatty acid oxidation, is the rate-limiting enzyme involved in mitochondrial fatty acid uptake (Stanley *et al*, 1997). Malonyl-CoA, which is produced by acetyl-CoA carboxylase (ACC), is a potent inhibitor of CPT 1 and acts at a site distinct from the catalytic site of CPT1. ACC is a very important determinant of malonyl-CoA levels and fatty acid oxidation rates in the heart (Awan & Saggerson, 1993, Kudo *et al*, 1995). A key kinase responsible for the control of ACC activity is the AMPK (Sakamoto *et al*, 2000) (see Fig 2.2). Thus AMPK is an important regulator of fatty acid oxidation in the heart, since it phosphorylates and inactivates ACC, resulting in a decrease in malonyl-CoA production and an increase in fatty acid oxidation rates (Kudo *et al*, 1995). It has been shown that the heart contains an active malonyl-CoA decarboxylase (MCD) that decarboxylates malonyl-CoA back to acetyl-CoA (Sakamoto *et al*, 2000).

Any activated intracellular fatty acid not oxidized can either be stored as triglycerides or transformed to structural lipids and incorporated into the membrane.

2.2.2 Fatty Acid Metabolism

The first step in fatty acid oxidation is the activation of fatty acids to acyl-CoA which is then transferred from the cytosol to within the mitochondria (see fig 2.2). On the outer surface of the inner mitochondrial membrane, the enzyme CPT1 catalyses the transfer of the acyl group from CoA to carnitine. The fatty acyl group is translocated across the membrane to the inner surface, where the enzyme CPTII catalyses the transfer of the acyl group to CoA from the inner matrix. β-oxidation then converts intramitochondrial long chain acyl-CoA into acetyl-CoA, and the fatty acid oxidation spiral then continuously removes acetyl-CoA from the carboxyl end of the chain, in the TCA (tricarboxylic acid) Cycle. The TCA, Citric Acid, or Krebs cycle is the major energy producing pathway in the body, and starts with the condensation of oxaloacetate to acetyl-CoA by citrate synthase to form citrate. As acetyl-CoA is oxidized to CO_2, electrons are donated to the oxidation-reduction coenzymes, FAD and NAD^+. Three NADH, 1 $FADH_2$, and 1 GTP are produced in the Citric Acid Cycle. The NADH and $FADH_2$ generate ATP by donating electrons to O_2 in the process of oxidative phosphorylation. ATP is also produced from GTP (substrate-level phosphorylation). One turn of the cycle generates 12 ATP molecules. (Marks, 1990, Davidson and Sittman, 1994).

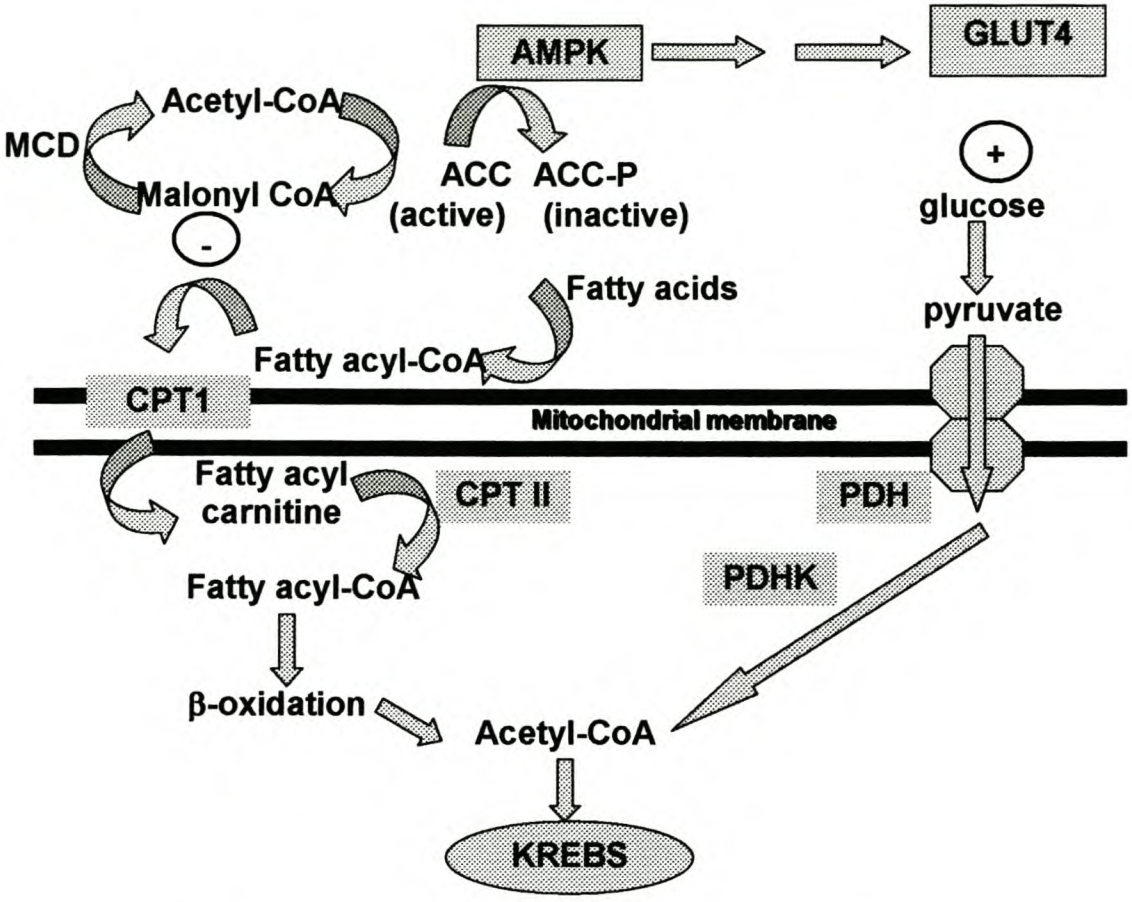

Figure 2.2 **A simplified schematic diagram showing the role of ACC, AMPK, and MCD in the regulation of fatty acid and glucose oxidation in the heart. Fatty acids are converted to fatty acyl-CoA by FACS. These fatty acyl-CoA esters are then converted to fatty acyl carnitines and shuttled into the mitochondria via the carnitine translocase system. Once inside the mitochondria, the fatty acyl carnitines are converted back into fatty acyl-CoA esters and enter into the β-oxidation spiral to produce acetyl-CoA. In addition, exogenous glucose is transported into the cell via the cell glucose transporters, and can be converted to pyruvate via glycolysis. Pyruvate enters the mitochondria via the pyruvate carrier and is converted to acetyl-CoA by the pyruvate dehydrogenase complex. Fatty acid-derived or glucose-derived acetyl-CoA enters into the Krebs cycle, which produces reduced equivalents that are used by the electron transport chain to produce ATP. (Adapted from Dyck & Lopaschuk, 2002).**
For abbreviations see Abbreviations list.

2.3 Insulin Signaling

Insulin affects many biological responses in cells like gene expression as well as cellular metabolism (Lee & Pilch, 1994). In the heart, insulin has direct effects on both glucose transport, glycolysis (Depre *et al*, 1998), glucose oxidation and glycogen synthesis (Belke *et al*, 2001). Insulin may also increase cardiac contractility (Ren *et al*, 2000) and has an anti-apoptotic effect on cardiomyocytes (Aikawa *et al*, 2000).

In order to affect cellular processes, insulin binds to specific insulin receptors on the cell surface, which are receptor tyrosine kinases composed of an external α-dimeric subunit and an internal β-dimeric subunit (Shepherd *et al*, 1998) (see Figure 2.3). When insulin binds to the α-subunit, the β-subunit auto-phosphorylates (White & Kahn, 1994). This autophosphorylation amplifies the effect of insulin and also stimulates an intrinsic receptor tyrosine kinase activity, which results in multi-site phosphorylation of the cytosolic insulin receptor substrate proteins (IRS-1, 2, 3 and 4) (Shepherd *et al* 1998; De Luca *et al* 1999; Wang *et al*, 1999). The major IRS protein in the heart is IRS-1.

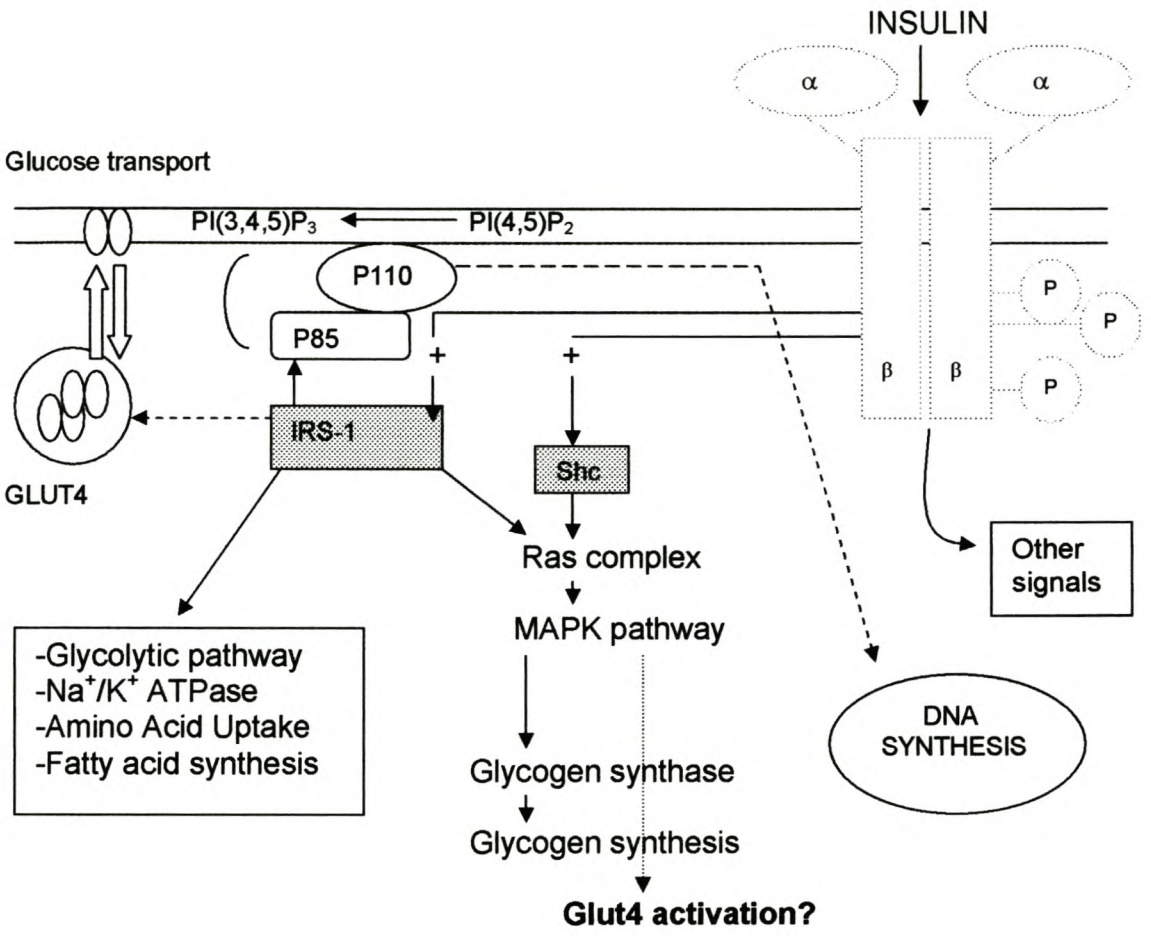

Figure 2.3. A schematic model of the IRS-1 signaling pathways mediated through activation of the insulin receptor kinase and phosphorylation of IRS-1 or Shc. Shc contains a PTB (phosphotyrosine binding) domain, and when phosphorylated, activates the MAPKinase pathway. (Adapted from White & Kahn, 1994 and Holman and Kasuga 1997)

IRS-1 in turn acts as a docking site for several proteins through its multiple tyrosine phosphorylation sites for proteins containing Src-homology 2 (SH2) recognition motifs. These phosphorylated sites act as binding domains, thus alerting signaling pathways to increase the activity of many crucial enzymes by phosphorylating them (White & Kahn, 1994). Three of these crucial enzymes are glycogen synthase, the rate limiting enzyme in glycogen storage (De Luca *et al*, 1999), pyruvate dehydrogenase (Opie, 1998) and phosphatidylinositol 3-kinase (PI3-K) (De Luca *et al*, 1999; Kirwin *et al*, 2000).

2.3.1 PI3-Kinase (PI3-K)

Activation of the insulin-receptor tyrosine kinase results in the rapid recruitment of phosphoinositide 3-OH-kinase (PI3-K) activity into signaling complexes, and current evidence indicates that class 1a PI3-K accounts for the majority of this increase (Shepherd *et al*, 1998). PI3-K enzymes are a family of lipid kinases present in all cell types and are characterized by their ability to phosphorylate the 3-OH position of the inositol ring of several different phosphoinositides (Duronio *et al*, 1998). PI3-K is a heterodimer composed of an 85kDa (p85) regulatory subunit and an 110kDa (p110) catalytic subunit (Kohn *et al*, 1996). The p85 subunit binds to other molecules via its Src-homology 2 (SH2) domain such as the tyrosine residues of the IRS-1, p110, phospholipase C (PLC), Ras GTPase-activating protein and others (White & Kahn, 1994). The p110 subunit phosphorylates the cellular lipids phosphatidylinositol mono- or bisphosphate (PIP or PIP_2) at the 3' position of the inositol rings (Meyers *et al*,

1994; De Luca *et al*, 1999), producing PtdIns(3,4)P_2 , PtdIns(3)P and PtdIns(3,4,5)P_3. G-protein regulated class 1b-PI3-K associates with a family of adapter subunits unrelated to those of class 1a-PI3-K, and there is no evidence that they are activated by insulin (Stephens *et al*, 1997). Although class 2 PI3-Ks are widely expressed and are activated by insulin, they seem unlikely to play a role in mediating any of the common insulin responses since they cannot use PI(4,5)P_2 as a substrate to produce PIP_3 (which is thought to be a key mediator in insulin signaling) and they are relatively resistant to the PI3-K inhibitors, while many insulin responses are very sensitive to these inhibitors (Domin *et al*, 1996).

The fungal inhibitor wortmannin has been shown to be a potent inhibitor of 1a (Ui *et al*, 1995), 1b (Stoyanova *et al*, 1997) and class 3 (Volinia *et al*, 1997) PI3-K activity (Powis *et al*, 1994). LY294002 is another highly specific inhibitor of class 1 PI3-Ks, although class 2 PI3-Ks are relatively resistant to this inhibitor (Domin *et al*, 1997).

Lipid products of PI3-K act as signaling molecules. PIP_3 is the main product of class 1a PI3-K and can directly modulate downstream events by specifically interacting with molecules in downstream signal transduction pathways:

i) by acting in an allosteric manner they may alter the catalytic activity of targets;

ii) by changing conformation the interactions may expose regulatory sites for phosphorylation, and iii) interactions may regulate co-localization with other PIP_3 - binding proteins to form specific signaling complexes at membranes (Shepherd *et al*, 1997). It acts to recruit pleckstrin-homology (PH)-domain-containing proteins such as

phosphatidylinositol-dependent protein kinases (PDKs) as well as protein kinase B (PKB/Akt) (Marte & Downward, 1997) to the cell membrane.

Evidence is emerging which suggests that PI3-K also plays a crucial role in activation of certain isoforms of protein kinase C (PKC epsilon) (Yatomi *et al*, 1992, Moriya *et al*, 1996, Shepherd *et al*, 1998).

The jun-N-terminal kinase (JNK) also lies downstream of PI3-K, as demonstrated by the findings that PI3-K activity is necessary for the growth factor stimulated activation of JNK (Lopez-Ilasaca *et al*, 1997) It is suggested that the activation pathway in this case involves the small GTP-binding proteins Rac or cdc42 as these lie upstream of JNK and the activation of Rac is PI3-K dependent (Coso *et al*, 1995, Hawkins *et al*, 1995).

2.3.2 Protein Kinase B (PKB/Akt)

The origins of PKB/Akt research can be traced back to the discovery of a transforming murine leukemia virus from mice with a high incidence of spontaneous lymphoma, by Staal and co-workers in 1977. This virus was termed AKT8 and had the ability to induce focus formation in other cell lines which suggested that the virus contained a previously undescribed oncogene. Staal and co-workers isolated and termed this oncogenic sequence *akt (*Staal *et al*, 1988). Human homologues AKT1 and AKT2 were also identified in gastric carcinomas and this supported the

hypothesis that this *akt* gene played a strong role in the pathogenesis of human malignancy and tumor formation (Staal *et al,* 1988).

In 1991 three independent research groups identified genes related to *akt.* Firstly, Jones *et al* identified a serine-threonine protein kinase, which they termed Rac (related to the A and C kinases), subsequently renamed PKBα/Akt1. Secondly Bellacosa *et al* described the similarity between v-Akt and protein kinase C. Lastly Coffer and Woodgett (1991) used PCR to identify a novel cDNA with significant homology to protein kinase C and protein kinase A, termed protein kinase B (PKB). Together with the discovery of a second form, PKBβ/Akt2 (Jones *et al*, 1991b), these papers established PKB/Akt as a novel phospho-protein kinase that was widely expressed , and paved the way for future research into its diverse cellular processes (Brazil & Hemmings, 2001).

Metabolic functions of PKB/Akt are diverse and include cellular functions such as regulation of glucose uptake and metabolism (Kohn *et al*, 1996), transcription, apoptosis, proliferation, migration, angiogenesis (Brazil & Hemmings, 2001), differentiation, inhibition of apoptosis, regulation of growth and cytoskeleton organisation (Duronio *et al*, 1998).

2.3.2.1 Structure of PKB/Akt

PKB/Akt has been described as a novel phospho-protein kinase that is widely expressed (Coffer & Woodgett, 1991). Three main isoforms have been identified in mammalian cells: PKBα/Akt1, PKBβ/Akt2 and PKBγ/Akt3. PKBα/Akt1 and PKBβ/Akt2 are widely expressed, with highest levels present in the brain, thymus, heart and lungs (Coffer & Woodgett, 1991). PKBγ/Akt3 is also expressed in the heart (Patrucco *et al*, 2004). Akt1, -2 and -3 are all expressed in both normal and tumor tissue of the lung, breast, prostate and colon, according to Zinda *et al* (2001). All tissues contain at least one form of PKB/Akt. (Coffer & Woodgett, 1998).

All three iso-forms of PKB/Akt contains a serine/ threonine kinase domain, as well as a pleckstrin-homology (PH) domain at its amino-terminal end and the integrity of this PH domain has been found to be crucial for activation of PKB/Akt in intact cells in response to PI3-K activation (Klippel *et al*, 1996). Alessi and colleagues in 1996 identified 4 sites on PKB/Akt that are phosphorylated in vivo. Thr-308 and Ser-473 are inducibly phosphorylated by extracellular stimuli, whereas Ser-124 and Thr-450 appear to be basally phosphorylated.

PKB/Akt is an important mediator of the physiological effects of insulin and is a target for PI3-K (Marte & Downward, 1997).

2.3.2.2 Activation of PKB/Akt

PKB/Akt has been shown to be activated by a wide variety of stimuli including cytokines, chemokines (Tilton *et al*, 1997), heat shock, hypoxia, integrins and growth factors (Andjelkovic *et al*, 1998).

PI3-K activation results in the production of PtdIns(3,4,5)P_3 and PtdIns(3,4)P_2. There is an essential role for the PH domain and binding of PIP_2 and PIP_3 in the activation and regulation of PKB/Akt (Klippel *et al*, 1997). Interaction of the PH domain of PKB/Akt with these lipids might cause it to translocate to the plasma membrane, which could be where the stimulating kinases are active. It could also promote conformational changes which would lead to enhanced phosphorylation by upstream kinases (Marte & Downward, 1997) (see Fig 2.4).

The assembly of the phosphoinositide-dependant protein kinases (PDKs) and PKB/Akt at the same site allows PKB/Akt to become phosphorylated at two residues. PDK-1 phosphorylates PKB/Akt at threonine-308 and PDK-2 phosphorylates PKB/Akt at serine-473. Phosphorylation of both is required for full activation of the kinase. (Alessi *et al*, 1996; Coffer *et al*, 1998).

PDK-1 is insensitive to wortmannin (Marte & Downward 1997), but PDK-2 is sensitive to wortmannin, suggesting that it is under the control of PI3-K (Alessi *et al*, 1996).

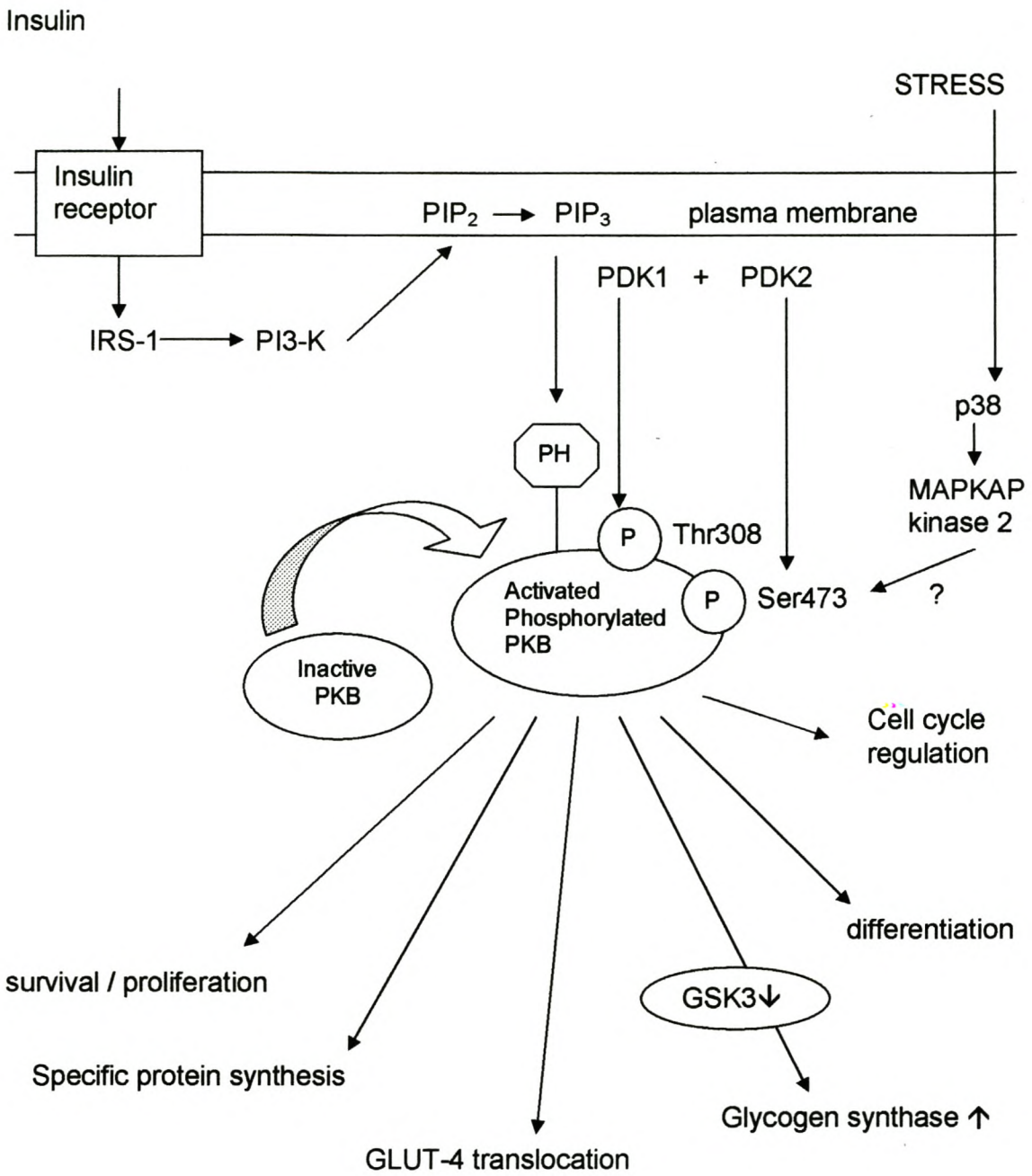

Figure 2.4 A model for PKB activation and downstream events (modified from Coffer *et al*, 1998)

2.3.2.3 Regulation of PKB/Akt

Regulation of PKB/Akt activity is of the utmost importance since constitutively active PKB/Akt has been shown to cause oncogenic transformation of cells (Mirza *et al*, 2000), and PKB/Akt isoforms have been shown to be overexpressed in breast cancer cell lines (Jones *et al*, 1991b), as well as ovarian (Cheng *et al*, 1992) and pancreatic (Cheng *et al*, 1996) cancers and gastric adenoma (Staal *et al*, 1987). On the other hand, dominant negative PKB/Akt cell lines show increased apoptosis in infected cells (Esfandiarei *et al*, 2004; Kim *et al*, 2004).

PTEN (phosphatase and tensin homologue deleted on chromosome ten), a novel tumour suppressor protein involved in PKB/Akt regulation, appears to control the activity of PKB/Akt by limiting the lipid substrate PtdIns(3,4,5)P_3 necessary for its activation (Brazil and Hemmings, 2001) by dephosphorylating it. Conversely, inactivation of PTEN could have significant implications for the activation state of PKB/Akt, for example Leslie *et al* showed in 2003 that oxidative stress activated PI3-K–dependent signaling via the inactivation of PTEN. It has been shown that mutations in PTEN that inactivate this lipid phosphatase function allow unregulated PKB/Akt activity and uncontrolled cell proliferation (Myers *et al*, 1998). Since PKB/Akt has been widely implicated in tumor genesis (Bao *et al*, 2004) PTEN (Hlobilkova *et al*, 2003), as well as PKB/Akt (Hanada *et al*, 2004) are thus potential targets for cancer therapy.

There are survival stimuli that activate PKB/Akt via mechanisms independent of PI3-K activation (Datta *et al*, 1999). Agonists of the PKA pathway can activate PKB (Sable *et al*, 1997) as can agents which raise intracellular calcium levels (Tilton *et al*, 1997). Calcium binds to calmodulin and the Ca^{2+}/calmodulin complex activates the calcium/calmodulin dependent kinase (CaMK), which then activates PKB/Akt by direct phosphorylation of Thr-308 (Yano *et al*, 1998).

Since PI3-K can also be stimulated by direct interaction with the Ras proto-oncogene GTPase Ras, PKB/Akt is also controlled by Ras. Activated Ras will stimulate PKB/Akt (Datta *et al*, 1996; 1999).

Cellular stresses such as heat shock and hyperosmolarity, both of which can stimulate the activity of p38/HOG1 kinase cascade, can stimulate the activity of PKB/Akt. Heat shock induces association of PKC with the PHδ domain of PKB/Akt.

Integrin-linked kinase (ILK), a serine threonine kinase that interacts with the cytoplasmic tail of integrin β subunits (Delcommenne *et al*, 1998) has also been suggested to regulate PKB/Akt by phosphorylation at Ser-473. ILK is directly regulated by $PI(3,4,5)P_3$, presumably through binding of lipids to a PH domain within ILK, however further studies are necessary to determine whether ILK activity alone is sufficient to activate PKB/Akt in vitro.

Since PKB/Akt is a downstream target of PI3-K, its action is also blocked by the inhibitor wortmannin (Ng *et al*, 2001).

2.3.2.4 Targets of PKB/Akt

One of the first important downstream target kinases that appears to be regulated by activities of PI3-K and PKB/Akt is glycogen synthase kinase 3 (GSK-3) (Marte and Downward, 1997). PKB/Akt was found to phosphorylate and inactivate GSK-3, which in turn regulates a number of substrates involved in cellular metabolism, including glycogen synthase (Cross *et al*, 1995).

PI3-K and PKB/Akt are well known as pro-survival factors, and one of the routes by which this is accomplished, is by the phosphorylation of an early downstream target identified as the pro-apoptotic factor BAD. This was shown to be phosphorylated on residue Ser-136 by PKB/Akt, and this phosphorylation, stimulated by ligands such as IGF-1, prevented BAD-induced cell death (Datta *et al*, 1997; del Pesto *et al*, 1997).

In Table 1 the complete list of PKB/Akt substrates can be seen. This includes the aforementioned BAD phosphorylation and GSK-3 inhibition. Included too are the phosphorylation and activation of eNOS to produce NO, the activation of phosphofructokinase (PFK2) to increase glycolysis, and the activation of mammalian target of rapamycin (mTOR).

Table 1. Current list of published protein kinase B (PKB)/Akt substrates (modified from Brazil and Hemmings, 2001).

Protein	Effect of phosphorylation
BAD	blocks BAD-induced apoptosis
C-Raf	inhibits C-Raf activity
B-Raf	inhibits B-Raf activity
BRCA-1	interferes with nuclear localization of BRCA-1
CREB	increased association with CBP and pl30
eNOS	activates eNOS and leads to NO production
FKHRL1	inhibits transcriptional activity of FKHRL1
GSK-3α	inhibits GSK-3 activity
GSK-3β	inhibits GSK-3 activity
I-κB-kinaseα	activates transcriptional activity of NF-κB
IRS-1	protects IRS-1 from the activity of PYPase
mTOR	activates mTOR activity
PDE 3B	inactivates PDE-3B
PFK-2	activates PFK-2
Rac1	inhibits Rac1-GTP binding
hTERT	enhances telomerase activity
p21CIP1	causes cytoplasmic localization of p21CIP1
Nur77	inhibits transcriptional activity of Nur77

2.3.2.5 PKB/Akt and Glucose Uptake

The final step in the preparation process for glucose uptake is the fusion of GLUT4-containing vesicles with the plasma membrane (Foster and Klip, 2000). Work by Tanti *et al* in 1997 with adipocytes suggests a direct link between PKB/Akt activation and GLUT4 translocation to the membrane. There is additional evidence that PKB/Akt interacts with the GLUT4 containing vesicles in the cell cytosol, and causes these vesicles to translocate to the cell surface and deposit their contents in the cell membrane in muscle cells (Wang *et al*, 1999b) and adipose cells (Cong *et al*, 1997; Calera *et al*, 1998).

2.3.2.6 Caveolae

Insulin receptor signal transduction has been demonstrated to depend on functional caveolae (Karlsson *et al*, 2001). Caveolae are small flask-shaped invaginations of the plasma membrane expressed in most terminally differentiated mammalian cell types (Shaul and Anderson, 1998). They are related to raft microdomains, and enriched in sphingolipids and cholesterol. They appear to form lipid rafts in the presence of the principal structural protein caveolin, which serves as their marker. These specialized microdomains are common in endothelial, muscle, and adipose tissues and appear to be involved in uptake of solutes into the cytosol and in signal transduction (Smart *el al*, 1999). Karlsson *et al* (2001) showed that GLUT4 in the plasma membrane is largely located in the caveolae in response to insulin stimulation.

2.4 Contraction and Exercise

The rate of glucose uptake is subject to the influence of three states: rest, physical activity (including the effects of hypoxia) and alimentation (including effects of fat and plasma free fatty acid (FFA) concentration) (Zierler 1999).

Acute exercise, similar to insulin, increases the uptake of glucose into muscle (Douen *et al*, 1990). Exercise, or muscle contractions, can increase the rate of glucose uptake into the cell 10 to 20 fold and this occurs despite a decrease in insulin concentrations (Wahren *et al*, 1971), thus via a mechanism that is independent of insulin (Holloszy, 2003).

In 1979 Soman *et al* showed that acute exercise led to a significant increase in insulin binding to monocytes, which returned to basal 24 hours after exercise. Spontaneously exercised rats show enhanced responsiveness to exogenous insulin at rest in the research of Mondon *et al* in 1980, while Koivisto *et al*, 1980, reported that, in previously untrained subjects, physical training resulted in a 35% rise in insulin binding to monocytes. Kirwan *et al* (2000) found that there was enhanced insulin sensitivity in skeletal muscle associated with exercise training.

The heart has a greater oxygen consumption both at rest and during exercise compared to skeletal muscle (Rowell, 1986). Kemppainen *et al* (2002) showed that during low- and moderate- intensity exercise, myocardial glucose uptake doubled as

compared to the resting state. This has been shown to be brought about by an increase in the number of glucose transporters (GLUT4) in the plasma membrane (Douen *et al*, 1989, Fushiki *et al*, 1989). Although the cardioprotective effects of exercise have been widely shown (Davidoff *et al*, 2004; Vona *et al*, 2004), it is currently unknown whether exercise will enhance cardiac insulin sensitivity.

However, if the intensity of the exercise is increased to a very high level, myocardial glucose uptake is lower than it is during lower intensity levels (Kemppainen *et al*, 2002). This indicates that during higher intensity levels the increased myocardial energy needs are provided for by substrates other than glucose.

The effects of exercise on glucose uptake have been shown to be additive to that of insulin (Koval *et al*, 1999; Kirwin *et al*, 2000). This finding strongly suggests that different biochemical pathways are involved in the effects of exercise/ contraction and insulin on glucose uptake.

Oxygen deprivation, which occurs in the muscle during exercise, induces a rapid stimulation of glycolysis, known as the Pasteur Effect (Randle and Morgan, 1962). This effect is brought about by activation of PFK-1 (phospho-fructo-kinase 1) due to the increase in the AMP:ATP ratio that occurs under these conditions. It has been shown that this effect is mediated by AMPK.

2.5 AMP-activated protein kinase (AMPK)

2.5.1 Structure of AMPK

AMPK is a heterotrimeric enzyme composed of a catalytic (α) subunit and two regulatory (β and γ) subunits (Hardie *et al*, 1998). Each subunit exists as alternate isoforms encoded by two or three genes (α1, α2, β1, β2, γ1, γ2, γ3) and all twelve different combinations of isoforms appear able to form complexes (Hardie, 2003). The predominant isoforms in most cells are α1, β1 and γ1 and skeletal and cardiac muscle also expresses α2, β2, γ2 and γ3 (Stapleton *et al*, 1996; Kemp *et al*, 1999). The core of the β subunit contains a conserved domain that has recently been recognized as a glycogen-binding domain (GBD) (Hudson *et al*, 2003; Polekhina *et al*, 2003).

2.5.2 Activation and regulation of AMPK

AMPK is activated by any stress treatment that interferes with ATP production where the ratio of AMP: ATP in the cell increases due to nutrient or exercise induced stress (Hardie and Hawley, 2001; Hardie 2003). Stresses include heat shock (Corton *et al*, 1994) metabolic poisons (Corton *et al*, 1994) glucose deprivation (Salt *et al*, 1998) and hypoxia and ischaemia in heart muscle (Kudo *et al*, 1995). These are all abnormal, pathological occurrences which decrease ATP production, but AMPK can also be activated by a physiological stress such as increased ATP consumption

induced by exercise (Winder and Hardie, 1996; Fujii *et al*, 2000). AMPK is activated by exercise or contraction in rodent (Winder and Hardie 1996) and human (Fujii *et al*, 2000) muscle, with activation being dependent on the duration as well as the intensity of the exercise (Stephens *et al*, 2002).

AMPK is allosterically activated by AMP, but also by phosphorylation by one or more upstream kinases, termed AMPK kinases (recently identified as LKB1 (Hawley *et al,* 2003 and Woods *et al,* 2003)) at threonine residue 172 within the "activation loop" of the α subunit kinase domain. Without this phosphorylation there is no detectable activity of AMPK (Hawley *et al*, 1996; Stein *et al*, 2000). LKB1's activation is also promoted by increased AMP levels (Weekes *et al*, 1994).

AMPK is allosterically inhibited by physiological concentrations of phosphocreatine (Ponticos *et al*, 1998) and this confirms the proposed physiological role of AMPK as a sensor of cellular energy status.

2.5.3 Role of AMPK

AMPK plays a key role in maintaining energy homeostasis in the cell (Hardie *et al*, 1998) since it is sensitive to AMP levels within the cell and is activated by a rising AMP/ATP ratio, indicative of energy depletion. It acts as an energy sensor in the cell because it recognizes ATP depletion (Hardie and Carling, 1997) and prevents any further ATP utilization by anabolic pathways, but also initiates changes to restore

cellular ATP levels (Kemp *et al,* 1999). Activated AMPK phosphorylates and inactivates key enzymes involved in ATP-utilizing pathways e.g. enzymes involved in glycogen, fatty acid and cholesterol synthesis, and stimulates enzymes controlling catabolism. In the heart and skeletal muscle AMPK plays an important role in accelerating fatty acid oxidation, glucose uptake, GLUT4 translocation, glycolysis, FAT/CD36 translocation and fatty acid uptake (Hardie and Hawley, 2001).

The AMPK signaling pathway provides an alternative to the insulin-dependant glucose uptake pathway in muscle. Resistance of muscle to the effects of insulin is one of the first defects leading to the development of type II diabetes mellitus. This reduction in insulin sensitivity is reflected in decreased insulin-stimulated glucose uptake (Fryer *et al*, 2000). Since AMPK activates glucose uptake via a distinctly different pathway to insulin, this AMPK path may present the perfect mechanism to manipulate pharmacologically to treat this disease. AMPK has also been found to be activated in the muscle of subjects with type II diabetes during exercise (Musi *et al*, 2001).

If activation of AMPK mediates the metabolic effects of exercise, and exercise sensitizes muscle to the effects of insulin, the biochemical pathway that results in AMPK activation, must cross-talk with the biochemical pathway that is activated by insulin.

Indeed, in insulin-resistant humans and rodents, regular exercise enhances insulin sensitivity (Seals *et al*, 1984; Trovati *et al*, 1984; Rogers *et al*, 1988; Cortez *et al,* 1991; Dela *et al*, 1992; Hughes *et al*, 1993; Houmard *et al*, 1999; Chibalin *et al*, 2000). Importantly, insulin-stimulated PI3-kinase activity is greater in skeletal muscle from young healthy individuals who do regular exercise compared to sedentary individuals (Kirwin *et al*, 2000). Therefore, enhanced insulin action after exercise may be due to improvements in insulin signal transduction (Kemppainen *et al*, 2003).

In 2001, Musi and coworkers were the first to demonstrate that an acute bout of exercise led to a significant increase in AMPKα2 activity in the skeletal muscle of individuals with type 2 diabetes. This finding supported the idea put forward by researchers (e.g. Winder 2000) that increasing glucose uptake by the muscle through pharmacological manipulation of AMPK (e.g. AICAR) could be an important strategy for the treatment of type 2 diabetes.

2.5.4 Targets of AMPK

As seen in Figure 2.5, AMPK has many targets and thus effects several physiological pathways.

2.5.4.1 Acetyl-CoA carboxylase

AMPK is involved in the regulation of acetyl-CoA carboxylase (ACC), the enzyme that catalyses malonyl-CoA synthesis (Kudo *et al*, 1995; Kemp *et al*, 1999; Saha *et al*,

2000). AMPK inhibits this enzyme by phosphorylating it, and thereby reduces the level of malonyl CoA. Malonyl CoA is an inhibitor of carnitine palmitoyl-transferse I (CPT1) (Saha *et al*, 2000) which is located on the outer surface of the mitochondrion and is responsible for the transport of long-chain fatty acids into the mitochondrion with carnitine for oxidation (Kemp *et al*, 1999). Therefore by increasing AMPK activation, fatty acid intake into the mitochondrion is increased and oxidation occurs. Decreases in malonyl-CoA concentration in muscle during exercise have been linked to decreases in ACC activity (Vavvas *et al*, 1997; Saha *et al*, 2000) as have increases in ACC phosphorylation been linked to increases in AMPKα2 activity (Stephens *et al*, 2002).

2.5.4.2 HMG-CoA Reductase

Through an acute, rapid effect of AMPK, 3-hydroxy-3-methylglutaryl-CoA (HMG-CoA) reductase activity is decreased and so too is sterol synthesis (Corton *et al*, 1994).

2.5.4.3 Creatine Kinase

The creatine kinase (CK)–phosphocreatine system plays a crucial role in the maintenance of ATP levels in tissues that have a high and fluctuating energy requirement. CK catalyses the interconversion of creatine (Cr) and ATP with phospho-creatine (PCr) and ADP (Walliman, 1994). Thus CK is presumed a prime target for AMPK action, and Ponticos *et al* demonstrated in 1998 that AMPK phosphorylates and inactivates the muscle specific isoform of CK (MM-CK). They

also demonstrated that not only was AMPK activity regulated by the ATP:AMP ratio, but by the PCr:Cr ratio as well.

2.5.4.4 Glycogen Synthase

Glycogen synthase is also phosphorylated and thereby inactivated by AMPK. Thus the synthesis of glycogen is halted (Carling and Hardie, 1989).

2.5.4.5 Glucose Uptake

The work of Hayashi *et al* (1998) also suggested that AMPK stimulates glucose uptake. These studies, involving exercise stimulated glucose transport as well as stimulation of AMPK with 5-aminoimidazole-4-carboxamide-1-β-D-ribonucleoside (AICAR), show enhanced glucose uptake via an insulin independent pathway and will be discussed in Chapter 2.6 as it has specific relevance to the current study.

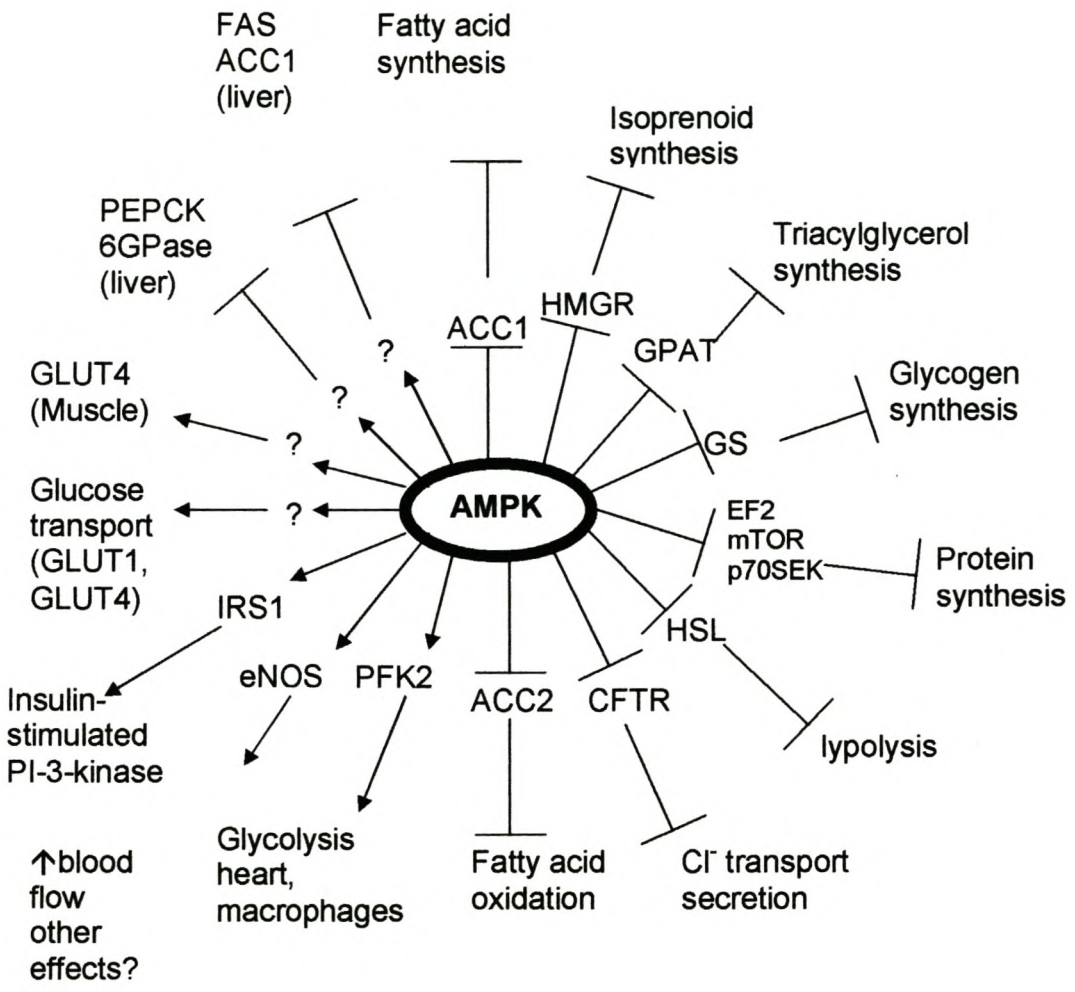

Figure 2.5 Physiological targets and pathways regulated by AMPK (from Hardie 2003).

2.6. 5'-aminoimidazole-4-carboxamide-1-β-D-ribonucleoside (AICAR)

AICAR is an adenosine analogue which is taken up into cells and converted to the monophosphorylated nucleotide, 5-aminoimidazole-4-carboxamide-ribonucleoside monophosphate (ZMP), by adenosine kinase (Sabina *et al*, 1985; Hardie 2003). It was described as a specific activator of AMPK (Corton *et al*, 1995) in intact cells. It has also been found that ZMP, an analogue of AMP, mimics the effect of AMP on allosteric activation of AMPK (Sullivan *et al*, 1994) and promotion of phosphorylation and activation of AMPK by LKB1 (Weekes *et al*, 1994).

It is important to note that stimulation with AICAR does not change the ATP/ADP or ATP/AMP ratios in the cells (Corton *et al*, 1995), which indicates that the conversion of ZMP to AMP is slow.

There are numerous studies showing that AICAR increases AMPK phosphorylation as well as glucose uptake in skeletal muscle. The latter was shown to be mediated by increased GLUT4 translocation (Lochhead *et al*, 2000; Ojuka *et al*, 2000; Buhl *et al*, 2001).

However, the matter of AMPK activation by AICAR is still controversial. A few studies have shown no increased AICAR-induced AMPK activity or glucose uptake in a diversity of tissues. For example Kaushik *et al* (2001) as well as Balon and Jasman (2001) showed that AICAR exposure did not stimulate glucose uptake in rat soleus muscle. On the other hand, convincing evidence has been presented for the

stimulation of glucose uptake in skeletal muscle by AICAR. AMPK activation by AICAR in the rat lateral and medial gastrocnemius led to increased glucose uptake (Bergeron *et al*, 1999). Similarly, work by Balon and Jasman also showed dramatic increases in glucose uptake in isolated mouse soleus muscle incubated with 2 mM AICAR (Balon and Jasman, 2001).

Exposure of rat epitrochlearis muscles to 0.5 mM AICAR activated AMPK and increased GLUT4 translocation (Ojuka *et al*, 2000), while chronic treatment with AICAR (1mg/g body wt subcutaneous injection per day for 5 days) increased insulin-stimulated glucose uptake and GLUT4 translocation in rat gastrocnemius muscle (Buhl *et al*, 2001). However in this same study by Buhl *et al* they showed no increase in these parameters in white twitch soleus muscle.

There is, however, only one study to date published on the effects of AICAR on the uptake of glucose in the heart. Russell *et al* showed in 1999 that AICAR increased glucose uptake in isolated rat ventricular papillary muscles.

Although there is evidence for the stimulation of glycogenolysis by AICAR in the heart (Longnus *et al*, 2003), it had no effect on glycolysis in rabbit cardiomyocytes (Javaux *et al*, 1995) which led to the theory that the effect of AICAR is dependent on the capacity of the cells to accumulate ZMP and the presence of target enzymes which are sensitive to ZMP (Javaux *et al*, 1995).

There have also been studies where it was found that treatment of cells with the combination of AICAR and insulin led to enhancement of the insulin signaling pathway as well as enhancement of insulin-stimulated glucose uptake (Buhl *et al*, 2001; Jessen *et al*, 2002). It was seen that chronic AICAR administration and long-term exercise both improved insulin-stimulated glucose uptake in skeletal muscle in a fiber type specific way with the most marked increase in muscles with high content of type II fibres, and this was associated with an increase in GLUT4 content (Jessen *et al*, 2002). Buhl *et al*, (2001) showed that rats subcutaneously injected with AICAR had a marked increase in maximally insulin-stimulated glucose uptake in epitrochlearis and extensor digitorum longus muscles, but not in soleus muscles. Similarly, combining insulin and AICAR led to a fully additive effect on glucose uptake in the epitrochlearis muscle according to Bergeron *et al* (1999). Furthermore, AICAR treatment improved glucose homeostasis in insulin resistant (ob/ob) mice in skeletal muscle and liver (Song *et al*, 2002).

In view of the above we hypothesized that stimulation of the heart with AICAR or ZMP would lead to a sensitization of the heart muscle for insulin stimulation, and we therefore aimed to determine:

i) Whether AICAR can activate AMPK in heart muscle

ii) Whether this pharmacological activation will mimic some of the physiological effects of exercise e.g. increased glucose uptake and GLUT4 translocation

iii) Whether AICAR, in any way, affects the biochemical pathway activated by insulin and leading to glucose uptake.

CHAPTER 3

MATERIALS AND METHODS

3.1 Animals

Male Wistar rats weighing between 250-350g were used in all experiments. The rats were allowed free access to food (standard rat chow) and water, and maintained in animal quarters at 22°C with a 12 hour day/night cycle. Animals were anaesthetised with an intraperitoneal injection of pentobarbitone sodium at a concentration of 0.12mg/gram. The project was approved by the Ethics committee of the Faculty of Health Sciences, University of Stellenbosch.

3.2 Materials

Materials purchased from Sigma

2-3,butane-dione monoxime (BDM), HEPES hemisodium salt technical grade minimum 99.5% titration, pyruvate, mercaptoethanol, N,N,N',N'-tetramethylethylenediamine (TEMED), ponceau S, phenylmethylsulphonyl fluoride (PMSF), Na-p-nitrophenylphosphate (p-NPP), 5-aminoimidazole-4-carboxamide-1-β-D-ribofuranoside (AICAR), 5'-aminoimidazole-4-carboxamide-ribonucleoside-phosphate (ZMP), wortmannin, insulin, triton-X-100, benzamidine, 8-cyclopentyl-1,3-dipropylxanthine (8-CPT).

Materials purchased from Merck NT laboratory supplies (Pty). LTD [Darmstadt, Germany]

d-glucose, sodium dodecyl sulphate (SDS), ammonium peroxodisulphate (APS), tris(hydroxylmethyl) aminomethane, trypan blue, (Analar grade).

Materials purchased from Worthington

type 2 collagenase.

Materials purchased from Roche Diagnostics

bovine serum albumin (BSA), fraction V, fatty acid-free.

Materials purchased from Millipore, UK.

Millipore immobilon-p polyvinylidene fluoride (PVDF) microporous membrane .

Materials purchased from Fluka

acrylamide

Materials purchased from Amersham Biosciences, UK Ltd

ECL Western blotting detection reagents, anti-rabbit Ig, horseradish peroxidase linked whole secondary antibody

Materials purchased from PerkinElmer Lifesciences, Boston

2-deoxy-D-[^{3}H]glucose

Materials purchased from Santa Cruz Biotechnology Inc.

GLUT4 (H-61): sc-7938 rabbit polyclonal antibody

Materials purchased from Cell Signaling technology

p38 MAP Kinase Antibody, phospho-PKB/Akt (Ser473) antibody, phospho-AMPK-α (Thr172) antibody

3.3 Isolation of cardiomyocytes

Rod-shaped ventricular cardiomyocytes from male Wistar rats were obtained by the method as described by Fischer *et al* (1991). Hearts were quickly removed from anaesthetised animals and immediately mounted on a perfusion rig via the aorta. Hearts were perfused by the method of Langendorff retrogradely with medium A (see addendum) nominally calcium-free, pH 7.4, 37°C, equilibrated with 95% O_2 / 5% CO_2, for 5 minutes in order to remove the blood from the coronary vessels. The perfusion was then switched to oxygenated medium B (see addendum) at 37°C, and perfused in a recirculating manner. After 15 minutes $CaCl_2$ was added to the medium to raise the calcium concentration to 100 μM; after 5 more minutes, the calcium concentration was raised to 200 μM. The calcium concentration was risen to physiological concentrations in a stepwise manner in order to create the minimum amount of stress for the cardiomyocytes and to prevent them from going into calcium overload.

Perfusion was continued to a total of 35 minutes; the heart was then cut off the catheter, carefully torn open and the incompletely digested tissue then gently minced with tweezers. The tissue was subsequently incubated in a shaking water bath (37°C, 60 strokes/min, 5cm/stroke) for 20 minutes in a mixture consisting of one part medium B and one part medium C (see addendum) under an oxygen atmosphere. During the last 5 minutes of incubation, the calcium concentration was raised in a stepwise manner to 1.25 mM.

After digestion the suspension was filtered through a nylon net (mesh size 200 x 200 μm) and gently spun down (10 x g, 3 min). The supernatant was rapidly aspirated and the loose pellet resuspended in medium D (see addendum) at room temperature. The cells were left to sediment for no more than 5 minutes, the supernatant was removed and the loose pellet resuspended in 15 ml medium D. The myocyte suspension was then kept in a slowly rotating, closed vial under an oxygen atmosphere at room temperature for at least 1 hour to allow recovery from the isolation procedure. Before the beginning of the experiments, the cardiomyocytes were washed three times with assay buffer, medium E (see addendum).

3.4 Cell viability

Osmotic fragility coupled to trypan blue exclusion (TBE) and cell morphology were used as indices for assessment of cell viability. (Adapted from Armstrong *et al*, 1994)

Approximately 12.5μl (representing 80 000-100 000 myocytes) of the myocyte cell pellet was removed after the hour of incubation at room temperature, washed with medium D, and resuspended for 3-5minutes in 100μl of hypotonic medium D. Thereafter the suspension was further diluted (1:1) with counting medium (see addendum). 10 μl of the final counting suspension was placed on a haemocytometer counting slide and examined light microscopically (100x magnification) to evaluate the absorption (non-viable) or exclusion (viable) of trypan blue dye. Blue cells were counted as non-viable as their membrane

integrity had been compromised leading to uptake of the blue dye. Yellow cells were counted as viable.

Time zero viability (viable cells calculated as a percentage of the total cells in a sample) varied between 70% and 80% and all cell isolates of less than 70% viability were discarded.

The use of myocyte morphology as an index of viability involved the same procedure as above, with the exception that the cells were suspended in an isotonic medium D and counting medium. Rod-shaped cells (length: width ratio ≥ 3:1) were considered viable whereas square-shaped (length: width ratio ≤ 3:1) and round cells were considered non-viable. Cell viability was expressed as the percentage rod-shaped cells present.

(Armstrong and Ganote, 1991)

3.5 Detection of Glucose Uptake

Myocyte uptake of 2-deoxy-D-[^{3}H]glucose (2DG) was measured in assay medium E, pH 7.4, 37°C, equilibrated with oxygen.

0.5ml of washed cell suspension (corresponding to approximately 1.5mg cell protein) was assayed in a total volume of 750µl of medium E with or without an appropriate dilution for one or several agents to be tested. Cells were incubated in flat-bottomed vials, at 37°C under an oxygen atmosphere in a shaking water bath (60 strokes/min, 5cm/stroke). 2DG accumulation in these cells was measured in the presence or absence of 400µM phloretin as described by Fischer *et al* (1991).

Phloretin at this concentration totally blocks glucose uptake by GLUT4 and GLUT1, therefore carrier mediated glucose uptake. Myocyte glucose uptake in the presence of phloretin was subtracted from all values to determine carrier mediated uptake.

The samples were incubated as indicated in Figure 2.1. After stimulation, the myocytes were further incubated in the presence of 2DG (3μCi/ml, final concentration 1.5μM) for an additional 30 minutes before 2DG uptake was stopped by adding phloretin (to a final concentration of 400μM). The samples were then immediately transferred into 1.5ml eppendorf tubes, and centrifuged at 10 000xg for 1minute at room temperature to separate the cells from the less dense incubation medium. The supernatants were aspirated and the pellet washed twice with medium A, whereafter the pellet was dissolved in 0.5N NaOH. An aliquot of this suspension was used in protein determination by the method of Lowry et al (see chapter 3.12), while 3 x 100μl of the rest was counted in 2ml of scintillation fluid in a liquid scintillation counter (Beckman). Specific, i.e. glucose-carrier-mediated 2-deoxy-D-glucose uptake was calculated by subtraction of uptake monitored in the presence of 400μM phloretin from values measured in the absence thereof (Fischer *et al* 1991).

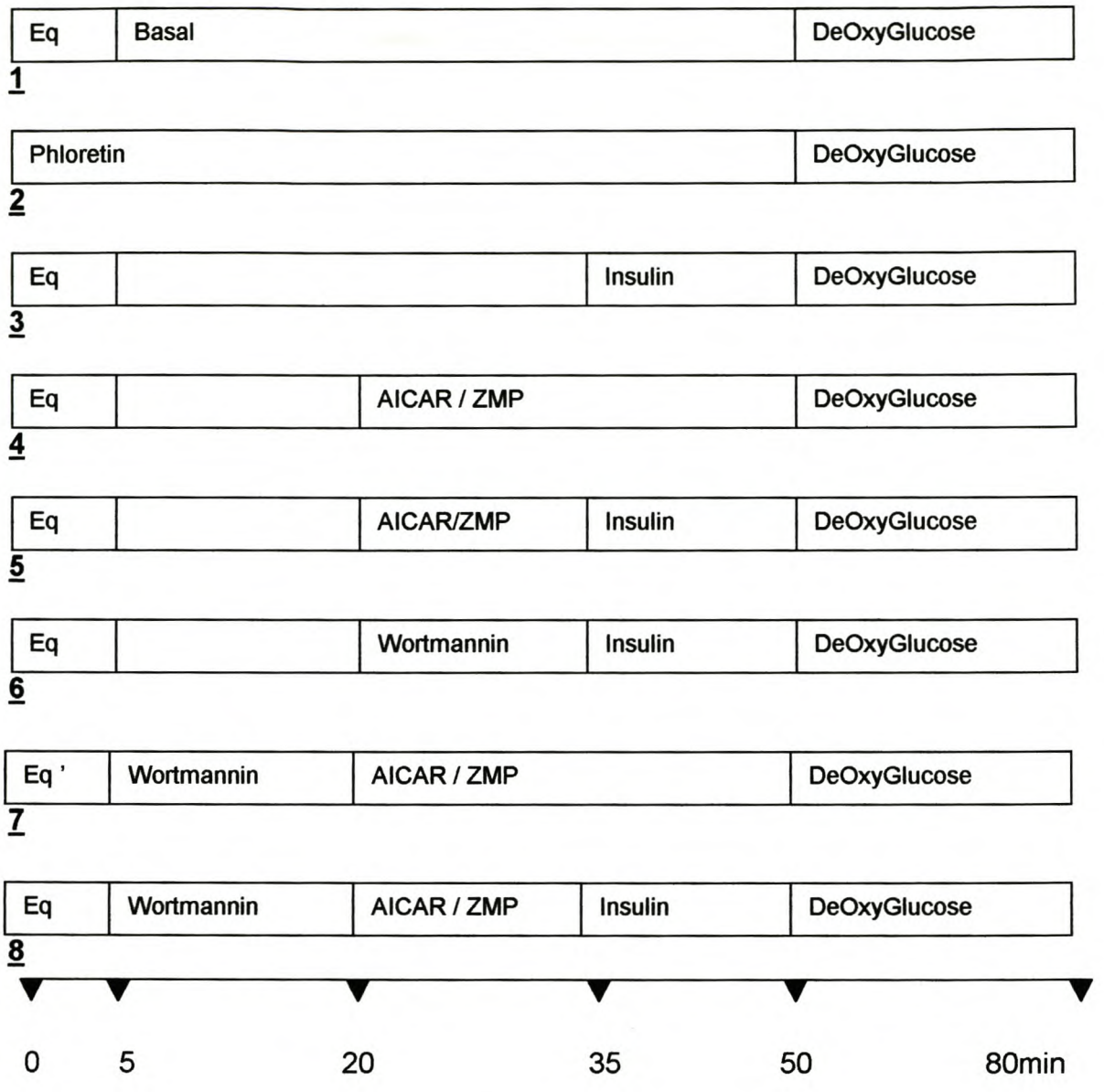

Figure 3.1 Diagram of cardiomyocyte protocol for glucose uptake

All groups were equilibrated for a 5minute period. Various agents were added in the following concentrations for the times indicated: Insulin (100nM) 15 minutes, AICAR (1mM) 30 minutes, ZMP (1mM) 30 minutes, Wortmannin (100nM) 15 minutes before either insulin or AICAR/ ZMP stimulation as indicated, Eq = equilibrium. Please note that once an agent was added, it remained in the medium until the end of the experiment.

1. *Basal 2DG uptake of the cells measured after 50 minutes incubation followed by 30 minutes incubation with radioactively labelled 2DG.*
2. *Phloretin was present throughout the duration of the experiment to act as a negative control.*
3. *Cells were stimulated with insulin for 15minutes before the addition of 2DG.*
4. *AICAR or ZMP (1mM unless otherwise indicated) were added 30minutes prior to addition of 2DG.*
5. *A combination of AICAR or ZMP and insulin were staggered by addition at the time points indicated prior to 2DG addition.*
6. *Wortmannin was added 15minutes before the addition of Insulin.*
7. *Wortmannin was added 15minutes before the addition of AICAR or ZMP.*
8. *Wortmannin was added 15minutes before the combination of AICAR, ZMP and insulin.*

All 2DG uptake reactions were stopped by addition of phloretin to a final concentration of 400μM.

3.6 Whole Heart Perfusion Protocol

Hearts were quickly removed from animals (anaesthetised with 0.12 mg/g body wt of sodium pentobarbitone) and immediately perfused by the method of Langendorff with Krebs-Henseleit bicarbonate buffer with or without 5 mM glucose as indicated. This concentration of glucose was used because it results in minimal basal glucose uptake, which allows for a maximal stimulatory effect of insulin to be observed on both glucose uptake and GLUT4 translocation. The perfusion

solution was gassed with 95% O_2, 5% CO_2 for 20 minutes before and throughout the experiment (see Fig 3.2).

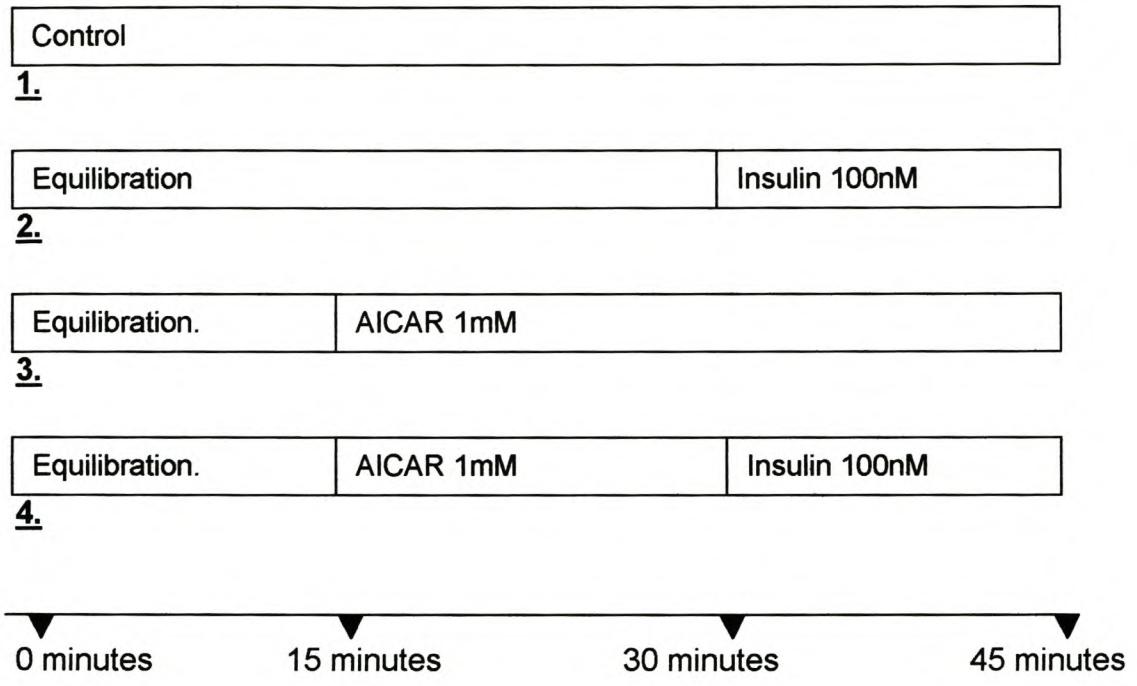

Figure 3.2 Diagram of whole heart perfusion protocol for Western blot analysis.

1 Hearts used as controls were continuously perfused for 45 minutes.

After a stabilisation period, the experimental hearts were either perfused with

2 Insulin (100nM) for 15 minutes,

3 AICAR (1mM) for 30 minutes or

4 AICAR (1mM) for 30 minutes and Insulin (100nM) for 15 minutes

Hearts were immediately freeze-clamped with Wollenberger tongs and stored in liquid nitrogen until further use.

3.7 Preparation of lysates for Western Blotting

3.7.1 Cardiomyocyte lysates

For the measurement of AMPK, PKB/Akt and GLUT4 phosphorylation patterns, the following procedure was followed to generate lysates for Western Blotting analysis.

As for 2DG uptake, 0.5 ml of washed cell suspension (corresponding to approximately 1.5 mg cell protein) was incubated in a total volume of 750 µl of medium E. This was done with or without an appropriate dilution for one or several agents to be assayed, in flat-bottomed-vials, at 37°C in a shaking water bath (60 strokes/min, 5 cm/stroke). Basal phosphorylation was measured on a vial where no other agents were added. The following agents were added as indicated in Figure 3.1 and Figure 3.3 to various samples at appropriate times for stimulation for the times indicated:

Insulin (100 nM) 15 minutes, AICAR (1 mM) 30 minutes, ZMP (1 mM) 30 minutes, Wortmannin (100 nM) 15 minutes before AICAR, ZMP or insulin.

Cardiomyocytes were stimulated as indicated in figure 3.1 and samples for determination of PKB/Akt, AMPK and GLUT4 were removed before addition of 2DG. The samples were immediately transferred to 1.5 ml eppendorf tubes and centrifuged at 10 000 x g for 1 minute at room temperature to separate the cells from the less dense incubation medium. After centrifugation tubes were

immediately placed on ice. The supernatants were aspirated and the remaining pellet sonicated for 3 cycles of 5 seconds each at maximum power in the appropriate lysis buffer (see addendum).

These lysates were then centrifuged at 12 000 x g at 4°C for 15 minutes to remove any particulate matter. The Bradford Method (Chapter 3.11) was used to determine protein content of the supernatant. It was then diluted with a 3 times Laemmli sample buffer (see addendum), boiled for 5 minutes, and stored at -20° for Western Blot analysis.

3.7.2 Tissue lysates from perfused hearts

After perfusion as shown in Fig 3.2, approximately 0.2g of liquid nitrogen frozen ventricular tissue was fully pulverised in a pre-cooled mortar and pestle at 4°C. Pulverised tissue was then added to Sorvall centrifuge tubes each containing 900µl of specific lysis buffer for either AMPK or GLUT4 extraction (see addendum). The tissue and lysis buffer was then homogenised mechanically with a polytron PT10 homogeniser for 2 cycles of 5 seconds each and spun down in a microfuge to remove the particulate matter. Protein determination for each sample was conducted using the Bradford protein determination method. Samples were then diluted with a 3 times Laemmli sample buffer (see Addendum), boiled for 5 minutes and stored at -20° for Western blot analysis.

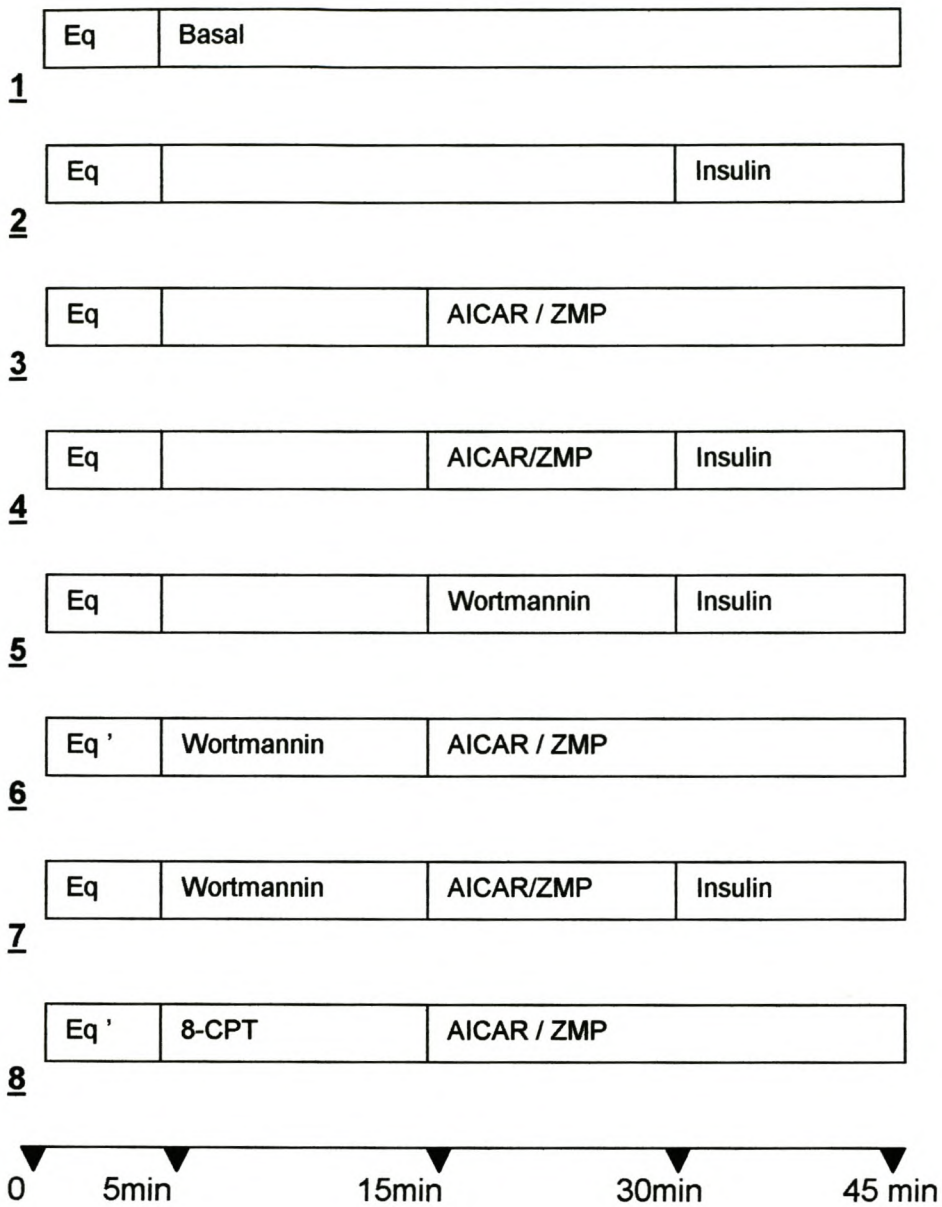

Figure 3.3 Diagram of cardiomyocyte protocol for Western blot analysis

All groups were equilibrated for a 5minute period. Various agents were added in the following concentrations for the times indicated: Insulin (100nM) 15 minutes, AICAR (1mM) 30 minutes, ZMP (1mM) 30 minutes, Wortmannin (100nM) 15

minutes before insulin / AICAR/ ZMP stimulation as indicated, 8-CPT (10μM) 15 minutes before AICAR/ ZMP stimulation.

1. *Basal levels of activation were measured after 45 minutes.*

2. *Cells were stimulated with insulin for 15 minutes*

3. *AICAR or ZMP were added for a stimulation period of 30 mintues.*

4. *A combination of AICAR- or ZMP and insulin were staggered by their addition at the time points indicated.*

5. *Wortmannin was added 15 minutes prior to the addition of insulin*

6. *Wortmannin was added 15 minutes prior to the addition of AICAR or ZMP*

7.*Wortmannin was added 15 minutes before the addition of AICAR- or ZMP and insulin*

8. *8-CPT, an adrenergic (purinergic) receptor antagonist, was added 15 minutes before the addition of AICAR or ZMP, to establish whether the effects of these two drugs involved the purinergic receptors at all.*

3.8 Western Blotting techniques

3.8.1 General

After boiling each sample for 5minutes, equal amounts (20-50μg as indicated) of sample protein from the various fractions were separated on a 12% SDS-polyacrylamide gel (see addendum) using the standard Bio-Rad Mini-PROTEAN III system (Biorad, Life Science group, US).

Electrophoretically separated proteins were transferred to a PVDF (polyvinylidene fluoride) membrane by electroblotting. After staining the membranes with Ponceau-S red (reversible staining) for visualisation and verification of transferral of the protein bands, membranes were scanned with laser scanning and saved as a record of equal loading. Membranes were then washed with TBS 0.1%Tween (TBST). Non-specific binding sites on the membranes were blocked with 5% fat-free milk powder in TBST for 2 hours at room temperature.

Following the blocking procedure membranes were washed thoroughly with TBST and incubated with the appropriate primary antibody (1:1000 dilution in TBST) for 5-16 hours at 4°C. After washing the membranes with TBST, the immobilised primary antibody was conjugated with a diluted (1:4000) horseradish peroxidase-labelled secondary antibody for 1 hour at room temperature. The membranes were again washed thoroughly with TBST. Bands were visualised with electro-chemiluminescence (ECL™) detection agents used according to the manufacturers instructions and quickly exposed to high performance

chemiluminescence film (Hyperfilm ECL) to detect the light emission. Bands were quantified by laser scanning densitometry and analysed with suitable software (UN-SCAN-IT, Silkscience, US).

3.8.2 PKB blots

Western blotting technique was carried out as stated (Ch 2.8.1) with minor adjustments for specificity. Fractions (20μg protein) were separated on a 12% SDS-polyacrylamide gel. Membranes were incubated with the phospho-Akt (Ser473) primary antibody (Cell Signaling Technology™) for 5 – 16 hours at 4°C.

3.8.3 GLUT4 blots

Western blotting technique was carried out as stated (Ch 2.8.1) with minor adjustments for specificity. Fractions (50μg protein) were separated on a 10% SDS-polyacrylamide gel, using the standard Bio-Rad Mini-PROTEAN III system (Biorad, Life Science group, US).

Membranes were incubated with the GLUT4 (H-61): *sc-7938* primary antibody (Santa Cruz Biotechnology, Inc) (1:1000 dilution in TBS 0.02% Tween) for 5 – 16 hours at 4°C.

From this point onwards the membranes were washed with TBS 0.02%Tween instead of TBS 0.1%Tween.

3.8.4 AMPK blots

Fractions (30μg protein) were separated on a 10% SDS-polyacrylamide gel, using the standard Bio-Rad Mini-PROTEAN III system (Biorad, Life Science group, US).

Membranes were incubated with the phospho-AMPK (Thr172) primary antibody (1:1000 dilution in TBS 0.1% Tween, 5% BSA and 5% blocking agent) for 5 – 16 hours at 4°C. 5% blocking agent was also added to the secondary , horse-radish peroxidase conjugated antibody.

3.9 Sarcolemmal Membrane and GLUT4 Isolation

GLUT4 translocates from an intracellular membrane compartment to the plasma membrane. In order to determine if translocation occurred, these two cell compartments needed to be carefully separated and the GLUT4 content per milligram membrane protein determined.

The fractionation protocol had to render a sarcolemmal membrane component, high in Na^+K^+ATPase activity and a cytosolic compartment containing no Na^+K^+ATPase activity, indicating an absence of contamination of the latter with sarcolemmal membrane fractions. Furthermore a clear movement of GLUT4 from the cytosolic to the membrane compartment should be detectable on Western blotting of membranes with GLUT4 after stimulation of hearts with insulin.

A number of protocols (Ch 3.9.1-3.9.3) were tested for the fractionation of membranes into sarcolemmal and cytosolic compartments before a final one (Ch 3.9.3) was selected as giving optimal pure fractions. Activity of the sarcolemmal Na^+K^+ATPase enzyme (Bers, 1979) was used as a marker for this membrane compartment, this enzyme only being present in the cell membrane. To validate the protocol, fractionation was done on samples from control and insulin-stimulated hearts. GLUT4 content of these membranes was then tracked via Western blotting.

When an optimal protocol was decided upon, cytosolic and membrane fractions were isolated and GLUT4 was visualised using the Western Blotting technique and the specific antibody [GLUT4 (H-61): *sc-7938* primary antibody as described above (Ch 3.8.3)

3.9.1 Protocol by Weber *et al*, 1988

Weber et al (1988) published a protocol for fractionation of rat adipocyte membranes to track GLUT4 trafficking.

For membrane fractionation, approximately 20mg of tissue, previously frozen in liquid nitrogen, was homogenised on ice by polytron (2 x 5sec at setting 5) in Buffer A (see addendum). These homogenates were centrifuged for 15minutes at 17000 x g (Sorvall RC-5B; rotor: SS34 with adapters for 12ml tubes; 12000rpm @ 4°C). The supernatant (S1) of this centrifugation was kept while the pellet of this centrifugation (P1) was washed once with Buffer A (SS34, 17000xg, 20min), before it was resuspended in 1.5ml Buffer A, layered on a sucrose cushion and

ultracentrifuged for 65 minutes at 65000 x g (Beckmann, SW 65, 25000rpm). The white interface was taken off, diluted with approximately 8ml Buffer A and the membranes pelleted at 48000 x g (Beckman Ti50) for 30 minutes. The pellet was then washed with 1ml Buffer A and the membrane fraction pelleted again, in an Eppendorf tube in special adapters, at 48000 x g (Ti50) for 30 minutes. This fraction was used as the membrane fraction.

To obtain a fraction containing the cytosolic glucose transporter pool, the supernatant of the first centrifugation (S1) was centrifuged for 30minutes at 48000 x g (Beckman Ti50). This resulted in the separation of a high-density microsome fraction (which appears in the pellet of this centrifugation and is contaminated with plasma membranes) and a low-density membrane fraction in the supernatant. This supernatant was therefore ultracentrifuged (rotor: Ti60, 50000 rpm) for 65minutes at 250000 x g while the pellet was discarded.

3.9.2 Protocol modified from technique by Philipson *et al*, 1980

Philipson *et al* developed a membrane fractionation protocol in 1980 to prepare purified sarcolemmal membranes from cardiac tissue.

Half a heart was homogenised in 5 ml of Buffer B (see addendum) by polytron on setting 4 for 2 X 5 seconds. The homogenate was filtered through one layer of nylon gauze (200 μM). 4 ml of Na-PPi-KCl solution (see addendum) was added to every 36 ml of homogenate. This was then poured into rotor tubes and spun down

for 60minutes in a Beckman Ultracentrifuge in the Ti50 rotor at 45 000 x g. The resultant supernatant was taken as the cytosolic fraction.

The pellet was re-homogenised in Buffer C (see addendum). This was then ultracentrifuged at 40 000 x g for 1 hour at 4°C (Beckman, rotor: Ti50), and the supernatant was used as the membrane fraction.

3.9.3. Protocol by Takeuchi *et al*, 1998

Myocardial content of GLUT4 glucose transporters was visualised by Takeuchi et al in 1998 by the following protocol.

Hearts perfused under control conditions and perfused with insulin and previously stored in liquid nitrogen were homogenised on ice in TES buffer (see addendum). The homogenate was centrifuged to remove particulate debris (1000 x g at 4°C for 10minutes).

The supernatant (crude extract) was further fractionated by ultracentrifugation for 90minutes at 40 000 x g at 4°C (Beckman, Ti50). The supernatant was considered to represent the cytosolic fraction, (no p-nitrophenylphosphatase activity was detectable, indicating that this fraction was devoid of sarcolemmal membrane elements). The pellet was suspended in the aforementioned buffer minus sucrose and containing 1% (vol/vol) Triton X-100 and left on ice for approximately half an hour.

Afterwards the suspension was ultracentrifuged at 40 000 x g for 1 hour at 4°C (Beckman, rotor:Ti50), and the supernatant used as the membrane fraction.

In each instance the cytosolic and membrane fraction protein concentration was determined using the Bradford method. The samples were diluted in 3X Laemmli sample buffer, boiled for 5 minutes and stored at -20°C. GLUT4 content and distribution were determined by Western Blotting.

3.10 Measurement of sarcolemmal ouabain-sensitive paranitrophenyl phosphatase activity

Sarcolemmal membranes and cytoplasmic compartments were isolated as described above. K^+-dependent p-nitrophenylphosphatase (K^+-pNPPase) was used as a marker enzyme for the sarcolemmal membrane.

The hydrolysis of p-nitrophenylphosphate (pNPP) by the Na^+K^+ATPase enzyme (K^+-stimulated-p-nitrophenyl phosphatase) i.e. Na^+K^+ATPase activity was measured in the appropriate reaction medium (see addendum). A duplicate assay was also run with 10mM ouabain present so that the K^+-stimulated and ouabain-inhibited portion of the phosphatase activity could be measured.

The tubes with 0.1ml of homogenate or membrane fraction were pre-incubated in a shaking waterbath at 25°C for 5 minutes before reaction medium (0.8ml) was added with 15 second intervals followed by 0.1ml p-NPP to start the reaction. All

enzyme incubations were carried out at 25°C. The reaction was quenched after 15 minutes by the addition of 1.5 ml 12% TCA.

The vials were then centrifuged at 12000 rpm at 4°C for 10 minutes. To the supernatant, an equal volume of 0.5N NaOH was added, and the p-NP (p-nitrophenol) produced was measured spectrophotometrically at 410 nm against a 0.5N NaOH blank.

Optical densities (ODs) obtained in the presence of ouabain were subtracted from values obtained in its absence. A standard of p-nitrophenol was used to calculate the activity of the enzyme which is expressed as nmol nitrophenol formed per minute per mg protein (Bers, D.M. 1979)

3.10.1 Choice of an optimal membrane isolation method

3.10.1.1 Protocol by Weber *et al*, 1988

Weber *et al* (1988) published a protocol for fractionation of rat adipocyte membranes to track GLUT4 trafficking.

In the resulting membrane pellet no ouabain sensitive p-nitrophenylphosphatase activity was detectable, indicating that this fraction was void of plasma membrane. Therefore this method was found to not be optimal for the isolation of a pure sarcolemmal membrane compartment.

3.10.1.2 Protocol modified from technique by Philipson *et al*, 1980

Philipson et al developed a membrane fractionation protocol in 1980 to prepare purified sarcolemmal membranes from cardiac tissue.

In the resulting membrane pellet no ouabain sensitive p-nitrophenylphosphatase activity was detectable, indicating that this fraction was void of plasma membrane. Therefore this method was found to not be optimal for the isolation of a pure sarcolemmal membrane compartment.

3.10.1.3. Protocol by Takeuchi *et al*, 1998

Myocardial content of GLUT4 glucose transporters was visualised by Takeuchi *et al* in 1998 by the protocol described in Chapter 3.9.3.

The resulting membrane pellet was enriched with the plasma membrane marker enzyme ouabain-sensitive p-nitrophenylphosphatase (see Chapter 3.10). Western blot analysis for GLUT4 was done on basal and insulin-stimulated membrane compartments. GLUT4 could be seen in the membrane fraction, as well as its increased translocation in the insulin-stimulated fraction compared to basal (See Figure 3.4). Therefore this method was found to be the optimal method for myocardial sarcolemmal membrane GLUT4 analysis.

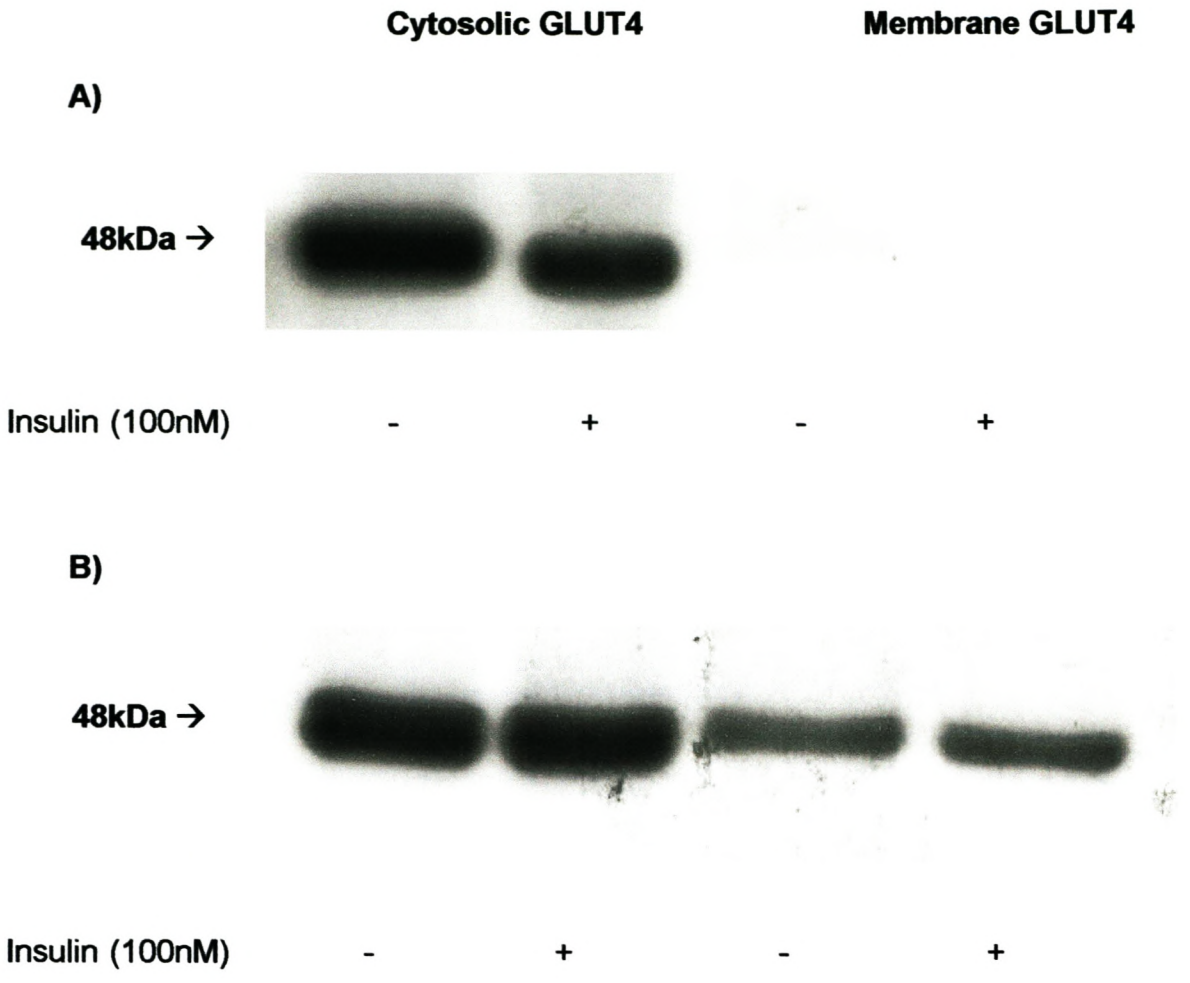

Figure 3.4 Western blot showing membrane compartment GLUT4, comparison between A) Protocol by Philipson *et al*, 1980 and B) Protocol by Takeuchi *et al*, 1998.

3.11 Bradford Protein Determination

The method of Bradford (Bradford, 1976) was used to determine the protein content of fractions known to have low concentration of protein.

For reagents see addendum.

Standard Curve

Protein standards (bovine serum albumin, BSA in dH_2O) containing 1 to 20 µg protein in a volume up to 0.1 ml was pipetted into 12 x 100 mm test tubes. The volume in the test tube was adjusted to 0.1 ml with Millipore H_2O. 0.9 millilitres of Bradford reagent (see addendum) was added to the test tube and the contents mixed either by inversion or by vortexing. The absorbance at 595 nm was measured after 15 minutes and before 30 minutes in 1ml cuvettes against a blank prepared from 0.1ml of Millipore H_2O and 0.9 ml of Bradford reagent. The standard curve obtained in this manner was used to determine the protein content of the unknown samples.

Protein assay

The membrane preparation was diluted 1 to 10 with dH_2O in order to dilute all detergents present (e.g. Triton-X) that may interfere with the assay. A suitable aliquot of this dilution (e.g. 5 µl) was adjusted to 0.1ml with dH_2O before the addition of 0.9ml Bradford reagent. The absorbance was measured in duplicate at 595 nM not less than 15 minutes but not more than 30 minutes after the addition

of the Bradford reagent. The amount of the protein was determined using the standard curve as described above.

The standard curve generated with Bradford reagent saturates at 20 µg of protein/ sample. Samples were therefore always diluted to fall on the linear portion of the curve.

3.12 Lowry Protein Determination

For reagents, see addendum.

1ml of 10% TCA was added to 100 µl of homogenate in a glass tube and left on ice for at least 30 minutes to precipitate all protein. The sample was then centrifuged at 2000 rpm for 10 minutes at 4°C and the supernatant carefully decanted and discarded. The sides of the tubes were carefully blotted dry. The precipitate was then dissolved in 1N NaOH in a water bath at 70°C. The solution was diluted 1:1 with dH2O, rendering a 0.5N NaOH solution.

The assay was done in triplicate on 50 µl of sample or standard (3 different BSA solutions of known concentration dissolved in 0.5N NaOH) or 0.5N NaOH (blank), in Lucham tubes.

1 ml of Work solution 2 was added to the 50 µl of sample or standard or blank, mixed well and allowed to stand for 10 minutes at room temperature. 0.1 ml of work solution 1 was added and very rapidly vortexed. After at least 30 minutes, the colour development was read in a spectrophotometer at 750 nm against the

blank. The unknown protein concentrations were plotted from the standard curve (Lowry et al, 1951).

3.13 STATISTICAL ANALYSES

In all instances, significance of observed effects was determined using Microsoft GraphPad Prism. The one way analysis of variance (ANOVA) with Bonferroni corrections for multiple comparisons or the paired Students t-test were used for comparisons between 2 groups. All values are expressed as mean ± standard error of the mean (SEM). A p-value smaller than 0.05 was considered significant.

ADDENDUM CHAPTER 3

Isolation of Cardiomyocytes:

Medium A: 6mM KCl,
1mM Na_2HPO_4,
0.2mM NaH_2PO_4,
1.4mM $MgSO_4$,
128mM NaCl,
10mM NaHEPES,
5.5mM D-glucose,
2mM pyruvate.

Medium B: medium A containing 0.7% fatty acid-free BSA,
1.1mg collagenase per ml
and 15mM BDM.

Medium C: medium A containing 400μM $CaCl_2$,
1%BSA,
and 1% fatty acid-free BSA.

Medium D: medium A containing 1.25mM $CaCl_2$
and 2% albumin, fatty acid-free, but no BDM.

Medium E: medium A without glucose, pyruvate or BDM
but with 2% albumin, fatty acid-free and 1.25 mM $CaCl_2$

Cell Viability

Hypotonic Medium D: medium D diluted 1:1 with deionised water, containing 5mM KCN.

Counting Medium: hypotonic medium D,

5mM KCN,

0.5% glutaraldehyde

and 1% trypan blue.

Detection of Glucose Uptake

Assay medium E: 6mM KCL,

1mM Na_2HPO_4,

1.4mM $MgSO_4$,

128mM NaCl,

10mM HEPES,

1mM $CaCl_2$,

2% BSA, fatty acid free.

PKB/Akt Lysis Buffer

20mM Tris-HCL (pH7.4),

1mM EGTA,

25mM NaCl,

1mM Na_3VO_2,

10mM NaF,

1% (vol/vol) Triton X-100,

leupeptin (10ug/ml),

aprotonin (10ug/ml),

1mM benzamidine

1mM phenylmethyl-sulphonyl fluoride (PMSF). (added immediately before use).

GLUT4 Lysis Buffers

Protocol by Weber et al (1988):

Buffer A : 20mM Tris,
1mM EDTA,
250mM sucrose; pH 7.4

Sucrose Cushion buffer: 38% (wt/vol) sucrose,
20mM Tris,
1mM EDTA; pH 7.4

Protocol by Phillipson et al (1980):

Buffer B: 20mM Tris,
1mM EDTA,
250mM sucrose; pH 7.4

Na-PPi-KCl solution : 0.25M sodium pyrophosphate (NaPPi)
3M KCl

Buffer C: Buffer B minus sucrose and
containing 1% (vol/vol) Triton X-100

Protocol by Takeuchi et al (1998):

TES buffer: Tris-HCl 20mM (pH 7.5),

sucrose 330mM,

EDTA 2mM,

EGTA 0.5mM,

PMSF 1mM and

25μg/ml leupeptin.

Laemmli Sample Buffer

3 x stock: 0.5M Tris (3.03g/50ml)

0.4% SDS (2ml of 10% /50ml)

pH 6.6 with HCl

take 33.3ml of this + 8.8g SDS

+20g glycerol

+ 0.01g bromo phenol blue

Make to 75ml with ddH_2O

850μl of the above + 150μl mercaptoethanol = sample buffer

Dilute sample 1 in 3 with sample buffer, boil for 5 minutes before freezing.

Perfusion Buffer

Krebs-Henseleit bicarbonate buffer: 119mM NaCl,

25mM $NaHCO_3$,

4.75mM KCl,

1.185mM KH_2PO_4,

0.6mM $MgSO_4$

0.6mM $NaSO_4$

1.25mM $CaCl_2.2H_2O$

5mM glucose

Perfusion buffer gassed with 95% O_2 / 5% CO_2

SDS-polyacrylamide gel

4% Stacking Gel: 3.05ml Millipore H_2O;

1.25ml 0.5M Tris-HCl pH 6.8;

50µl 10% SDS;

500µl Acrylamide;

50µl APS (0.1g/ml);

10µl TEMED.

12% Separating Gel: 3.35ml Millipore H_2O;

2.5ml 1.5M Tris-HCl, pH 8.8;

100µl 10% SDS,

3ml Acrylamide;

50µl APS (0.1g/ml) and

20µl TEMED.

10% Separating Gel: 4.9ml Millipore H_2O;

2.5ml 1.5M Tris-HCl, pH 8.8;

100µl 10% SDS,

2.5ml Acrylamide;

50µl APS (0.1g/ml) and

20µl TEMED.

Ouabain-sensitive pNPPase activity assay

Reaction medium, ouabain free: 50mM imidasole (pH 7.5, HCl),

5mM $MgCl_2$,

5mM EGTA,

10mM KCl

Reaction medium, containing ouabain: 50mM imidasole (pH 7.5, HCl),

5mM $MgCl_2$,

5mM EGTA,

10mM KCl

1mM ouabain

Nitrophenol Standard: 50 µM

Bradford Reagents

Coomassie Brilliant Blue G-250 (100mg) was dissolved in 50ml 95% ethanol. To this solution 100ml 85% (w/v) phosphoric acid was added. The resulting solution was diluted to a final volume of 1 litre. Final concentrations in the reagent were 0.01% (w/v) Coomassie Brilliant Blue G-250, 4.7% (w/v) ethanol, and 8.5% (w/v) phosphoric acid.

Lowry Reagents

Stock Solutions:

Reagent A: 10% cold TCA

Reagent B: 2% Na-K-Tartrate in dH_2O.

Reagent C: 1% $CuSO_4.5H_2O$ in dH_2O

Reagent D: 2% Na_2CO_3 in dH_2O

Reagent E: Folin-Ciocalteu's phenol reagent

Albumin stock standard

500mg albumin / 10ml H_2O, dissolve; dilute 50µl with 5ml H_2O

read at 280nm against H_2O to determine concentration

Molar extinction coefficient: 1.51

Work Solutions

Work solution 1: Mix 0.5ml Reagent B and 0.5ml Reagent C with 49ml Reagent D.

Work solution 2. Dilute Folin 1 in 3.

Standard: dilute albumin stock standard 1 in 200 with 0.5N NaOH.

CHAPTER 4

RESULTS

4.1 AMPK activation

To determine whether the 2 pharmacological substances, AICAR and ZMP, could exert physiological effects via activation of AMPK, the ability of these compounds to elicit phosphorylation of the kinase was determined. This was accomplished by measuring AMPK activation in terms of its phosphorylation on Thr 172 via Western Blotting and a specific antibody (Cell Signaling) as described in Materials and Methods (Chapter 3). In cardiomyocytes treated with AICAR (1 mM for 30 minutes) and ZMP (1 mM for 30 minutes) it was found that both substances resulted in phosphorylation of AMPK, increasing levels significantly above basal (see Figure 4.1). A heart subjected to ischaemia was included as a positive control.

4.2 AICAR concentration curve

To evaluate which concentration of AICAR was optimal, a concentration curve of glucose uptake was established in cardiomyocytes using 50 μM, 100 μM, 500 μM, 1 mM, 2 mM, 5 mM and 10 mM of AICAR. Glucose uptake was also measured as 2DG uptake in the presence of these AICAR concentrations and 100 nM Insulin. AICAR attenuated glucose uptake at all concentrations. AICAR was also seen to attenuate insulin stimulated glucose uptake in dose dependent manner. At 1 mM AICAR a significant attenuation of both basal and insulin mediated glucose uptake

was noticed. This, and the fact that this concentration was used in the other literature (Russell et al, 1999), led us to use 1 mM AICAR in the following experiments (see Fig 4.2).

4.3 AICAR and ZMP Time Curves

In order to select an optimal time for stimulation with the pharmaceutical agents in these experiments, a time curve was done. Cardiomyocytes were stimulated with AICAR (1 mM as previously established) for 15 minutes, 30 minutes and 60 minutes (see figure 4.3) and with ZMP (1 mM) for 15 minutes, 30 minutes and 60 minutes (see Fig 4.4). Glucose uptake was then assessed by measurement of 2DG uptake. AICAR and ZMP stimulation for 30 minutes gave reproducible and reliable results while stimulation for the longer time periods nearly abolished all glucose uptake and therefore 30 minutes was chosen as the time of stimulation for following experiments.

4.4 GLUCOSE UPTAKE

4.4.1 AICAR effect on glucose uptake

The mean response of cardiomyocytes to 1 mM AICAR over a 30 minute period with regards to glucose uptake was determined. This was done in the presence or absence of insulin (100 nM, 15 minutes). While stimulation with insulin (100 nM) increased glucose uptake significantly in isolated cardiomyocytes from basal (1 standardised unit ± 0) to 4.5 ±0.6 fold ($p<0.05$), AICAR (1 mM) was seen to elicit a glucose uptake of 0.7 ±0.1 which was significantly lower ($p<0.05$) than basal levels of glucose uptake. In the presence of AICAR, insulin-stimulated glucose uptake was significantly attenuated (2.6±0.48 vs 4.5±0.6 fold $p<0.05$)) (see Fig 4.5).

4.4.2 ZMP effect on glucose uptake

Javaux *et al* (1995) reported that rabbit cardiomyocytes were unable to phosphorylate AICAR to ZMP. Because of the observed inability of AICAR to elicit glucose uptake in rat cardiomyocytes we tested the ability of ZMP to affect glucose uptake. This was again done in the presence or absence of insulin (100 nM, 15 minutes). As above, insulin was seen to significantly stimulate glucose uptake from basal levels (1 ±0 to 7.3 ±0.8 fold, $p<0.05$). ZMP significantly lowered basal glucose uptake levels to 0.8 ±0.2 and was able to significantly attenuate insulin stimulated glucose uptake to 4.1 ±0.7($p<0.05$) when the ZMP (1 mM) was administered 15 minutes before the insulin (see Fig 4.6).

However, this attenuation of insulin stimulated glucose uptake was abolished when the insulin was administered only 5 minutes before the ZMP instead of 15 minutes after ZMP (see Figure 4.7). Insulin was then present throughout the experiment.

4.5 PKB/Akt PHOSPHORYLATION

Ponceau-S reversible staining was routinely used to determine equal protein loading and transfer during Western blotting. Figure 4.8 is an example of such a stain.

4.5.1 AICAR effect on PKB/Akt phosphorylation

Since there was a noticeable attenuation in insulin stimulated glucose uptake by AICAR, and since basal glucose uptake was suppressed by the drug, PKB/Akt phosphorylation patterns were measured by Western blotting to determine whether this pathway of glucose uptake was affected or not. Cardiomyocytes were again incubated with AICAR (1 mM, 30 minutes) in the presence or absence of insulin (100 nM, 15 minutes). The cells were then lysed, total protein isolated and subjected to Western blotting to determine phosphorylation on the Ser473 by use of a specific antibody (Cell Signaling) as described in Materials and Methods (Chapter 3).

Both 100 nM insulin alone (4.2 $\pm$ 0.5 arbitrary densitometry units) and 100 nM insulin plus 1 mM AICAR (4.0 $\pm$ 0.5 arbitrary densitometry units) stimulated

PKB/Akt phosphorylation to a similar extent above basal levels (1 ± 0.0 standardised arbitrary densitometry unit; $p<0.01$; $n=12$). The presence of AICAR therefore did not attenuate insulin stimulated PKB phosphorylation. AICAR 1 mM (0.8 ± 0.2) however, was unable to affect PKB/Akt phosphorylation beyond basal levels (See Fig 4.9 & 4.10).

4.5.2 ZMP effect on PKB/Akt phosphorylation

Cardiomyocytes were again incubated with ZMP (1 mM, 30 minutes) in the presence or absence of insulin (100 nM, 15 minutes). The cells were then lysed and subjected to Western blotting done to determine phosphorylation on the Ser473 by use of a specific antibody (Cell Signaling) as described in Materials and Methods (Chapter 3).

Insulin 100 nM significantly increased PKB/Akt phosphorylation (3.3 ± 0.4 arbitrary densitometry units, $p<0.05$) above basal levels. ZMP (1 mM) was not seen to have an effect on PKB/Akt phosphorylation. Similar to AICAR, ZMP (1 mM) did not attenuate the level of PKB/Akt phosphorylation elicited by 100 nM insulin. The combination of ZMP and insulin showed a tendency towards an accumulative effect. However this was not statistically significant (4.9 ± 1.3 arbitrary densitometry units). The attenuation of the effect of insulin by ZMP seen in the glucose uptake, was therefore not evident in the PKB/Akt phosphorylation pattern (see figure 4.11) observed under identical conditions.

4.6 Effect of Wortmannin on Glucose Uptake

It is known that inhibition of PI3-K with wortmannin inhibits insulin-stimulated glucose uptake by cardiomyocytes (Lefebvre *et al*, 1996). It is also stated that wortmannin does not inhibit AMPK mediated glucose uptake (Hayashi *et al*, 1998). We assessed in our cardiomyocyte system, the effects of wortmannin on insulin, AICAR and ZMP mediated effects. Cells were incubated with AICAR (1 mM, 30 minutes), insulin (100 nM, 15 minutes) and wortmannin (100 nM, 15 minutes before addition of either insulin, AICAR or ZMP) in the combinations set out in Chapter 3.

100 nM wortmannin abolished glucose uptake stimulated by insulin (Figure 4.13 and 4.14) having no effect on the response of AICAR and ZMP. In the presence of AICAR, wortmannin abolished insulin mediated glucose uptake while in the presence of ZMP, it was observed that glucose uptake was not completely suppressed.

4.7 Effect of Wortmannin on PKB/Akt phosphorylation

In view of the known link between activation of PKB/Akt by insulin and insulin-stimulated glucose uptake, we determined the effect of wortmannin on PKB/Akt phosphorylation after stimulation with insulin in the presence or absence of AICAR and ZMP.

4.7.1 Wortmannin and AICAR effect on PKB/Akt phosphorylation

The effect of wortmannin and AICAR on the phosphorylation of PKB/Akt was determined using Western blotting techniques and a specific Ser473 antibody (Cell Signaling Technology) as described in Chapter 3. Cells were incubated with AICAR (1 mM, 30 minutes), insulin (100 nM, 15 minutes) and wortmannin (100 nM, 15 minutes before addition of either insulin, AICAR or ZMP) in the combinations set out in Chapter 3.

As was expected, wortmannin inhibited insulin stimulated PKB/Akt phosphorylation from 4.2 ±0.5 arbitrary densitometry units to 1.3±0.1 ($p<0.05$) as well as PKB/Akt phosphorylation seen with insulin in combination with AICAR (4.0±0.5 arbitrary densitometry units to 1.9±0.3, $p<0.05$). It had no effect on either basal (1.0±0 to 1.0±0) or AICAR stimulated PKB/Akt phosphorylation (0.8±0.2 arbitrary densitometry units to 1.0±0.2) (See Fig 4.15 and Fig 4.16).

3.7.2 Wortmannin and ZMP effect on PKB/Akt phosphorylation

The effect of wortmannin and ZMP on the phosphorylation of PKB/Akt was determined using Western Blotting techniques and a specific Ser473 antibody (Cell Signaling Technology) as described in Chapter 3. Cells were incubated with ZMP (1 mM, 30 minutes), insulin (100 nM, 15 minutes) and wortmannin (100 nM, 15 minutes before the addition of either insulin, AICAR or ZMP) in the combinations set out in Chapter 3.

As was expected, wortmannin inhibited insulin stimulated PKB/Akt phosphorylation from 3.3 ±0.4 arbitrary densitometry units to 0.72 ± 0.02 arbitrary densitometry units ($p<0.05$), while having no effect on basal phosphorylation of PKB/Akt (1.0±0.01 to 0.9±0.06). The PKB/Akt phosphorylation elicited by the combination of insulin and ZMP (4.9±1.3 arbitrary densitometry units) was decreased by the addition of wortmannin (2.7±0.8 arbitrary densitometry units)($p<0.05$). However the addition of wortmannin to ZMP significantly increased phosphorylation levels of PKB/Akt from that of ZMP alone (1.1 ± 0.05 to 1.9±0.3, $p<005$) (See Fig 4.17 and Fig 4.18).

4.8 Effect of 8CPT on AMPK phosphorylation

ZMP is the phosphorylated form of AICAR. According to current knowledge such a phosphorylated molecule should not be able to enter the cell. It was speculated that perhaps ZMP, because of its AMP analogue nature, was exerting its intracellular effects like phosphorylation of AMPK, by binding to the adenosine receptors (purinergic receptors). Similarly AICAR could bind to the receptors to elicit effects. To investigate this possibility, a blocker of these receptors, 8CPT, was used in conjunction with AICAR and ZMP. Cells were incubated with the blocker 15 minutes before stimulation with either AICAR (1 mM, 30 minutes) or ZMP (1 mM, 30 minutes). Western blot analysis was then carried out using phosphorylated AMPK Thr 172 specific antibodies (Cell Signaling Technology).

ZMP and AICAR both resulted in phosphorylation of AMPK above basal levels (ZMP: 1.5 ±0.1, AICAR: 1.8 ±0.2, $p<0.05$). 8CPT had no significant effect on ZMP

or AICAR induced phosphorylation of AMPK (See Fig 4.19 & Fig 4.20) confirming that both substances did not act through activation of the purinergic receptors to affect AMPK phosphorylation.

4.9 GLUT4 Translocation in cardiomyocytes

GLUT4 is the glucose transporter that is recruited to the cell membrane of insulin and stress stimulated cells (see Chapter 2). It translocates from the cytosol to the membrane, and is responsible for glucose uptake. Because of the observed inhibitory effects of AICAR and ZMP on insulin-stimulated glucose uptake but not on PKB/Akt phosphorylation, as well as results showing activation of AMPK by these substances but not glucose uptake, we assessed GLUT4 translocation under these conditions. GLUT4 translocation was assessed by treating the cells with various sequences of AICAR (1 mM, 30 minutes), ZMP (1 mM, 30 minutes), and insulin (100 nM, 15 minutes), fractionating the cells into cytosolic and membrane compartments, and then doing Western Blots with specific GLUT4 antibody on these two compartments (See Figs 4.21 - 4.25).

4.9.1 GLUT4 Content in the cytosolic compartment

No significant difference in cytosolic GLUT4 content could be seen between basal (1.0 ± 0.02 arbitrary densitometry units) and insulin stimulated cells (0.9 ± 0.1 arbitrary densitometry units), but the standard error in this group was quite large. There was however a significant decrease in the cytosolic GLUT4 content of

AICAR (0.9 ± 0.04) and ZMP (0.9±0.05) ($p<0.05$) stimulated cells, showing a translocation away from the cytosol (See Fig 4.21 & 4.22).

4.9.2 GLUT4 Content in the membrane compartment

A significant increase in GLUT4 translocation could be seen between basal (1.1±0.01arbitrary densitometry units) and insulin stimulated cells (1.5±0.2), as well as between basal and AICAR (1.3±0.10) and basal and ZMP treated cells (1.6±0.1). This shows that the GLUT4 translocated away from the cytosol and into the membrane in insulin, AICAR and ZMP stimulated cells (See Fig 4.23 & 4.24). However, when insulin was added in combination with either AICAR or ZMP, only the AICAR + insulin combination gave a significantly higher than basal GLUT4 translocation (1.2±0.2, $p<0.05$), whilst ZMP + insulin (1.2±0.3) was not significantly increased (see Fig 4.25).

4.10 GLUT4 translocation in whole hearts

Since a very small amount of protein is obtained from cardiomyocyte preparations, the whole heart was used to see whether similar results could be obtained. Whole hearts were perfused with either AICAR (1 mM) for 30 minutes, ZMP (1 mM) for 30 minutes, or insulin (100 nM) for 15 minutes, in both 5 mM glucose medium and in glucose free medium. The latter was included because myocytes were treated in a glucose-free medium. Lysates were then made and Western blots done on the protein for GLUT4 (See Figs 4.26 - 4.30).

4.10.1 GLUT4 content in cytosolic compartment

In the whole heart no significant GLUT4 translocation could be detected from the cytosolic fraction in either the glucose free or the 5 mM glucose perfused hearts. Basal (1±0 arbitrary densitometry units), insulin (1.1±0.1), AICAR (0.9±0.1) and AICAR + insulin (1.3±0.3) GLUT4s showed no significant differences (See Fig 4.26) when perfused with 5 mM glucose medium. Basal (1±0 arbitrary densitometry units), insulin (1.0±0.1), AICAR (1.0±0.04) and AICAR + insulin (1.0±0.06) GLUT4s showed no significant differences (See Fig 4.29) in the cytosolic fraction of hearts perfused with a glucose free medium.

4.10.2 GLUT4 content in membrane compartment

In the whole heart although a pattern can be seen in increasing GLUT4 translocation to the membrane with insulin, AICAR and ZMP, these differences were not significant due to large standard errors (See Fig 4.27, 4.28 and 4.30). Basal (1±0 arbitrary densitometry units), Insulin (1.4±0.2), AICAR (1.6±0.5) and the AICAR, insulin combination (2.0±0.8) GLUT4s showed no significant differences in 5 mM perfused hearts (see Fig 4.27). Basal (1±0 arbitrary densitometry units), insulin (1.1±0.2), AICAR (1.2±0.3) and AICAR plus insulin (1.6±0.42) GLUT4s showed no significant difference in whole hearts perfused with glucose free medium (see Fig 4.29).

4.11 p38 MAPKinase

It has been put forward (Xi et al, 2001) that MAPKinases, especially p38 MAPK, play a role in glucose uptake. Therefore glucose uptake was measured in the presence and absence of SB203580 (Calbiochem), a specific blocker of p38. Cells were stimulated with ZMP, insulin, and a combination of the two, in the presence or absence of 1 μM SB203580, and the glucose uptake measured.

1 μM SB203580, added 5 minutes before ZMP, had no effect on glucose uptake in the basal (1±0 standardised unit and 0.6±0.5), insulin (8.3±2.4 and 7.7±2.4), ZMP (1.4±0.4 and 0.6±0.4) or combination ZMP and insulin stimulated cells (3.3±1.1 and 4.7±1.8) (See Fig 4.31).

Due to time constraints only one Western blot was done on the p38 MAPK phosphorylation pattern (See Fig 4.32). When the p38 MAPK phosphorylation pattern was analysed, it was seen that the phosphorylation of p38 MAPK increased from basal (1 arbitrary densitometry unit) with insulin stimulation (1.705 arbitrary densitometry units) and further increased with ZMP activation (2.3 arbitrary densitometry units). The insulin and ZMP combination was 1.8 arbitrary densitometry units, similar to insulin-stimulated levels (see Fig 4.32).

ADDENDUM CHAPTER 4

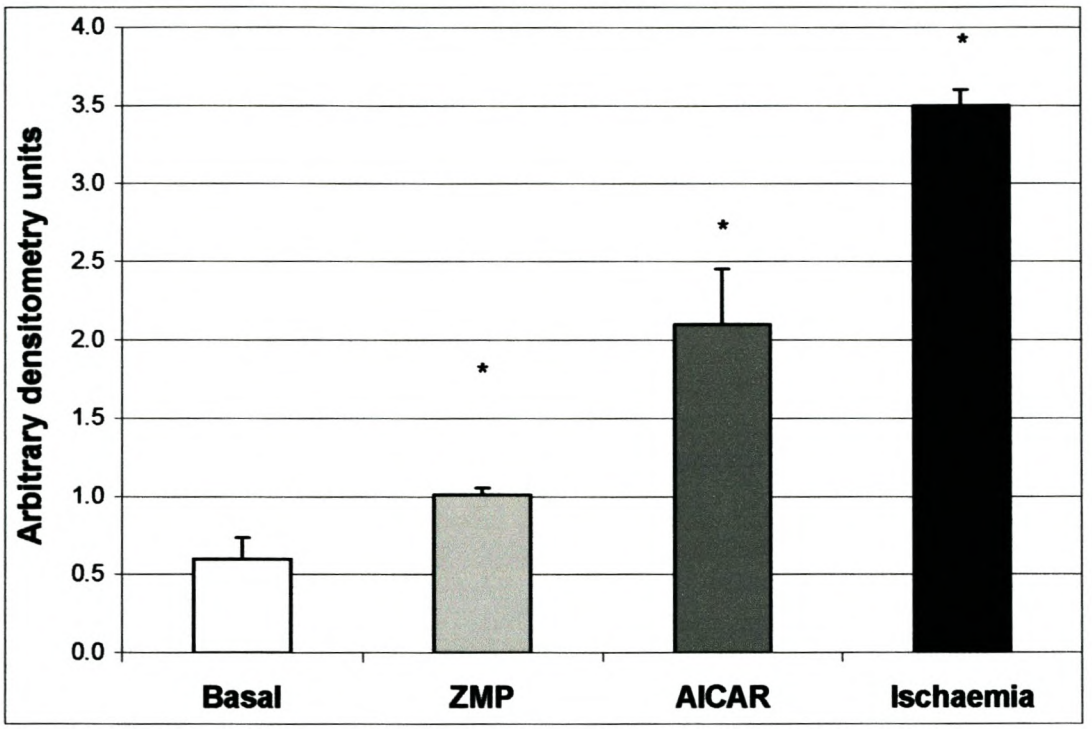

Figure 4.1: Phosphorylation of AMPK on Thr 172 in cardiomyocytes in control conditions, when activated by 30 minutes stimulation with ZMP (1mM) or AICAR (1mM) and when under stress i.e. ischaemia (positive control).

All values are expressed as mean ± SEM (n = 4),

* $p<0.05$ vs basal

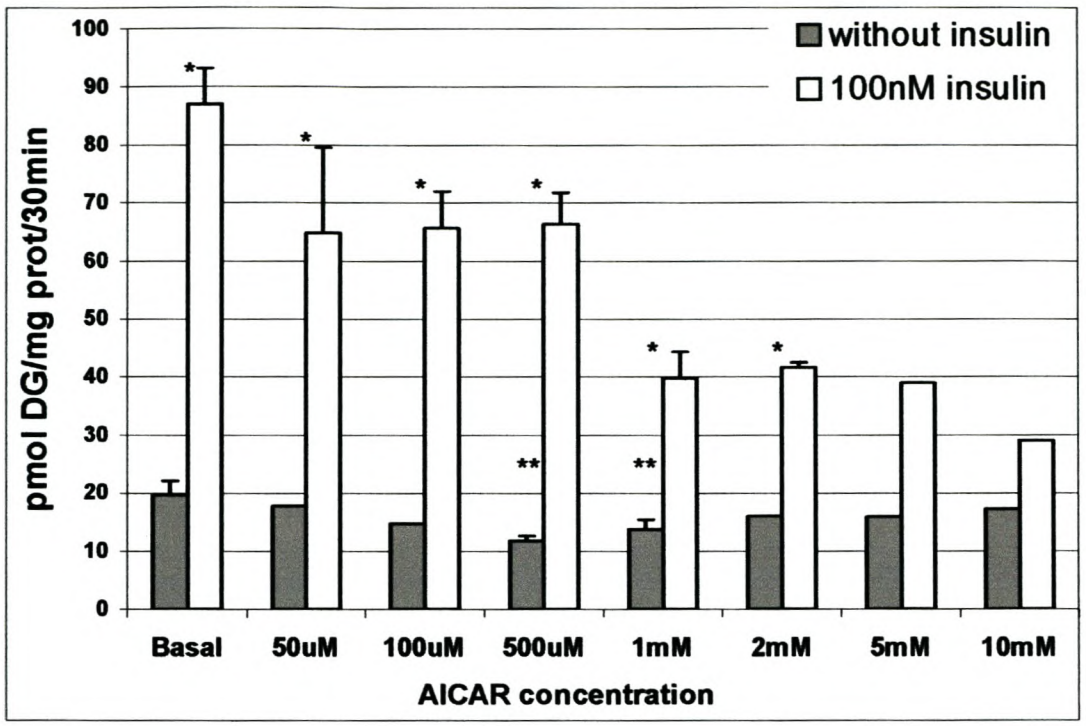

Figure 4.2 Concentration curve of the effect of AICAR (30 min stimulation) on cardiomyocyte glucose uptake with and without insulin. Insulin (100 nM) was added to cells 15 min after the addition of ZMP, total incubation time 30 min, before the addition of 2DG for a further 30 min incubation.

All values expressed as mean ± SEM (n=2-4)

* $p < 0.05$ - vs + insulin

**$p<0.05$ AICAR vs basal

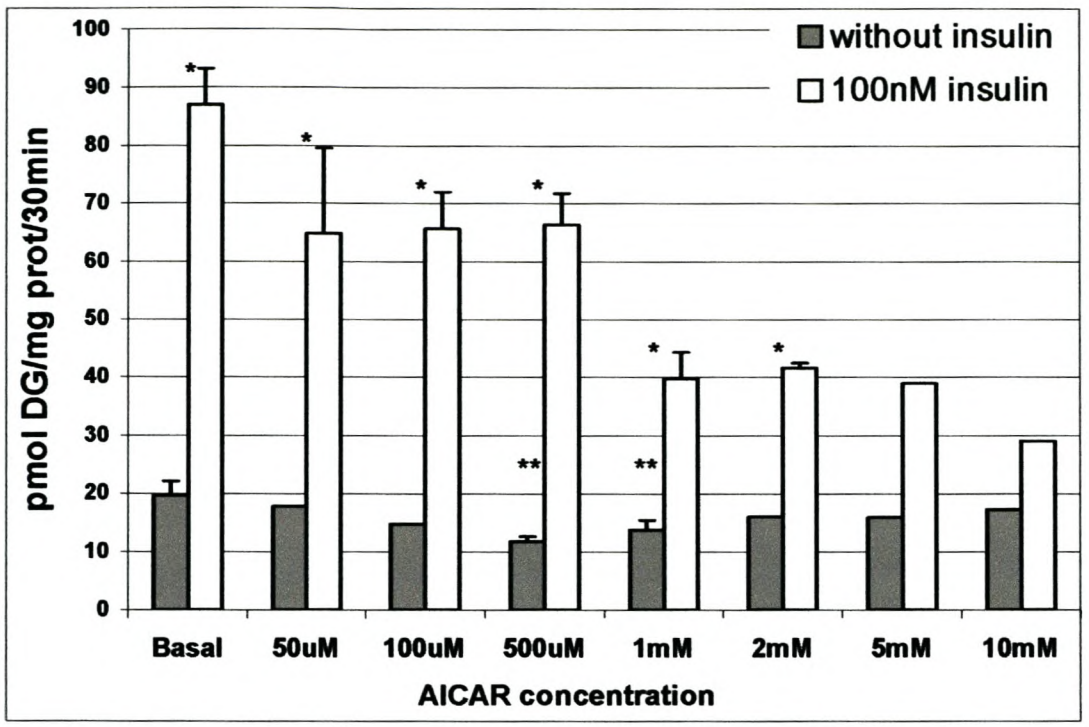

Figure 4.2 Concentration curve of the effect of AICAR (30 min stimulation) on cardiomyocyte glucose uptake with and without insulin. Insulin (100 nM) was added to cells 15 min after the addition of ZMP, total incubation time 30 min, before the addition of 2DG for a further 30 min incubation.

All values expressed as mean ± SEM (n=2-4)

* $p < 0.05$ - vs + insulin

**$p<0.05$ AICAR vs basal

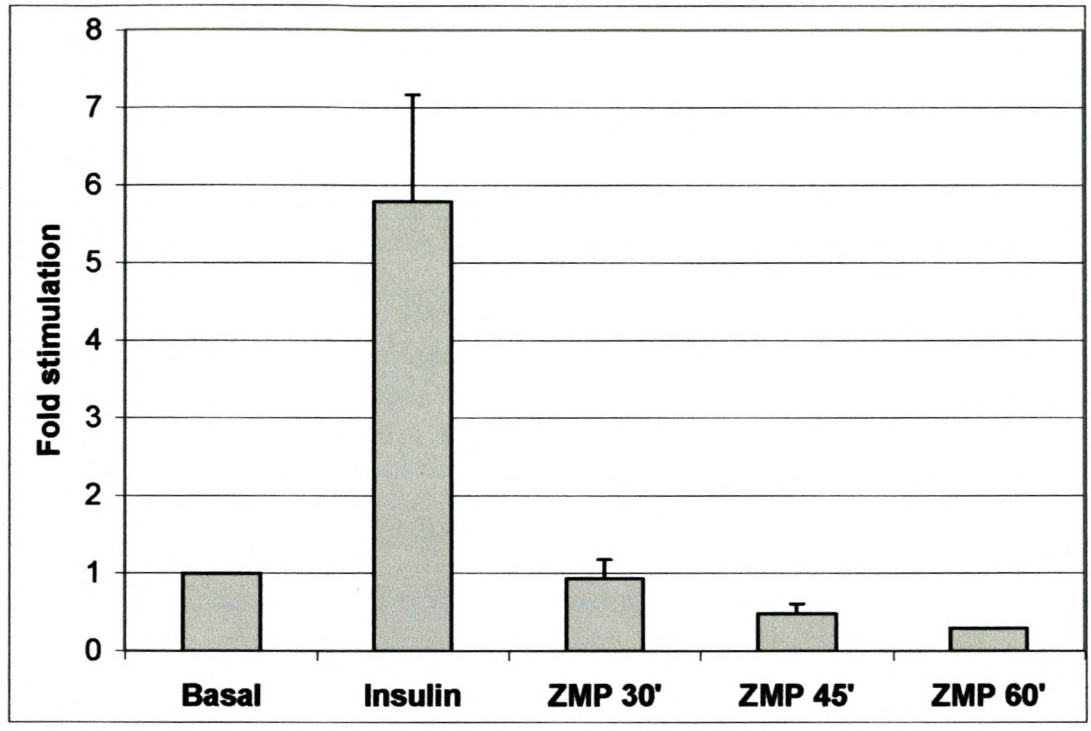

Figure 4.4: The effect of ZMP (1 mM), given for varying time periods, on cardiomyocyte glucose uptake. Insulin was given for 15 min and used as a positive control.

All values expressed as mean ± SEM (n = 1-6, assayed in duplicate)

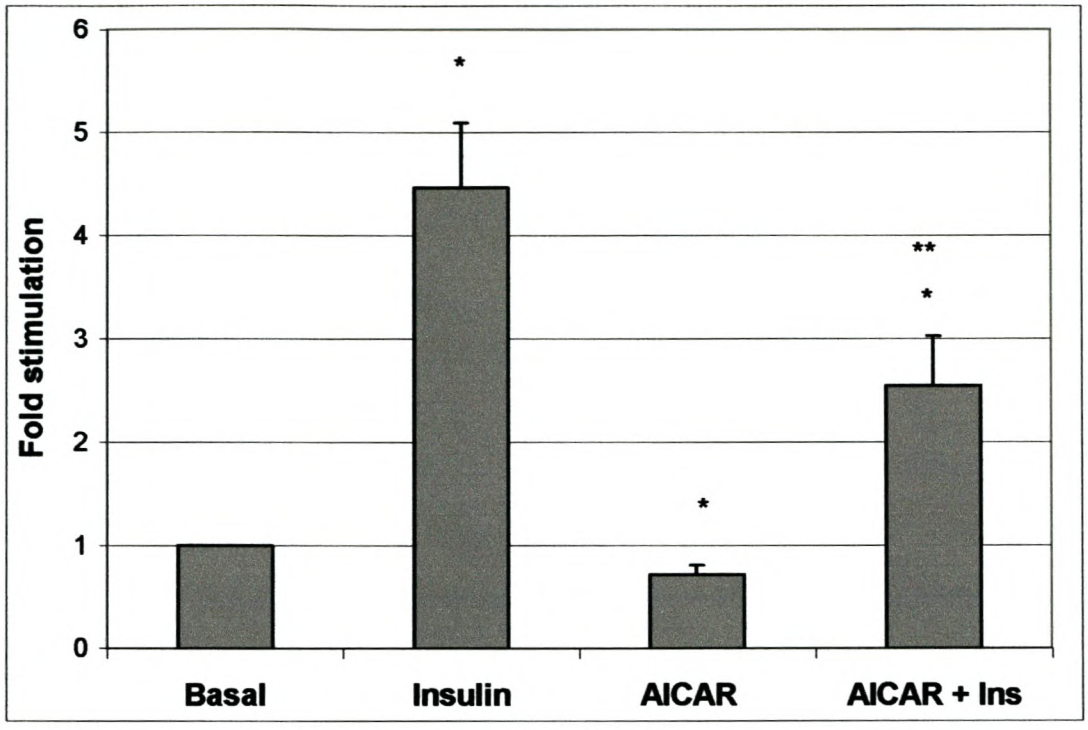

Figure 4.5: Effect of AICAR (1 mM) and insulin (100 nM) on cardiomyocyte glucose uptake when insulin was administered 15min after the addition of AICAR – total stimulation time 30 min before the addition of 2DG.

All values expressed as mean ± SEM (n=11, assayed in duplicate)

* $p<0.05$, vs basal,

** $p < 0.05$, vs insulin

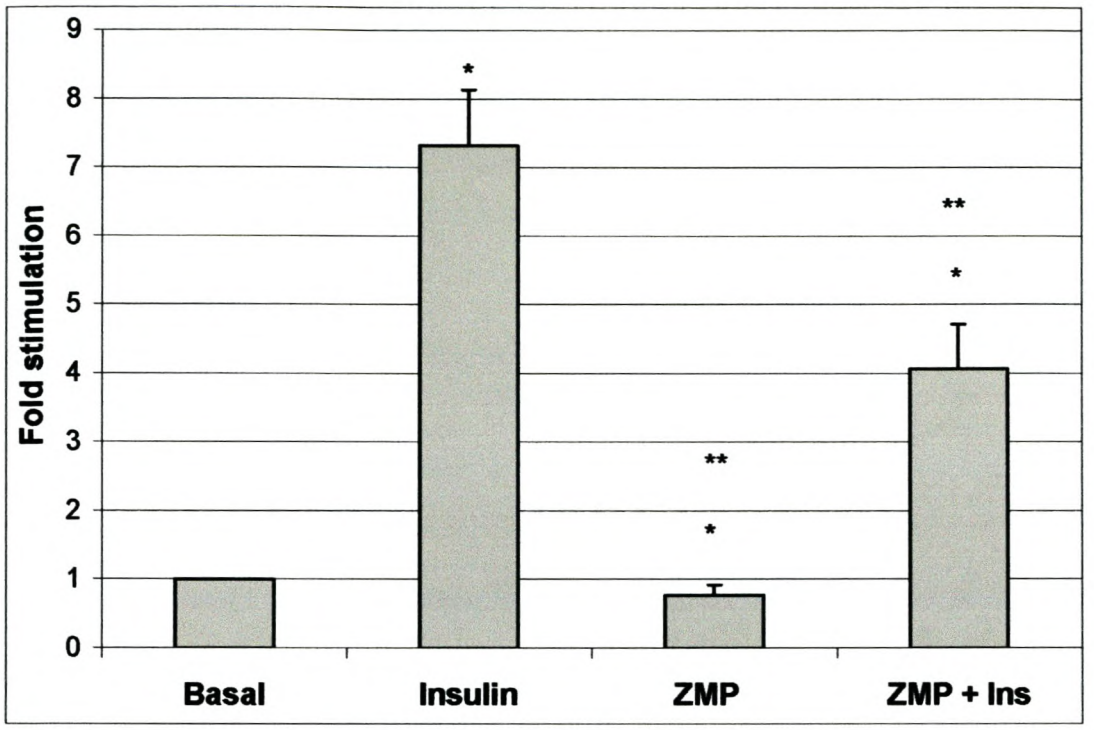

Figure 4.6: Effect of ZMP (1 mM) and insulin (100 nM) on cardiomyocyte glucose uptake, when insulin was administered 15 min after ZMP administration. Total incubation time 30 min before addition of 2DG.

All values expressed as mean ± SEM (n=8, assayed in duplicate)

* $p<0.05$ vs basal,

** $p<0.05$ vs insulin

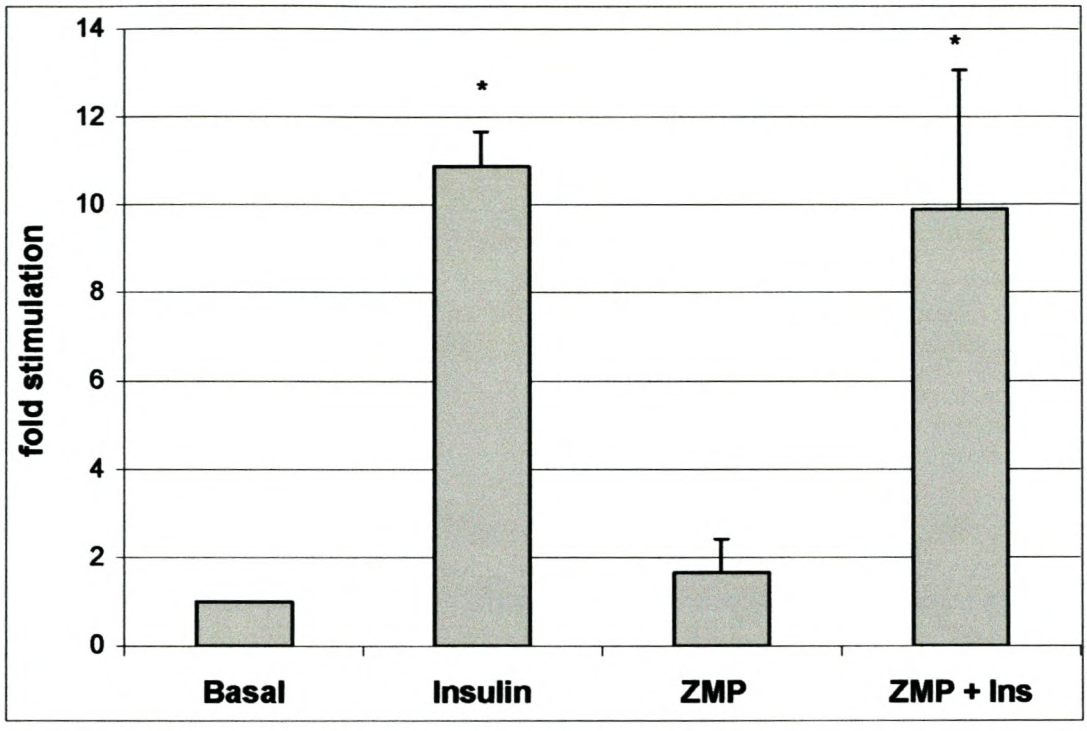

Figure 4.7: Effect of ZMP (1 mM) and insulin (100 nM) on cardiomyocyte glucose uptake when insulin was administered 5 min before ZMP administration. Total incubation time 35 min before the addition of 2DG.

All values expressed as mean ± SEM (n=7, assayed in duplicate)

* $p<0.05$ vs basal,

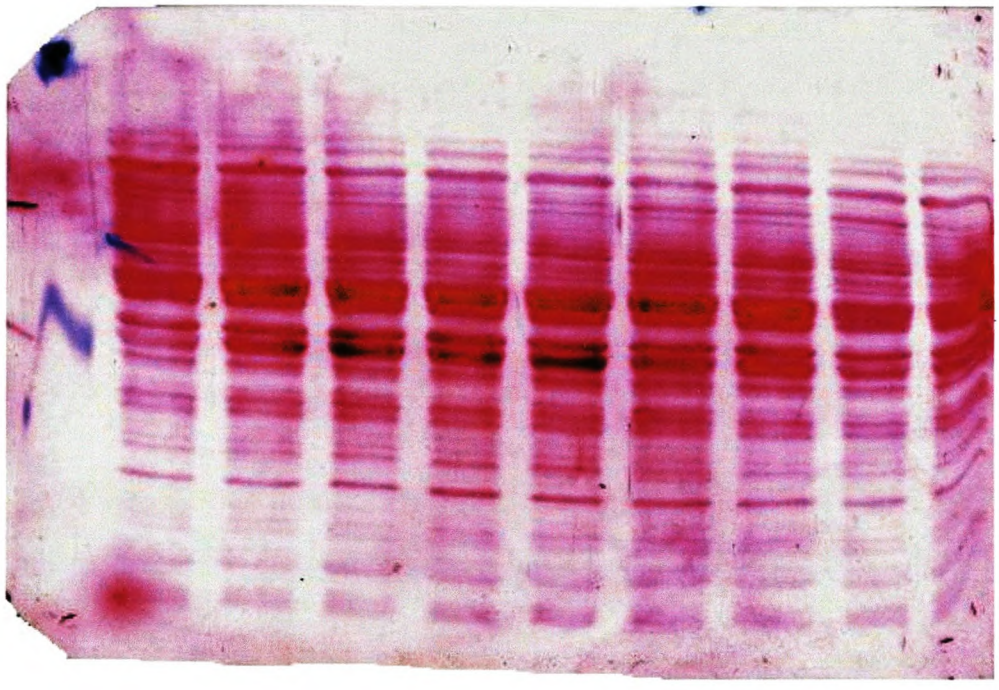

Figure 4.8: Ponceau S scan of a Western Blot to show equal concentration of bands and adequate transfer of proteins to the membrane.

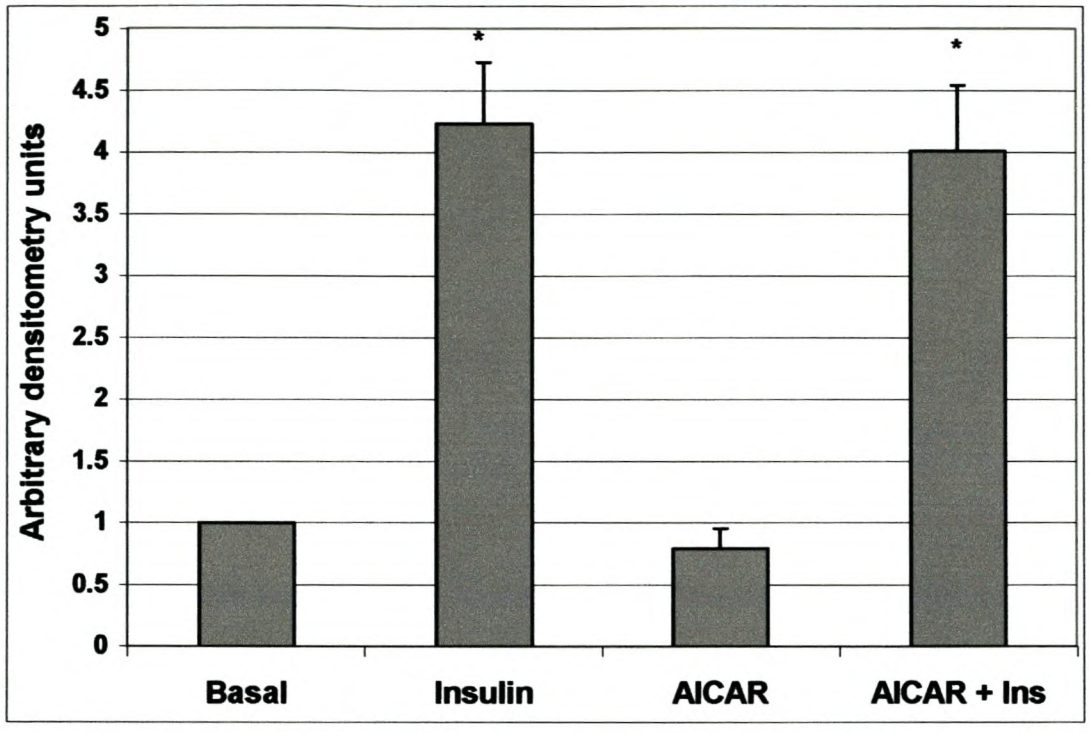

Figure 4.9: Effect of AICAR (1 mM) and insulin (100 nM) on PKB/Akt phosphorylation. Cells were stimulated with AICAR for 30 min and with insulin for 15 min.

All values expressed as mean ± SEM (n=12).

$p < 0.05$ vs basal

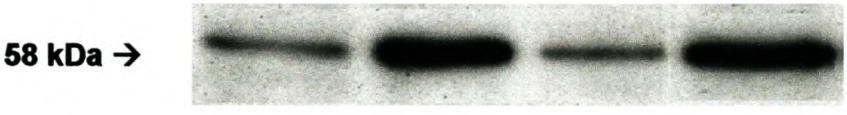

Insulin	-	+	-	+
AICAR	-	-	+	+

Figure 4.10: Western blot showing phosphorylation pattern of PKB/Akt on Ser473 phosphorylation by 1mM AICAR (30min) and 100nM insulin (15min).

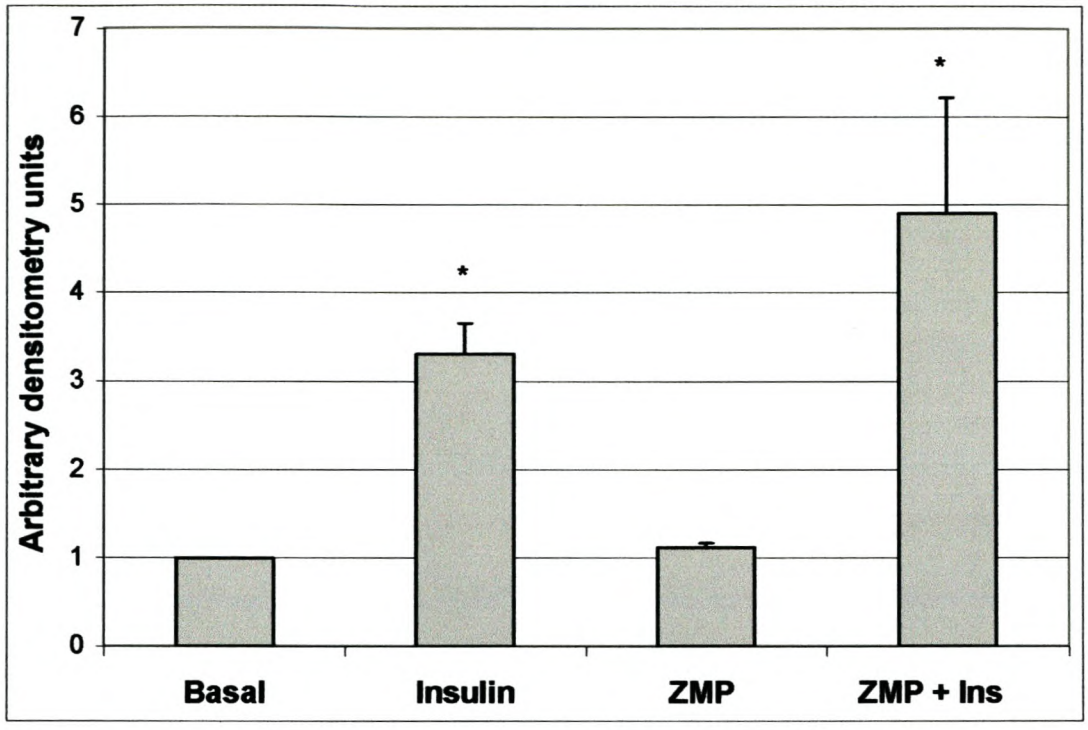

Figure 4.11: Effect of ZMP (1 mM) and insulin (100 nM) on PKB/Akt phosphorylation. Cells were stimulated with ZMP for 30 min and with insulin for 15 min.

All values expressed as mean ± SEM (n=9)

$p < 0.05$ vs basal

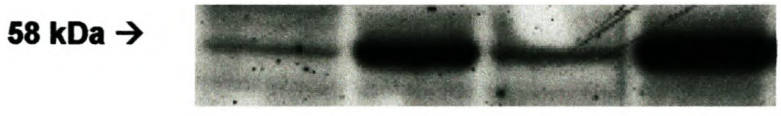

Insulin	-	+	-	+
ZMP	-	-	+	+

Figure 4.12: Western blot showing PKB/Akt phosphorylation pattern (Ser473) by 1mM ZMP (30 min) and 100nM insulin (15 min).

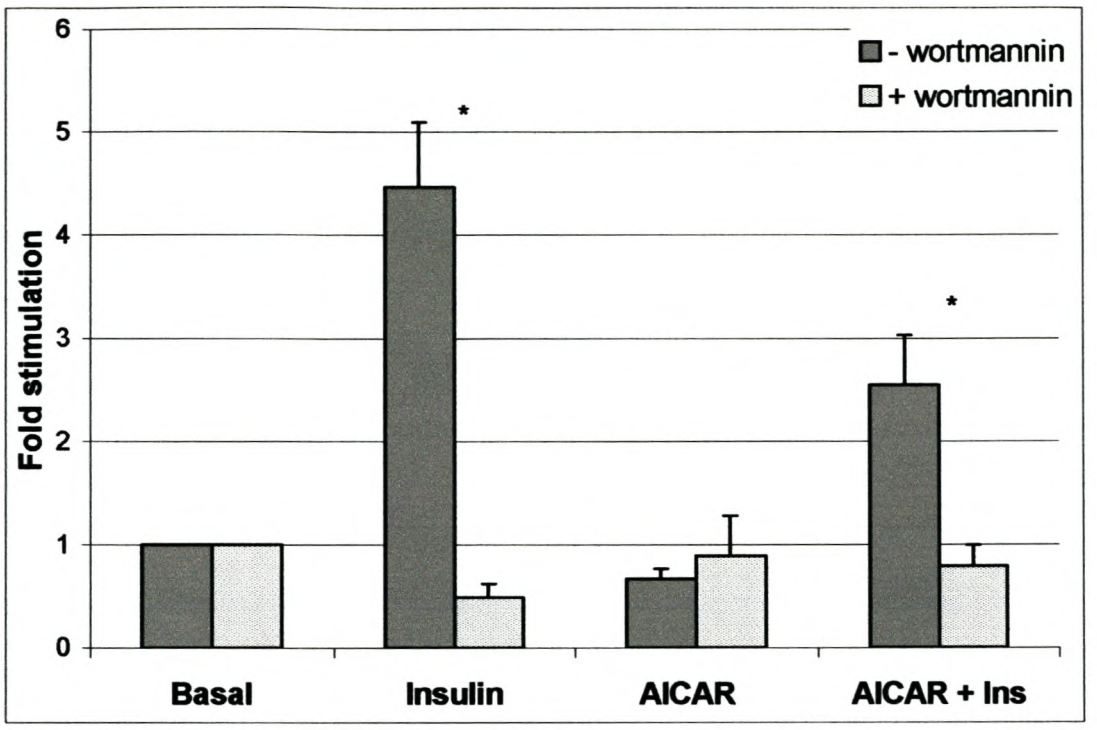

Figure 4.13: Effect of wortmannin (100nM) on glucose uptake in insulin (100 nM) and AICAR (1 mM) stimulated cardiomyocytes. Wortmannin was administered 15 min before the addition of either AICAR or insulin, and remained in the incubation medium for the duration of the experiment. Cells were stimulated with AICAR for 30 min and with insulin for 15 min.

All values expressed as mean ± SEM (n= 3-12, assayed in duplicate)

* $p < 0.05$ –wortmannin vs + wortmannin

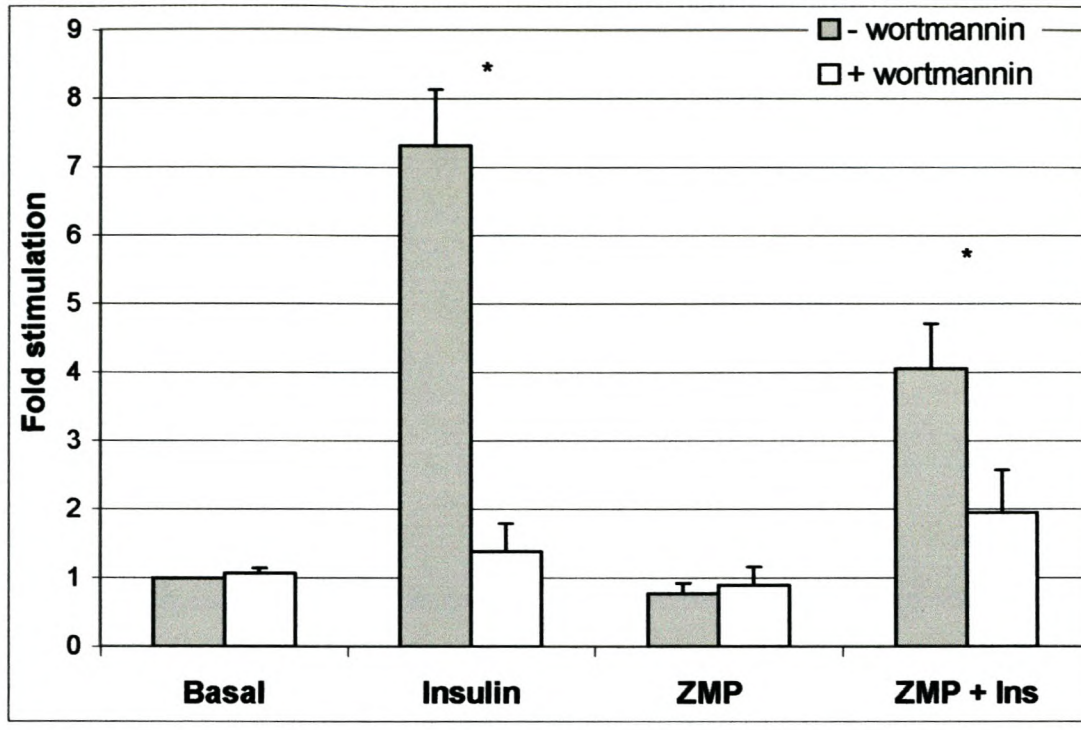

Figure 4.14: Effect of wortmannin (100 nM) on glucose uptake in insulin (100 nM) and ZMP (1 mM) stimulated cardiomyocytes. Wortmannin was administered 15 min before the addition of either ZMP or insulin, and remained in the incubation medium for the duration of the experiment. Cells were stimulated with ZMP for 30 min and with insulin for 15 min.

All values expressed as mean ± SEM (n= 3-12, assayed in duplicate)

* $p < 0.05$ –wortmannin vs + wortmannin

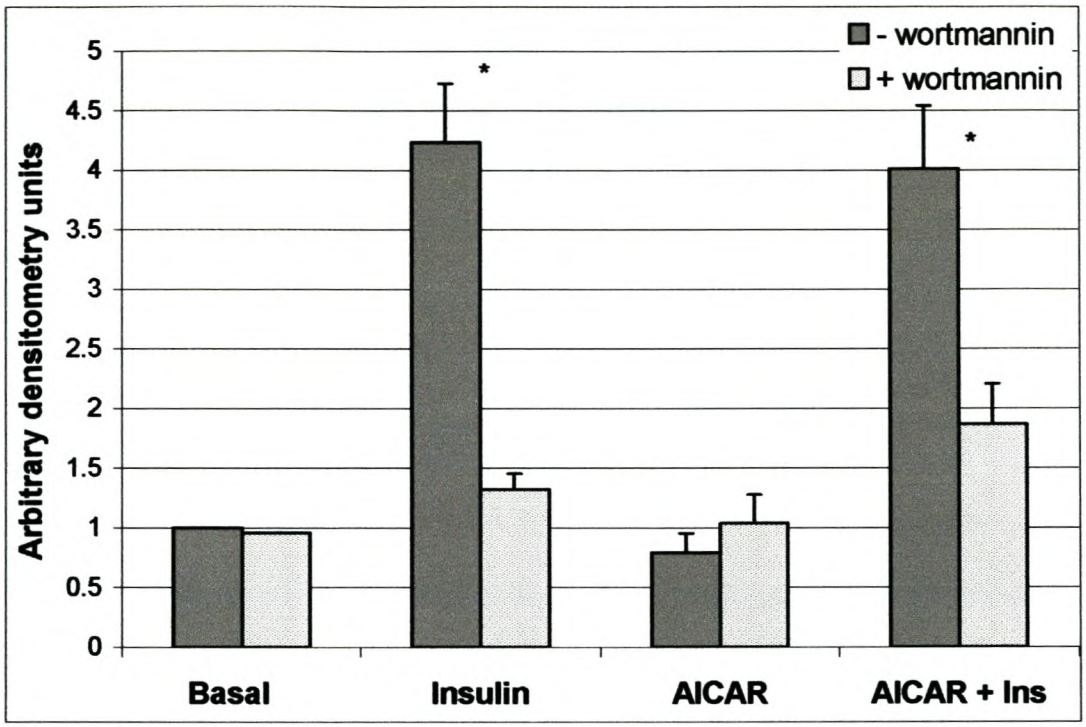

Figure 4.15: Effect of wortmannin (100 nM) on PKB/Akt phosphorylation in insulin (100 nm) and AICAR (1 mM) stimulated cardiomyocytes. Wortmannin was added 15 min before the addition of either AICAR or insulin, and remained in the medium throughout the experiment. Cells were stimulated with AICAR for 30 min and insulin for 15 min.

All values expressed as mean ± SEM (n=8-12)

* $p<0.05$ – wortmannin vs + wortmannin

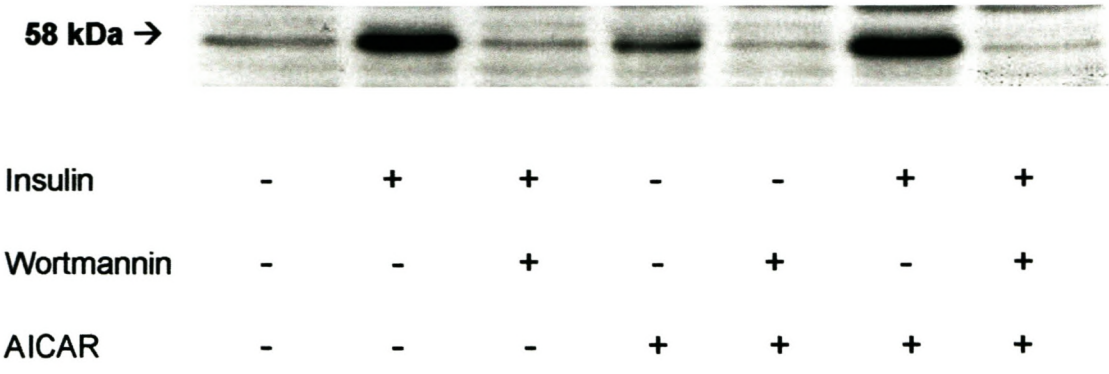

Figure 4.16: Western blot showing PKB/Akt phosphorylation pattern (Ser 473) in cells stimulated with AICAR (1 mM), insulin (100 nM) and wortmannin (100 nM) as indicated in Fig 4.15.

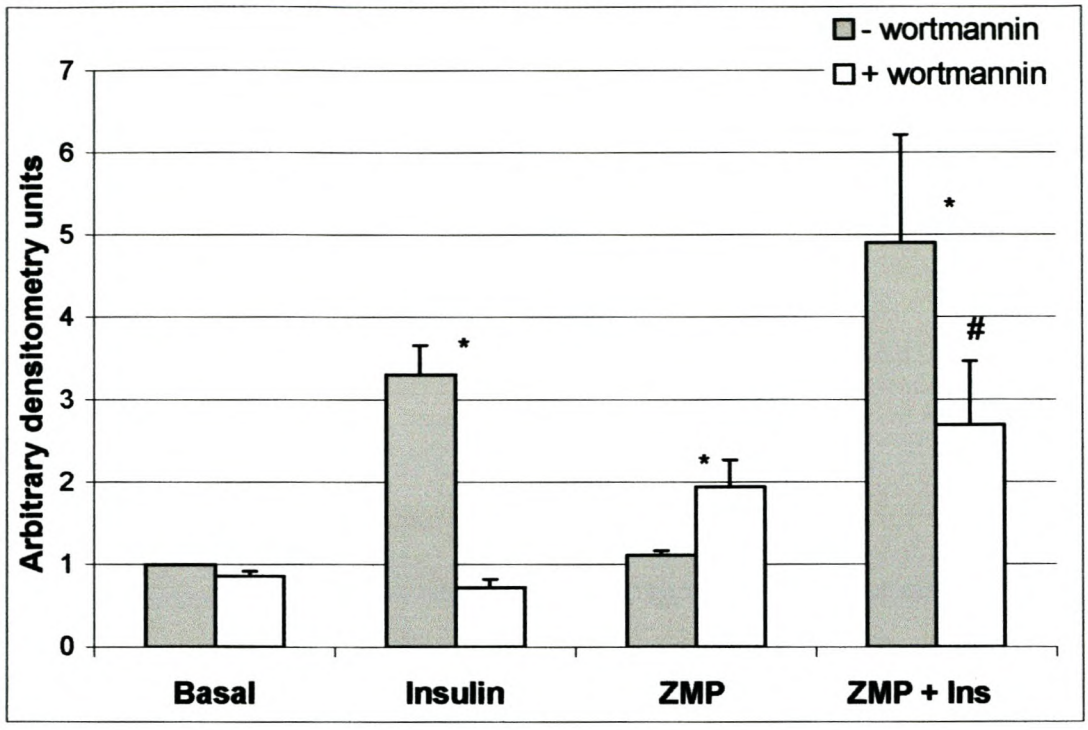

Figure 4.17: Effect of wortmannin (100 nM) on PKB/Akt phosphorylation in insulin (100 nm) and ZMP (1 mM) stimulated cardiomyocytes. Wortmannin was added 15 min before administration of ZMP or insulin, and present throughout the experiment. Cells were stimulated with ZMP for 30 min, and with insulin for 15 min.

All values expressed as mean ± SEM (n=5-10)

* $p<0.05$ -wortmannin vs + wortmannin

# $p<0.05$ vs insulin +wortmannin

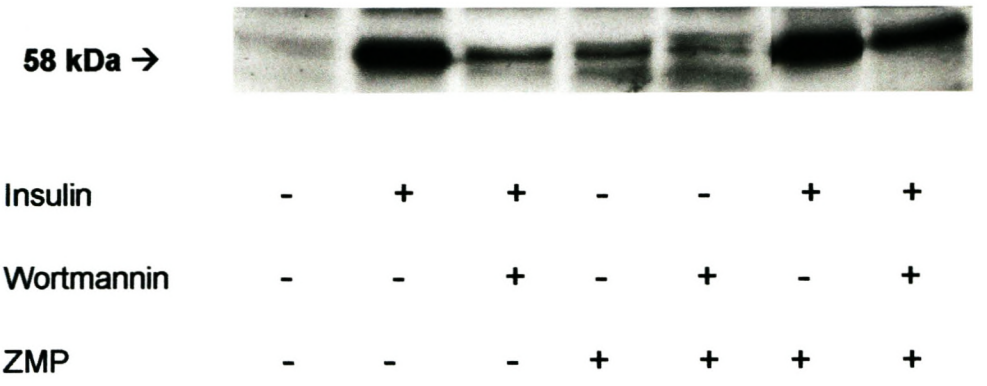

Figure 4.18: Western blot showing PKB/Akt phosphorylation pattern (Ser 473) in cardiomyocytes stimulated with ZMP (1 mM), insulin (100 nM) and wortmannin (100 nM) as indicated in Fig 4.17.

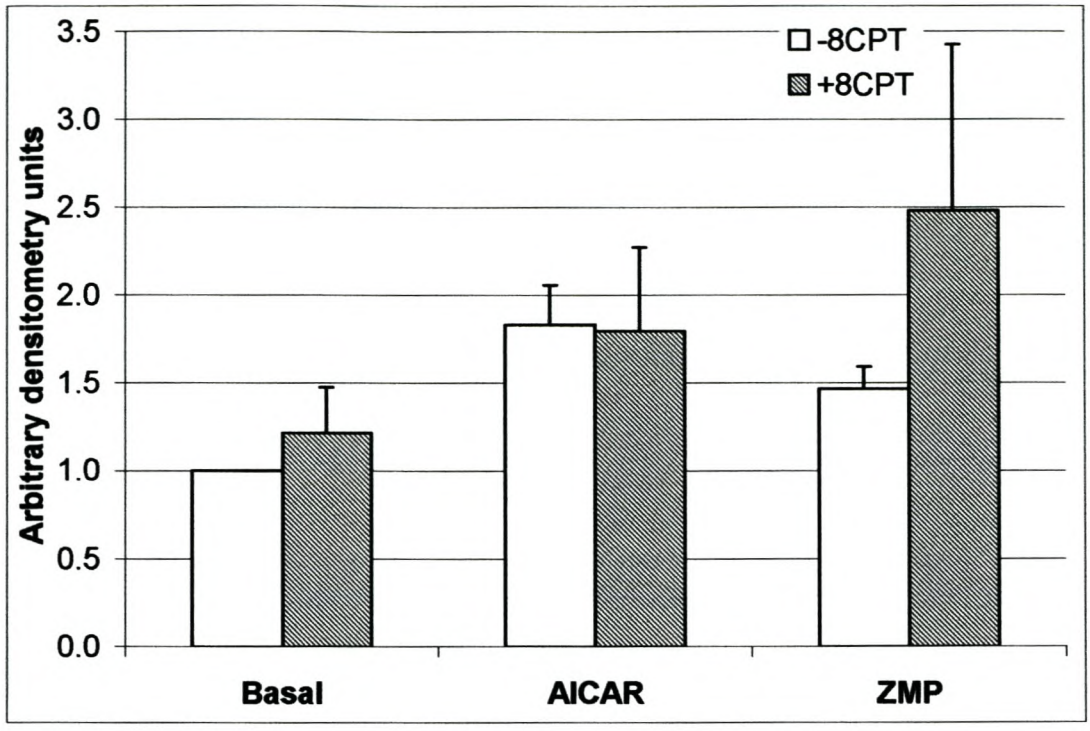

Figure 4.19 The effect of the purinergic receptor blocker, 8CPT (10 μM), on AICAR (1 mM) and ZMP (1 mM) phosphorylation of AMPK on Thr 172 in cardiomyocytes. 8CPT was added to cells 15 min before the addition of AICAR (1 mM) or ZMP (1 mM). Cardiomyocytes were stimulated with AICAR or ZMP for 30 min.

All values are expressed as mean ± SEM (n = 4),

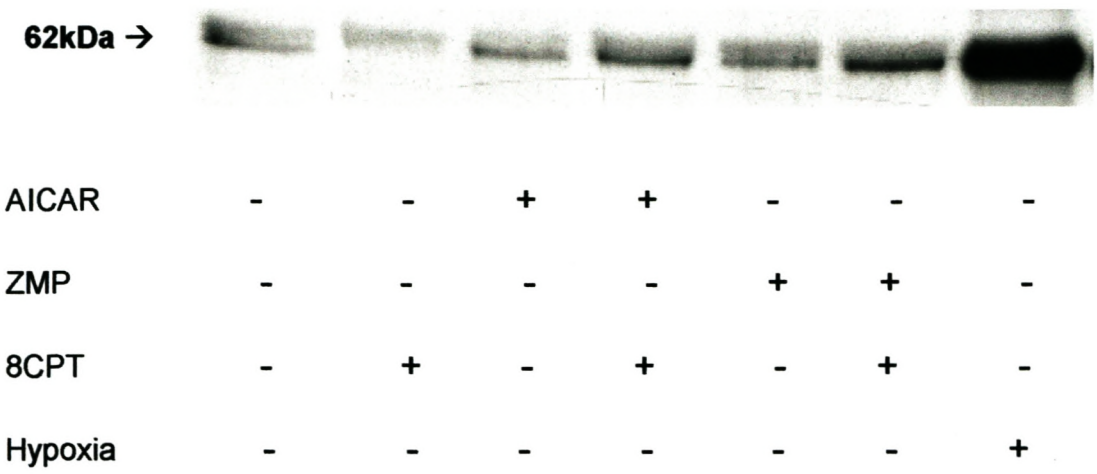

Figure 4.20 Western blot to show AMPK phosphorylation on Thr 172 in cells treated with AICAR (1 mM) or ZMP (1 mM) and blocked with 8CPT (10 µM). Hypoxic cells were used as a positive control.

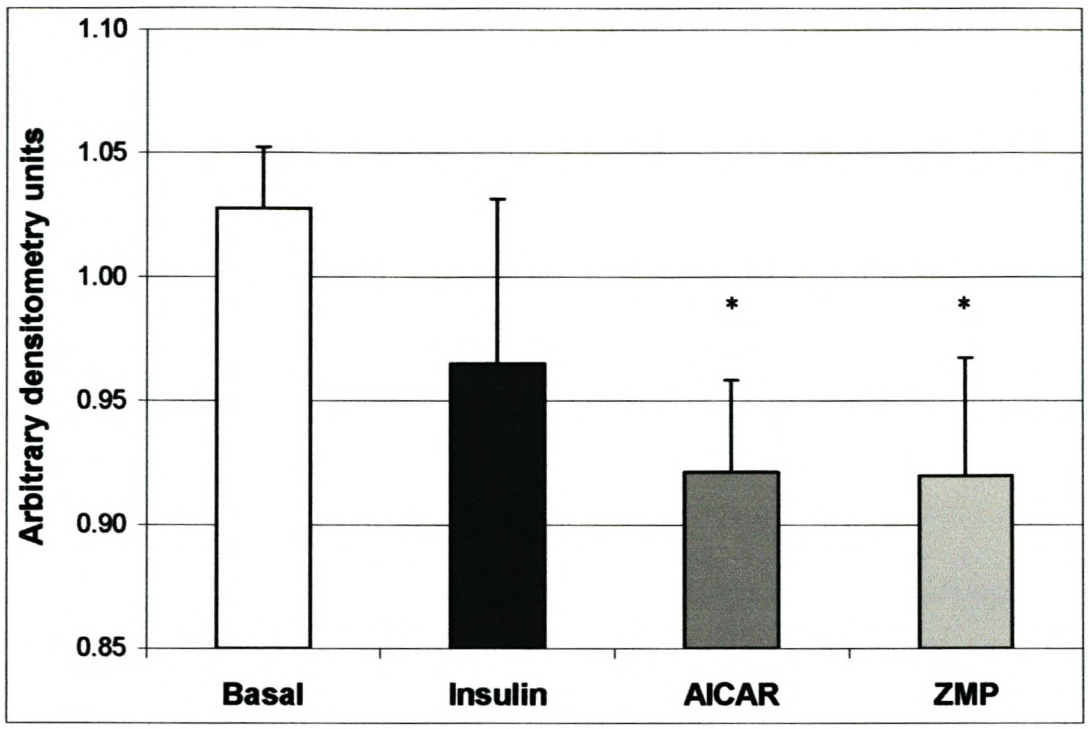

Figure 4.21 Cytosolic distribution of GLUT4 in basal, insulin (100 nM), AICAR (1 mM) and ZMP (1 mM) treated cardiomyocytes. Cells were stimulated with AICAR or ZMP for 30 min or with insulin for 15 min.

All values are expressed as mean ± SEM (n = 12),

* = $p<0.05$ vs basal

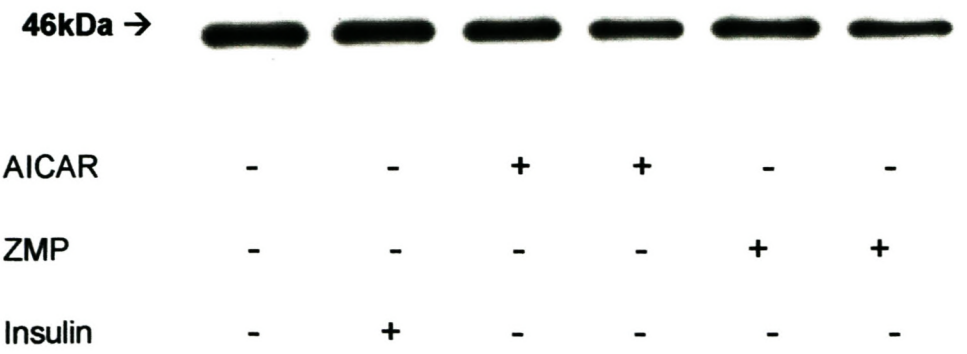

Figure 4.22 Western blot to show content of GLUT4 in the cytosol of cardiomyocytes treated with AICAR (1 mM), ZMP (1 mM) and insulin (100 nM).

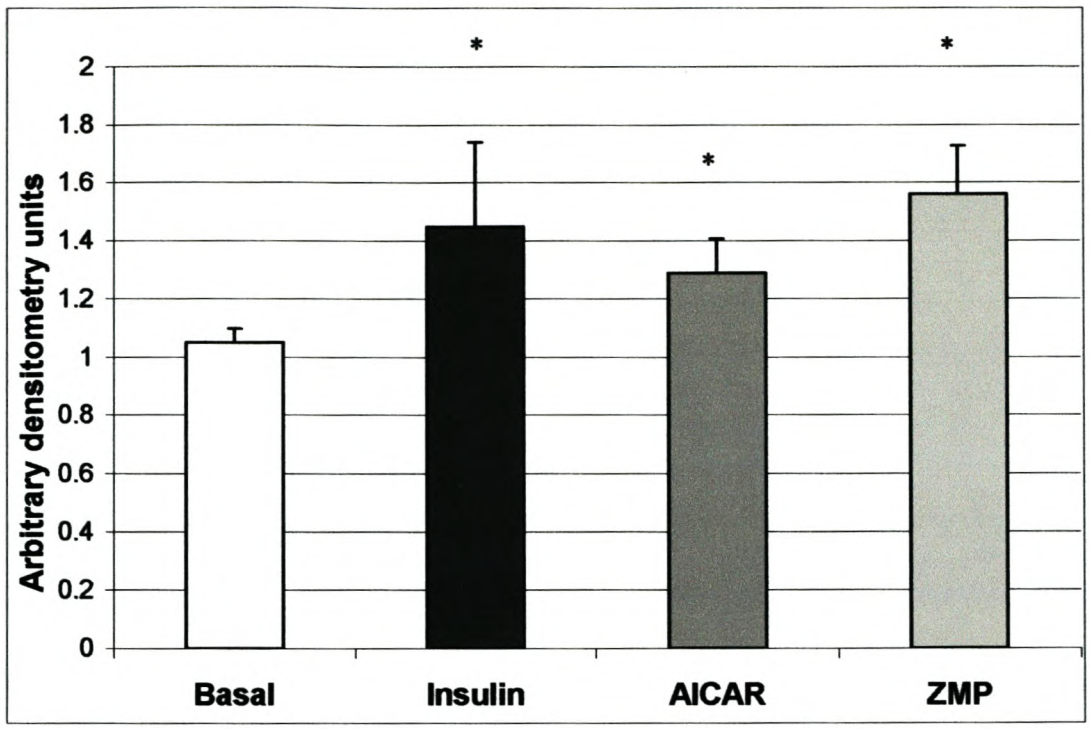

Figure 4.23 Membrane compartment distribution of GLUT4 in basal, insulin (100 nM), AICAR (1 mM) and ZMP (1 mM) treated cardiomyocytes. Cells were stimulated with AICAR or ZMP for 30 min or with insulin for 15 min.

All values are expressed as mean ± SEM (n = 12),

* = $p<0.05$ vs basal

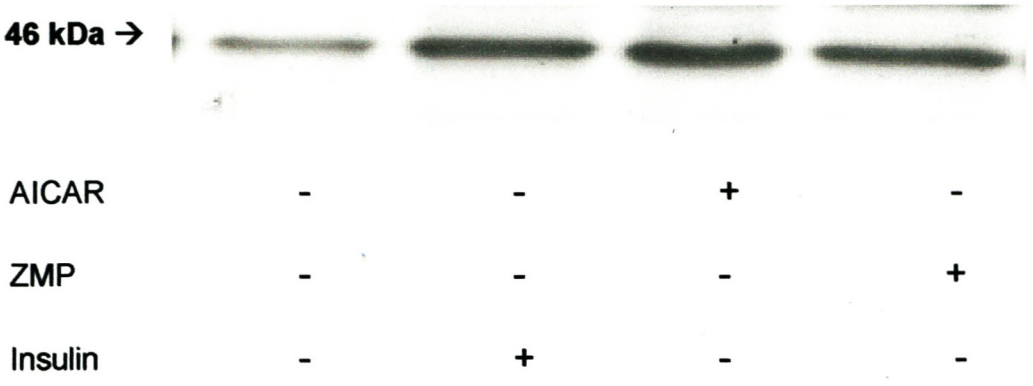

Figure 4.24 Western blot to show content of GLUT4 in the membrane of cardiomyocytes treated with AICAR (1 mM), ZMP (1 mM) and insulin (100 nM).

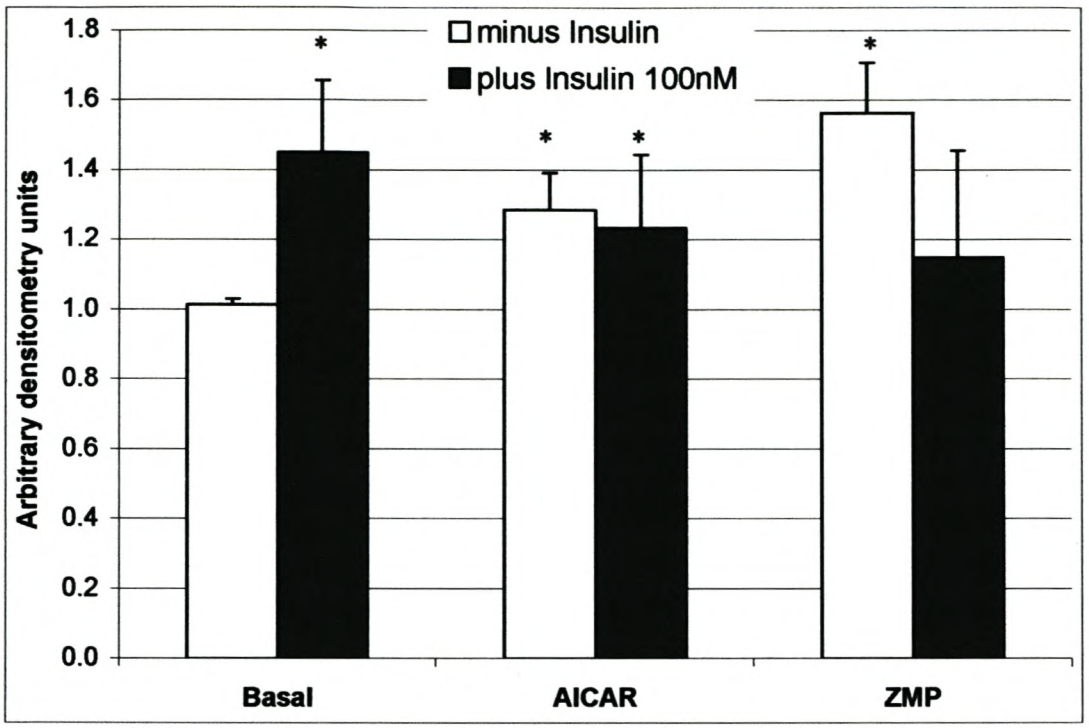

Figure 4.25 Membrane compartment distribution of GLUT4 in basal, insulin (100 nM), AICAR (1 mM), ZMP (1 mM) and a combination of AICAR and insulin or ZMP and insulin treated cardiomyocytes. Stimulation with insulin was for 15 min, and with AICAR or ZMP for 30 min.

All values are expressed as mean ± SEM (n = 5-15),

* = $p<0.05$ vs basal

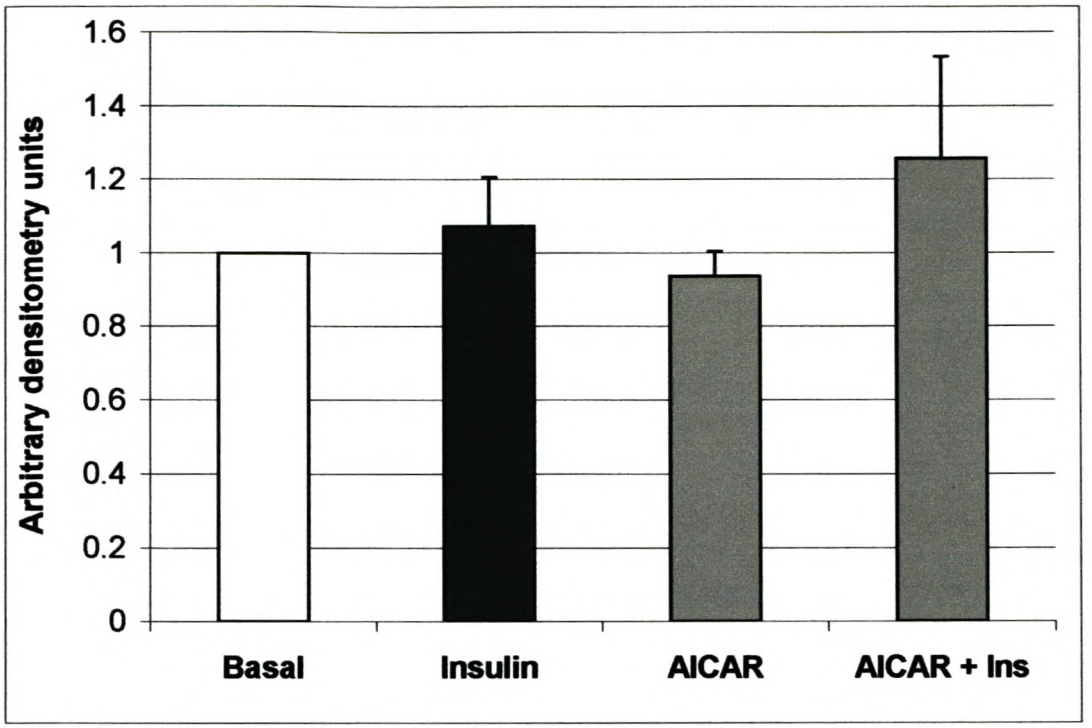

Figure 4.26 GLUT4 content of the cytosolic fraction of whole hearts perfused with 5 mM glucose under basal, insulin (100 nM), AICAR (1 mM) and a combination of AICAR and insulin conditions. Cells were stimulated with insulin for 15 min, and with AICAR for 30 min.

All values are expressed as mean ± SEM (n = 6)

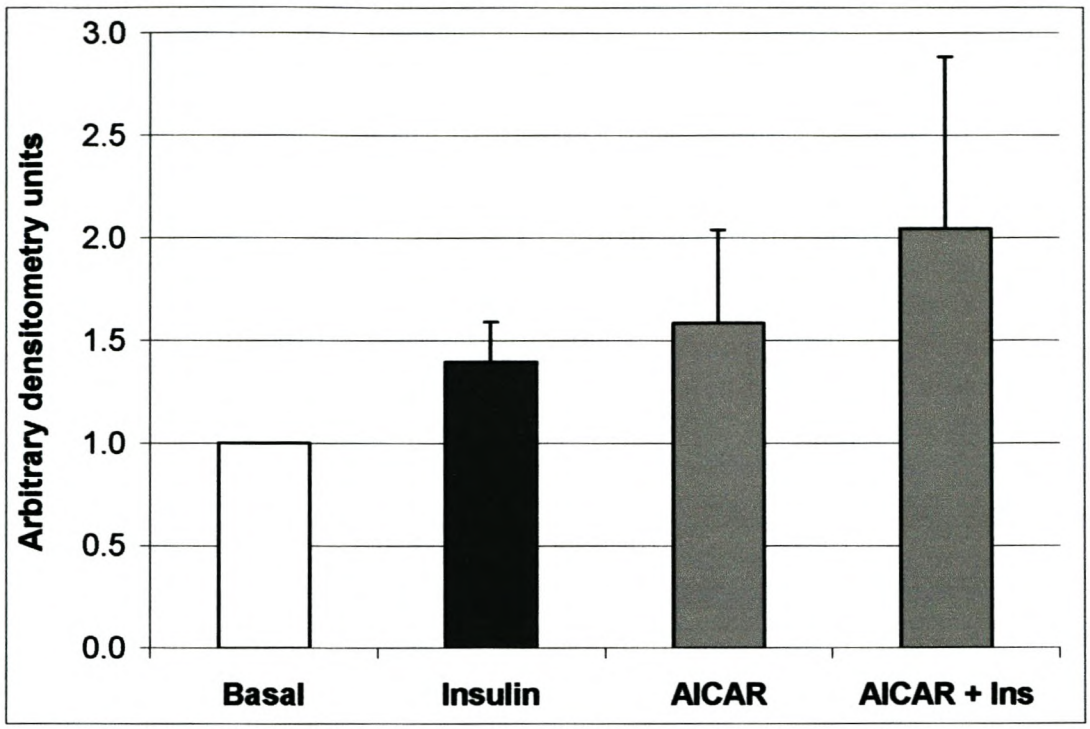

Figure 4.27 GLUT4 content of the membrane fraction of whole hearts perfused with 5 mM glucose under basal, insulin (100 nM), AICAR (1 mM) and a combination of AICAR and insulin conditions. Cells were stimulated with insulin for 15 min, and with AICAR for 30 min.

All values are expressed as mean ± SEM (n = 6)

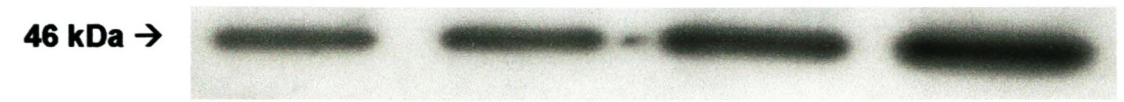

AICAR	-	-	+	+
Insulin	-	+	-	+

Figure 4.28 Western blot to show membrane content of GLUT4 in whole hearts perfused with 5 mM glucose under basal, insulin (100 nM), AICAR (1 mM) and a combination of AICAR and insulin conditions.

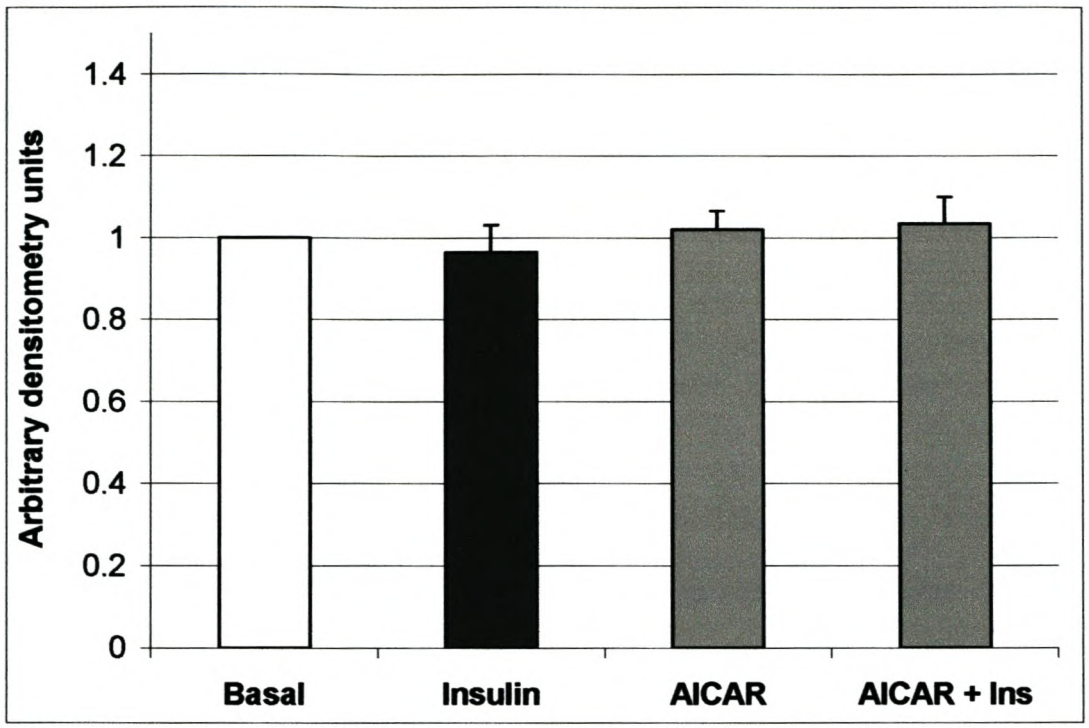

Figure 4.29 GLUT4 content of the cytosolic fraction of whole hearts perfused with glucose free medium under basal, insulin (100 nM), AICAR (1 mM) and a combination of AICAR and insulin conditions. Cells were stimulated with insulin for 15 min, and with AICAR for 30 min.

All values are expressed as mean ± SEM (n = 7)

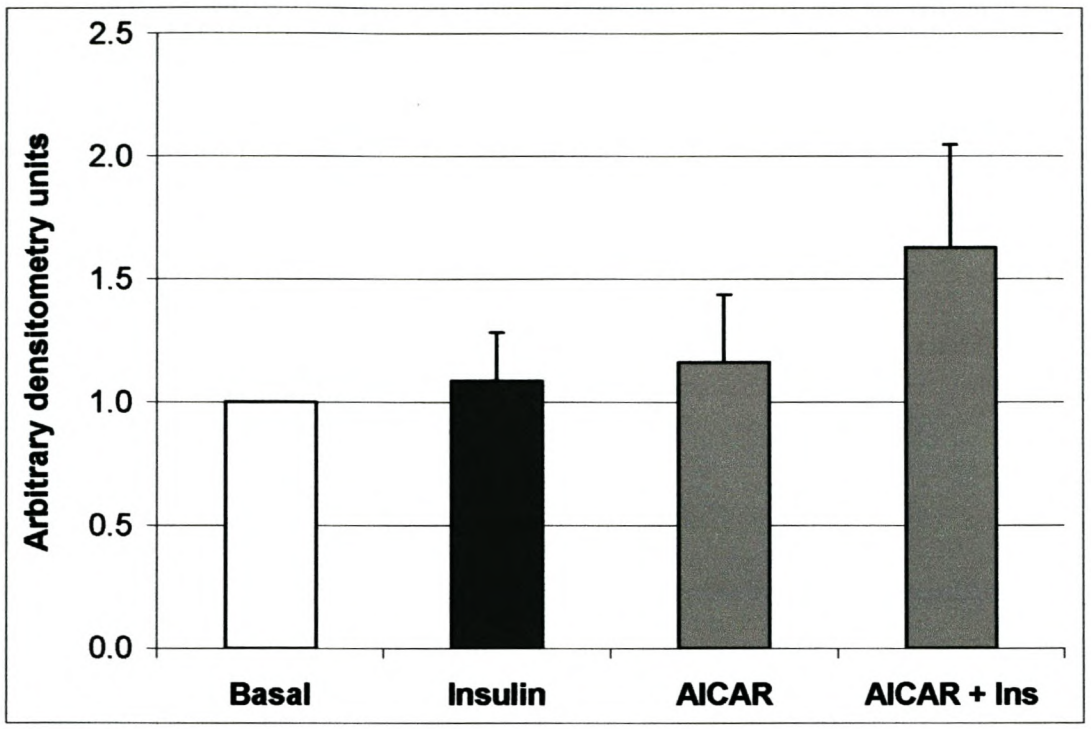

Figure 4.30 GLUT4 content of the membrane fraction of whole hearts perfused with glucose free medium under basal, insulin (100 nM), AICAR (1 mM) and a combination of AICAR and insulin conditions. Cells were stimulated with insulin for 15 min, and with AICAR for 30 min.

All values are expressed as mean ± SEM (n = 7)

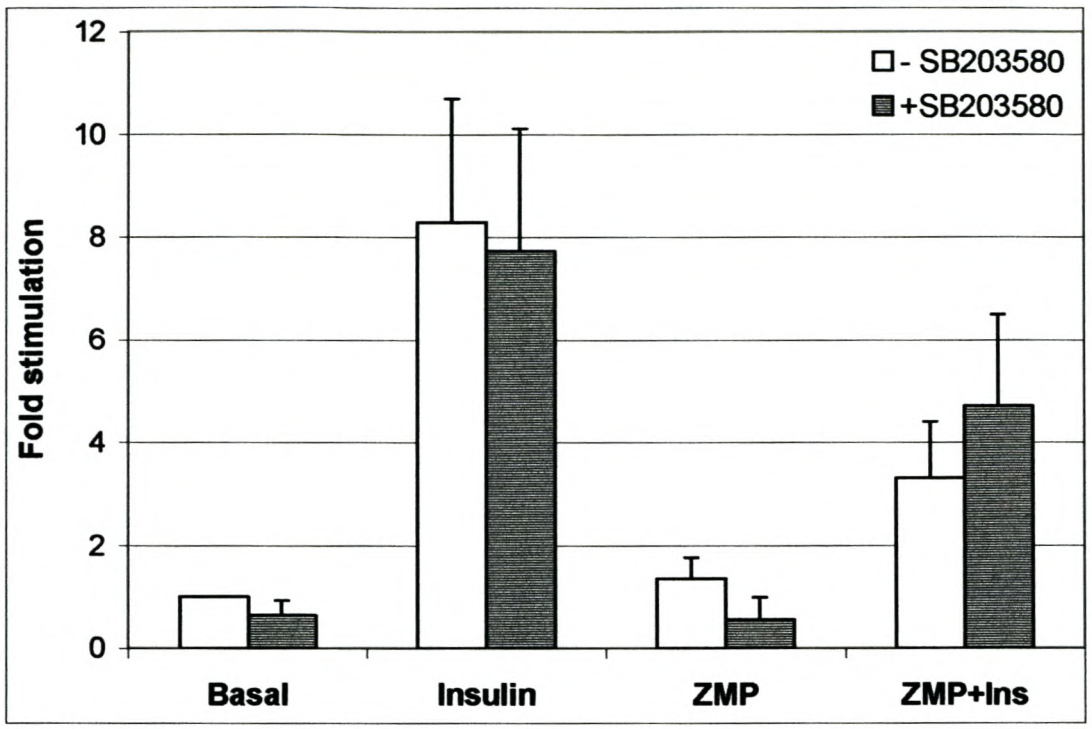

Figure 4.31: Effect of SB203580 (p38-MAPK inhibitor, 10 µM) on glucose uptake in insulin and ZMP (1 mM) treated cardiomyocytes. SB203580 was added 5 minutes before either insulin, ZMP or AICAR and left in the medium for the duration of the experiment. Cells were stimulated with ZMP for 30 min, and with insulin for 15 min.

All values are expressed as mean ± SEM (n = 3)

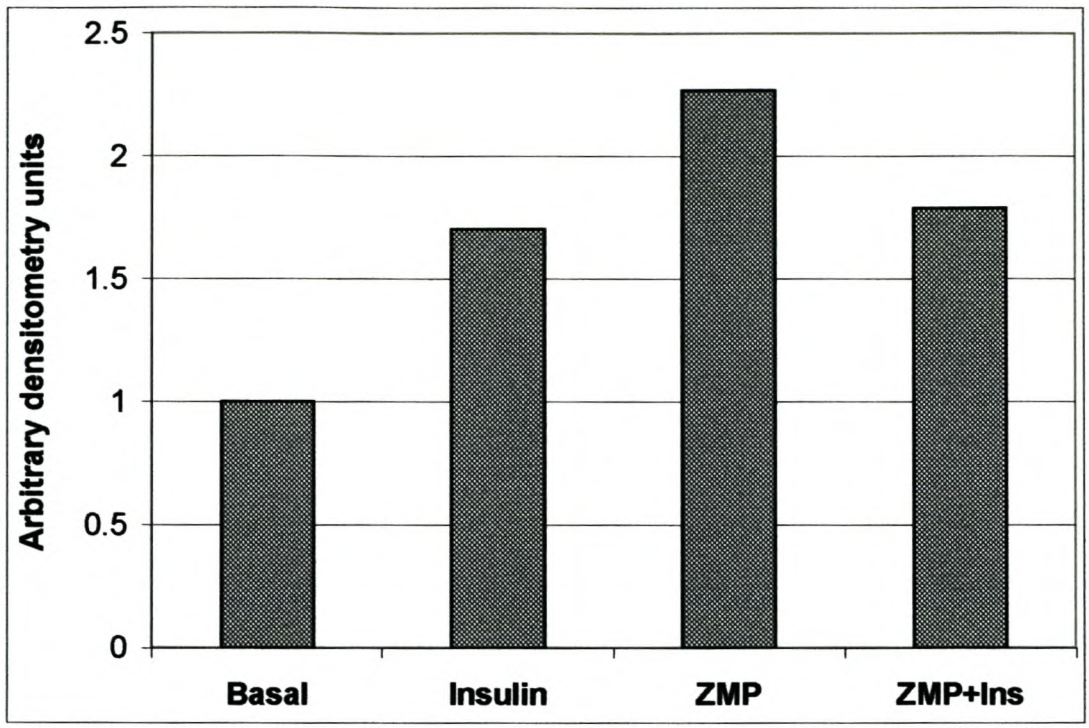

Figure 4.32: p38-MAPK phosphorylation in insulin (100 nM), ZMP (1 mM) and ZMP and insulin stimulated cardiomyocytes. Cells were stimulated with ZMP for 30 min, and with insulin for 15 min.

All values are expressed as mean ± SEM (n = 1)

Chapter 5

DISCUSSION

Regular exercise enhances insulin sensitivity in insulin resistant humans and rodents (Davis *et al*, 1986; Braun *et al*, 1995). This is manifested in increased insulin stimulated glucose uptake (Braun *et al*, 1995). Exercise leads to increased AMPK activity (Musi *et al*, 2003). It is therefore postulated that the AMPK biochemical pathway will cross talk with the insulin biochemical pathway. AICAR is said to activate AMPK (Corton *et al*, 1995), therefore pharmacological manipulation with AICAR should affect an increased insulin stimulated glucose uptake or insulin stimulated PKB/Akt phosphorylation as evidence of increased insulin signaling.

In view of the above we hypothesized that stimulation of the heart with AICAR or ZMP would lead to a sensitization of the heart muscle for insulin stimulation, and we therefore aimed to determine:

i) Whether AICAR can activate AMPK in heart muscle

ii) Whether this pharmacological activation will mimic some of the physiological effects of exercise e.g. increased glucose uptake and GLUT4 translocation

iii) Whether AICAR, in any way, affects the biochemical pathway activated by insulin and leading to glucose uptake.

5.1 AMPK phosphorylation

Adult ventricular myocytes were stimulated with AICAR (1 mM) for 30 minutes. This increased AMPK phosphorylation of Thr 172 significantly (see Fig 4.1). This result corroborates findings in EDL skeletal muscle (Lemieux *et al*, 2003) and hypothalamic cells (Perrin *et al*, 2004). However, Longnus *et al* (2003) were unable to elicit AMPK activation with AICAR in ventricular tissue. In view of the findings by Javaux *et al*, 1995 that in cardiomyocytes, AICAR is probably not phosphorylated to ZMP, we similarly tested the effect of ZMP on AMPK phosphorylation (see Fig 4.1) and found increased phosphorylation of Thr 172, indicating that ZMP indeed results in phosphorylation of AMPK in isolated cardiomyocytes. However, neither the activity of AMPK nor the activity of downstream targets of AMPK e.g. ACCβ and glycogen syntase were measured, suggesting a possibility that AMPK was phosphorylated but not actually activated.

There has also been positive evidence for ZMP activation of AMPK in hepatocytes (Corton *et al*, 1995). It was postulated that ZMP, due to its AMP analogue nature, acted via the purinergic receptors and thus bringing about its intracellular effect (Fischer *et al*, 1999). In order to ascertain or rule out this hypothesis, the cells were treated with ZMP and a blocker of the purinergic receptors, 8CPT. This showed to have no effect on the phosphorylation of AMPK elicited by ZMP (see Fig 4.19) ruling out the involvement of purinergic receptors in the effect of ZMP on AMPK phosphorylation in cardiomyocytes.

5.2 GLUCOSE UPTAKE

An increase in AMPK activity leads to stimulation of glucose uptake in skeletal muscle (Merrill *et al*, 1997; Hayashi *et al*, 1998). However, the significant AMPK phosphorylation noted in our study was not accompanied by a concomitant increase in cardiomyocyte glucose uptake (see Fig 4.5 and Fig 4.6). On the contrary, there was a significant decrease in glucose uptake seen in both the AICAR and ZMP treated cardiomyocytes.

This is similar to work by Jessen *et al* (2002) where he showed that, although AICAR increased insulin-stimulated glucose uptake in a fiber specific manner (higher in type II muscle fibers than type I fibers), basal non-insulin stimulated glucose transport in AICAR exposed animals was significantly lower in all muscles when compared with controls and exercised animals. Our findings are consistent with the results of Jessen *et al* in that AICAR stimulation alone decreased basal glucose uptake. Additionally, in recent work, Al-Khalili *et al* (2004) showed that AICAR-induced AMPK activation in primary human skeletal myocytes does not lead to a subsequent increase in glucose uptake. This work was done on both chronic and short-term exposure to 2mM AICAR.

However, in contrast to the above, Russell *et al* (1999) showed that in heart papillary muscle incubations with AICAR increased glucose uptake almost twofold and led to AMPK phosphorylation and GLUT4 translocation. The concentration of AICAR used

both in this study and by Russell and coworkers was 1 mM. Both in this study and in their study, the cells or muscle were incubated for 30 minutes prior to the addition of 2DG. However, Russell and colleagues incubated the papillary muscle with the 2DG for a further 60 minutes, whereas in our study it was only incubated for 30 minutes after the addition of 2DG. The incubation medium used in our study was a HEPES based buffer, and Russell *et al* used a PBS medium. These differences in protocol as well as the difference in model, might serve as some explanation for the differences in results.

In addition to the effects of AICAR and ZMP on cardiomyocyte glucose uptake, pre-treatment with the drugs attenuated insulin (100 nM) -stimulated glucose uptake. This is contrary to the findings of Fisher *et al* (2002) who found that the activation of AMPK enhanced the sensitivity of skeletal muscle glucose transport to insulin. However, our findings are similar to the previously mentioned work by Al-Khalili *et al* (2004), who also found that AICAR-induced AMPK activation in human skeletal myocytes did not lead to a subsequent increase in insulin-stimulated glucose uptake, in fact it lead to a 16-17% decrease in insulin-stimulated glucose uptake.

This attenuation was not seen, however, when we reversed the protocol and gave insulin to the cells only 5 minutes before AICAR or ZMP (see Fig 4.7). A maximal insulin-stimulated glucose uptake is seen at 7 minutes according to Somwar *et al* (2001), with a two-fold increase in basal glucose uptake occurring at 5 minutes already. Thus, in view of this rapid response, it appears that AICAR and ZMP

inhibition of insulin-stimulated glucose uptake can no longer occur. These observations suggest that AICAR and ZMP stimulation, when preceding insulin stimulation, unleashed as yet unidentified inhibitory effects on glucose uptake.

According to Shearer and colleagues (2004), using an in vivo perfusion system, stimulation of AMPK with AICAR leads to a rapid translocation of FAT/CD36 and uptake of fatty acids into the heart. This will inhibit glucose uptake, according to the mechanism of Randle (1963). However, in our system of measuring glucose uptake, glycolysis is inhibited by the presence of 2DG, therefore we measured glucose taken up by the GLUT4. Inhibition via the uptake and metabolism of fatty acids is therefore not a plausible explanation. Furthermore our system contains fatty acid free BSA that will sequester all fatty acids in the system, ruling out any role for fatty acids in our cardiomyocyte model.

5.3 PKB/Akt phosphorylation

Since insulin stimulates glucose uptake (Fischer *et al*, 1991; Berger *et al*, 1994), and so does AMPK (Fryer *et al*, 2000; Hyashi *et al*, 1998) by translocation of GLUT4 to the cell membrane (Fischer *et al*, 1997; Russell *et al*, 1999) it is very likely that cross talk occurs between these two pathways of glucose uptake. Although not much is known about the cross-talk between AMPK-stimulated and insulin-stimulated glucose uptake pathways, it was reported that stimulation of the AMPK glucose uptake pathway enhances the sensitivity of skeletal muscle glucose transport to insulin

stimulation (Fisher *et al*, 2002) involving a step beyond PKB in the insulin-stimulated pathway. In contrast it was also reported by Beauloye *et al* (2001) that pre-treatment of isolated hearts with 100 nM insulin antagonized the activation of AMPK during ischaemia at 5 minutes and onwards, showing definite inhibitory cross-talk between pathways.

For this reason, PKB/Akt phosphorylation was also analysed in this study (see Fig 4.9 to Fig 4.12). It was found that the basal stimulation of PKB\Akt was not inhibited by AICAR or ZMP, despite the observed inhibition of basal glucose uptake. This agrees with the viewpoint that basal glucose uptake is not a GLUT4 mediated event, therefore not dependent on PKB/Akt activation. Interestingly, the effect of pre-treatment with AICAR or ZMP on insulin stimulation of PKB/Akt phosphorylation was the same as that of insulin alone, not showing the attenuation seen in glucose uptake. Thus the inhibitory action of AICAR and ZMP on insulin-stimulated glucose uptake has its effect downstream from PKB/Akt phosphorylation.

5.4 Effect of Wortmannin

The fungal inhibitor wortmannin is a potent inhibitor of PI3-K activity (Stoyanova *et al*, 1997) and therefore has downstream effects inhibiting PKB/Akt phosphorylation. It was also reported by Jakobsen *et al* (2001) that AMPK, in response to AICAR, had the ability to phosphorylate IRS-1 on Ser-789 in mouse C2C12 myotubes suggesting an upstream link between the insulin-stimulated pathway and the AMPK pathway of

glucose uptake. We therefore decided to treat cells with wortmannin in combination with AICAR or ZMP and insulin and noted the effects (see Fig 4.13 to Fig 4.18).

5.4.1 Effect on Glucose Uptake

As was expected, wortmannin inhibited all insulin stimulated glucose uptake back to basal levels. This is consistent with the findings of others (Berger *et al*, 1994; Ueki *et al*, 1998). The presence of wortmannin did not alter the inhibitory effect of AICAR and ZMP on cardiomyocyte glucose uptake (see figures 4.13 and 4.14), indicating that PI3-K is not involved in these reactions.

5.4.2 Effect on PKB phosphorylation

AICAR and ZMP supposedly act via activation of AMPK, an event not associated with activation of PI3-K as discussed above. Interestingly, our work showed that in cells stimulated with ZMP in the presence of wortmannin, there was an unexpected significant increase in PKB/Akt phosphorylation. This same increase could be seen in PKB/Akt phosphorylation in the presence of AICAR and wortmannin, although it was not as outspoken. This can perhaps be explained by an effect of AICAR and ZMP on PKB/Akt phosphatases, where the dephosphorylation of PKB/Akt is diminished and the effect thereof is only unmasked in the presence of inhibition of further phosphorylation of PKB/Akt via PI3-K. It may of course also be the result of the actions of some unknown kinase only triggered by the abovementioned combination.

It is well known that wortmannin inhibits PKB/Akt phosphorylation via inhibition of PI3-K (Ng *et al*, 2001) and our findings are consistent with this (see figure 4.15 to 4.18) in that insulin-stimulated PKB/Akt phosphorylation was blocked by wortmannin administration to cardiomyocytes, having no effect on basal phosphorylation. As this study showed that the effects of both AICAR and ZMP on insulin-stimulated glucose uptake lie downstream of PKB/Akt phosphorylation in the signaling cascade, no effect of wortmannin on this event was expected. There is no literature to date describing the effect of wortmannin on AICAR and ZMP stimulated PKB/Akt phosphorylation in cardiomyocytes.

In the presence of AICAR or ZMP, wortmannin was also not able to totally abolish insulin stimulated PKB/Akt phosphorylation confirming an effect of these substances in modifying the PKB/Akt phosphorylation state. However the exact mechanism of this observation and the importance thereof would only be shown through further research.

5.5 GLUT 4 Translocation

GLUT4s are the glucose transporters recruited to the cell membrane in response to insulin stimulation (Fischer *et al*, 1997; Calera *et al*, 1998; Becker *et al*, 2001). They are also reported to be up regulated in response to AMPK activation by a single subcutaneous injection of AICAR (1mg/g body weight) peaking at 13 hours post-injection (Zheng *et al*, 2001; Holmes *et al*, 1999) and translocate to the cell

membrane to enhance glucose uptake during muscle contraction (Till *et al*, 1997). In heart papillary muscle, AICAR stimulated AMPK activation (Russell *et al*, 1999) also leads to GLUT4 translocation. In view of the observation made in this study that these drugs stimulate AMPK activation but not glucose uptake, it was decided to investigate the content of GLUT4 in cytosolic and membrane compartments of isolated myocytes and in perfused hearts to quantify the movement of GLUT4 after various stimuli.

5.5.1 GLUT4 content in the cytosol in isolated cardiomyocytes

Both ZMP and AICAR stimulated cardiomyocytes showed a significant decrease in cytosolic GLUT4 content, indicating that the transporters moved away from the cytosol in response to AICAR and ZMP stimulation (see Fig 4.21 & Fig 4.22). We have no explanation why such variable results were found with insulin, using the same experimental protocol, but it is possibly due to significantly elevated amounts of GLUT4 present in the cytosol, which makes it very difficult to quantify removal of small quantities.

5.5.2 GLUT4 content in the membrane in isolated cardiomyocytes

An increase in GLUT4 content was found after stimulation with insulin, AICAR and ZMP in the membrane compartment (see Fig 4.23 & Fig 4.24). We therefore conclude that GLUT4 translocation indeed occurred from the cytosolic compartment

to the membrane in insulin, AICAR- and ZMP-stimulated cardiomyocytes, even though no glucose uptake was elicited with either AICAR or ZMP. When insulin was added to myocytes pre-treated with either AICAR or ZMP, a significant increase in GLUT4 translocation could only be seen with the combination of insulin and AICAR.

5.5.3 GLUT4 content in the whole heart

As can be seen in Figures 4.26 & 4.29, no significant differences in GLUT4 content could be seen in cytosolic compartments in insulin-, AICAR- or ZMP-stimulated hearts, regardless of whether the perfusate contained glucose (5 mM) or not. When looking at the membrane fractions of both 5mM and glucose free perfused hearts, a definite tendency could be seen towards GLUT4 translocation to the membrane (see Fig 4.27, 4.28 & 4.30). Unfortunately the standard errors of these groups were very high, not allowing for these increases in translocation to be significant. This could be due to the fact that the technique for isolation and purification of sarcolemmal membrane is a rather crude method that does not yield enough protein for analysis. It is suggested that a more stringent and accurate method be developed and used to refute or prove the results obtained. However, the convincing results obtained with the cardiomyocyte preparation, lead us to believe that AICAR and ZMP do indeed cause translocation of GLUT4 from the cytosol to the sarcolemma.

5.6 Glucose uptake versus GLUT4 translocation

The two major findings of the current study is that (i) neither AICAR nor ZMP could stimulate glucose uptake in isolated cardiomyocytes while both substances were able to phosphorylate AMPK and elicit translocation of the GLUT4 transporter from the cytosol to the cell membrane and (ii) both AICAR and ZMP inhibited insulin stimulated glucose uptake while insulin-induced translocation of GLUT4 was not affected.

These findings highlight the concept put forward by the group of Amira Klip (Furtado *et al,* 2002) that GLUT4 translocation and GLUT4 activation to transport glucose are two independent, though interrelated occurrences that can be separated from one another. To substantiate this statement, Sweeney *et al* (2004) demonstrated that intracellular delivery of PIP_3 results in GLUT4 translocation and incorporation into the membrane, but no associated glucose uptake while Funaki *et al* (2004) created a cell-permeable phosphoinositide-binding peptide that could induce GLUT4 translocation to the plasma membrane in adipocytes, without increasing glucose uptake. This has lead investigators to search for the second signal involved in the activation of glucose transport, as discussed below.

Using isolated ventricular cardiomyocytes for measurement of both GLUT4 translocation and glucose uptake, it is apparent that insulin has the ability to stimulate both translocation and activation of GLUT4 while AICAR and ZMP stimulate GLUT4

translocation but not activation. It would also seem as if, once AICAR and ZMP have accomplished this translocation, insulin loses its ability to activate the transporters, the mechanism of which remains to be established. On the other hand, once translocation by insulin has been accomplished (according to Somwar *et al* (2001) this takes less than 5 minutes), AICAR and ZMP have no effect. Clearly further work is required to elucidate the mechanisms involved. We are currently developing a flow cytometric analyses of GLUT4 translocation in cardiomyocytes using a cell impermeable probe that binds only to translocated GLUT4 on the outer membrane surface. This has only become available after completion of the current project.

5.6.1 p38 MAPK

A study by Xi *et al*, (2001) reported that AMPK stimulated glucose uptake via p38 MAPK activity. These findings were supplemented by Somwar *et al* (2001) who found that a dominant negative p38 MAPK mutant and selective inhibitors of p38 MAPK reduce insulin-stimulated glucose uptake in adipocytes without affecting GLUT4 translocation. Furthermore Lemieux *et al* (2003) showed that AICAR stimulated p38 activation in skeletal muscle.

For these reasons we treated cells with the p38 inhibitor SB 203580, measuring the effect on glucose uptake, in the presence of ZMP. In cardiomyocytes, we did not observe any effect on the inhibition of glucose uptake by ZMP. Thus it was concluded that p38 MAPK activation does not play a role in our observations.

Role of NOS?

In a recent publication by Li *et al* (2004), it was proposed that nitric oxide might play a role in AMPK-mediated glucose uptake and GLUT4 translocation. It has been described before that AMPK phosphorylates endothelial nitric oxide synthase (eNOS) on Ser^{1177} (Chen *et al*, 1999, Chen *et al*, 2000) leading to NOS activation. This was confirmed by Li *et al* (2004). Several studies have indicated that insulin activates endothelial NOS via protein kinase B (PKB/Akt)-mediated phosphorylation at Ser^{1177} in endothelial cells (Trovati *et al*, 1999; Ribiere *et al*, 2002). In skeletal muscle from mice deficient in eNOS, there is decreased insulin stimulated glucose uptake, suggesting that activation of nitric oxide by PKB/Akt may play a key role in glucose uptake (Browne *et al*, 1999; Duplain *et al*, 2001). Shearer *et al* (2004) and Fryer *et al* (2000) showed that NOS inhibition with L-NAME (N^{ω}-nitro-L-arginine) in skeletal muscle reduced AICAR stimulated glucose uptake. Li and coworkers (2004) incubated rat left ventricular papillary muscle with AICAR (1mM) and found increased glucose uptake and GLUT4 translocation along with the increased eNOS phosphorylation. Low concentrations of nitric oxide donors were found to increase papillary muscle glucose uptake as well as GLUT4 translocation, and NOS inhibitors partially blocked AICAR stimulated glucose uptake.

According to the available literature, activation of eNOS is an event occurring downstream of PKB/Akt phosphorylation after stimulation with insulin (Salt *et al*,2003; Kim et al, *2001*), making this a possible candidate. It is possible that in a myocyte

preparation, the available eNOS is not able to produce enough NO to trigger GLUT4 activation. In contrast, in papillary muscle, endothelial eNOS may play a major role, supplying the necessary NO. This would explain why glucose uptake takes place on stimulation with AICAR in a papillary muscle model but not in the isolated myocyte preparation. We will be able to test this possibility by supplying isolated cardiomyocytes with nitric oxide donors in conjunction with stimulation with AICAR and ZMP to see whether such treatment will induce glucose uptake.

CONCLUSION

In conclusion, treatment of cardiomyocytes with AICAR and ZMP, two AMPK-activating pharmacological agents, did not result in an increased glucose uptake. In fact, both AICAR and ZMP resulted in a decreased glucose uptake response, even though PKB/Akt phosphorylation and GLUT4 translocation were evident in both AICAR and ZMP treated cells. An attenuated insulin-stimulated glucose uptake was shown when AICAR or ZMP were given to cells before insulin, and this affect was absent when cells were stimulated with insulin before AICAR or ZMP. This attenuation was also not seen in the PKB/Akt phosphorylation patterns. An increase in phosphorylation of PKB/Akt was shown when cardiomyocytes were pre-treated with wortmannin and then stimulated with ZMP.

Our results, and those of others lead us to speculate that for AICAR or ZMP to induce glucose uptake, the whole muscle needs to be present, and individual isolated myocytes cannot be stimulated by these substances to induce increased glucose uptake. It is possible that the presence of endothelial cells may play a large role in these whole muscle preparations.

Finally, the mechanism whereby AICAR and ZMP inhibit activation of the GLUT4 transporter after its translocation to the cell membrane remains to be established. In order to do so, a more sensitive technique to measure GLUT4 translocation in heart or myocytes, needs to be developed.

REFERENCES

Aikawa R, Nawano M, Gu Y, Katagiri H, Asano T, Zhu W, Nagai R and Komuro I. Insulin prevents cardiomyocytes from oxidative stress-induced apoptosis through activation of PI3 kinase/ Akt. *Circulation.* 102(23): 2873-2879, 2000.

Alessi DR, Andjelkovic M, Caudwell B, Cron P, Morrice N, Cohen P and Hemmings B.A. Mechanism of activation of protein kinase B by insulin and IGF-1. *EMBO J* 15: 6541-6551, 1996.

Al-Khalili L, Krook A, Zierath JR and Cartee GD. Prior serum- and AICAR-induced AMPK activation in primary human myocytes does not lead to subsequent increase in insulin-stimulated glucose uptake. *Am J Physiol Endocrinol Metab* 287: E553-E557, 2004.

Andjelkovic M, Suidan HS, Meier R, Frech M, Alessi DR and Hemmings, BA. Nerve Growth Factor promotes activation of the alpha, beta and gamma isoforms of protein kinase B in PC12 pheochromocytoma cells. *Eur J Biochem.* 251: 195-200, 1998.

Armstrong SC, Ganote CE. Effects of 2,3-butanedione monoxamine (BDM) on contracture and injury of isolated rat myocytes following metabolic inhibition and ischemia. *J Mol Cell Cardiol.* 23: 1001-1014, 1991.

Armstrong S, Downey JM and Ganote CE. Preconditioning of isolated rabbit cardiomyocytes: induction by metabolic stress and blockade by the adenosine antagonist SPT and calphostin C. a protein kinase C inhibitor. *Cardiovasc Res.* 28: 72-77, 1994.

Awan MM and Saggerson ED. Malonyl-CoA metabolism in cardiac myocytes and its relevance to the control of fatty acid oxidation. *Biochem J* 295: 61-66, 1993.

Balon TW and Jasman AP. Acute exposure to AICAR increases glucose transport in mouse EDL and soleus muscle. *Biochem Biophys Res Commun.* 282(4): 1008-1011, 2001.

Bao S, Ouyang G, Bai X, Huang Z, Ma C, Liu M, Shao R, Anderson RM, Rich JN and Wang XF. Periostin potently promotes metastatic growth of colon cancer by augmenting cell survival via the Akt/PKB pathway. *Cancer Cell* 5(4): 329-39, 2004.

Beauloye C, Marsin AS, Bertrand L, Krause U, Hardie DG, Vanoverschelde JL, Hue L. Insulin antagonizes AMP-activated protein kinase activation by ischemia or anoxia in rat hearts, without affecting total adenine nucleotides. *FEBS Lett* 505(3): 348-52, 2001.

Becker C, Sevilla L, Tomàs E, Palacin M, Zorzano A and Fischer Y. The endosomal compartment is an insulin-sensitive recruitment site for GLUT4 and GLUT1 glucose transporters in cardiac myocytes. *Endocrinolgy* 142(12): 5267-5276, 2001.

Belke DD, Larsen TS, Gibbs EM and Severson DL. Glucose metabolism in perfused mouse hearts overexpressing human GLUT4 glucose transporter. *Am J Physiol Endocrin Metab.* 280: E420-E427, 2001.

Bellacosa A, Testa JR, Staal SP, Tsichlis PN. A retroviral oncogene, *akt*, encoding a serine-threonine kinase containing an SH2-like region. *Science.* 254: 274-277, 1991.

Berger J, Hayes N, Szalkowski DM, Zhang B. PI 3-kinase activation is required for insulin stimulation of glucose transport into L6 myotubes. *Biochem Biophys Res Commun.* 205(1): 570-576, 1994.

Bergeron R, Russel III RR, Young LH, Ren JM, Marcucci M, Lee A and Shulman GI. Effect of AMPK activation on muscle glucose metabolism in conscious rats. *Am J Physiol Endocrinol Metabol.* 276(5): E938-944, 1999.

Bers DM. The isolation and characterisation of cardiac sarcolemma. *Biochem Biophys Acta.* 555: 131-146, 1979.

Bing RJ, Siegel A, Ungar I and Gilbert M. Metabolism of the human heart II. Studies on fat, ketone and amino acid metabolism. *Am J Med.* 16: 504-515, 1954.

Bonen A, Luiken JJFP, Arumaugam Y, Glatz JFC and Tandon NN. Acute regulation of fatty acid uptake involves the cellular redistribution of fatty acid translocase. *J Biol Chem.* 275: 14501-14508, 2000.

Bradford MM. A sensitive method for the quantification of protein utilizing the principle of protein-dye binding. *Ana Biochem* 71: 248-254, 1976.

Brazil DP and Hemmings BA. Ten years of protein kinase B signaling: a hard Akt to follow. *Trends Biochem Sci.* 26(11): 657-664, 2001.

Browne SE, Ayata C, Huang PL, Moskowitz MA, Beal MF. The cerebral metabolic consequences of nitric oxide synthase deficiency: glucose utilization in endothelial and neuronal nitric oxide synthase null mice. *J Cereb Blood Flow Metab* 19(2): 144-148, 1999.

Bruan B, Zimmerman MB and Kretchmer N. Effects of exercise intensity on insulin sensitivity in women with insulin-dependant diabetes mellitus. *J Appl Physiol* 78(1): 300-306, 1995.

Buhl ES, Jessen N, Schmitz O, Pedersen SB, Pedersen O, Holman GD and Lund S. Chronic treatment with 5-aminoimidazole-4-carboxamide-1-β-D-ribofuranoside increases insulin-stimulated glucose uptake and GLUT4

translocation in rat skeletal muscles in a fibre type-specific manner. *Diabetes* 50: 12-17, 2001.

Calera MR, Martinez C, Hongzhi L, El Jack AK, Birnbaum M, and Pilch PF. Insulin increases the association of Akt-2 with GLUT4-containing vesicles. *J Biol Chem.* 273(13): 7201-7204, 1998.

Carling D and Hardie DG. The substrate and sequence specificity of the AMP-activated protein kinase. Phosphorylation of glycogen synthase and phosphorylase kinase. *Biochem Biophys Acta.* 1012: 81-86, 1989.

Cheatham B, Volchuk A, Kahn CR, Wang L, Rhodes CJ and Klip A. Insulin stimulated translocation of GLUT4 glucose transporters requires SNARE-complex proteins. *Proc Natl Acad Sci U.S.A.* 93: 15169-15173, 1996.

Chen ZP, Mitchelhill KI, Michell BJ, Stapleton D, Rodriguez-Crespo I, Witters LA, Power DA, Ortiz de Montellano PR and Kemp BE. AMP-activated protein kinase phosphorylation of endothelial NO synthase. *FEBS Lett.* 443: 285-289, 1999.

Chen ZP, McConell GK, Michell BJ, Snow RJ, Canny BJ and Kemp BE. AMPK signaling in contracting human skeletal muscle: acetyl-CoA carboxylase and NO synthase phosphorylation. *Am J Physiol.* 279: E1202-E1206, 2000.

Cheng JQ, Godwin AK, Bellacosa A, Taguchi T, Franke TF, Hamilton TC, Tsichlis PN and Testa JR. AKT2, a putative oncogene encoding a member of a subfamily of protein-serine/threonine kinases, is amplified in human ovarian carcinomas. *Proc Natl Acad Sci U.S.A.* 89: 9267-9271, 1992.

Cheng JQ, Ruggeri B, Klein WM, Sonoda G, Altomare DA, Watson DK and Testa JR. Amplification of AKT2 in human pancreatic cells and inhibition of AKT2 expression and tumorigenicity by antisense RNA. *Proc Natl Acad Sci U.S.A.* 93: 3636-3641, 1996.

Chibalin AV, Yu M, Ryder JW, Song XM, Galuska D, Krook A, Wallberg-Henriksson H and Zierath JR. Exercise-induced changes in expression and activity of proteins involved in insulin signal transduction in skeletal muscle: differential effects on insulin-receptor substrates 1 and 2. *Proc Natl Acad Sci U.S.A.* 97: 38-42, 2000.

Coffer PJ and Woodgett JR. Molecular cloning and characterisation of a novel putative protein- serine kinase related to the cAMP-dependent and protein kinase C families. *Eur J Biochem.* 201: 475-481, 1991.

Coffer PJ, Jing J and Woodgett JR. Protein Kinase B (c-Akt): a multifunctional mediator of phosphatidylinositol-kinase activation. *Biochem J.* 335: 1-13, 1998.

Cong L-N, Hui C, Yunhua L, Lixin Z, McGibbon MA, Taylor SI and Quon MJ. Physiological role of Akt in insulin-stimulated translocation of GLUT4 in transfected rat adipose cells. *Mol Endocrin.* 11 (13): 1881-1890, 1997.

Cortez MY, Torgan CE, Brozinick JT and Ivy JL. Insulin resistance of obese Zucker rats exercise trained at two different intensities. *Am J Physiol.* 261: E613-619, 1991.

Corton JM, Gillespie JG, Hardie DG. Role of the AMP-activated protein kinase in the cellular stress response. *Current Biol.* 4: 315-324, 1994.

Corton JM, Gillespie JG, Hawley SA and Hardie DG. 5-Aminoimidazole-4-carboxamide ribonucleoside: A specific method for activating AMP-activated protein kinase in intact cells? *Eur J Biochem* 229: 558-565, 1995.

Coso OA, Chiariello M, Yu J, Teramoto H, Crespo P, Xu N, Miki T and Gutkind JS. The small GTP-binding proteins Rac1 and Cdc42 regulate the activity of the JNK/SAPK signaling pathway. *Cell.* 81: 1137-1146, 1995.

Cross DA, Alessi DR, Cohen P, Andjelkovich M and Hemmings BA. Inhibition of glycogen synthase kinase-3 by insulin mediated by protein kinase B. *Nature.* 378: 785-789, 1995.

Datta K, Bellacosa A, Chan TO and Tsichlis PN. Akt is a Direct Target of the Phosphatidylinositol 3-Kinase. ACTIVATION BY GROWTH *FACTORS, v-src* and *v-Ha-ras,* in Sf9 and mammalian cells. *J Biol Chem* 271: 30835-30839, 1996.

Datta SR, Brunet A and Greenberg ME. Cellular Survival: a play in three Akts. *Genes Dev.* 13: 2905-2927, 1999.

Datta SR, Dudek H, Tao X, Masters S, Fu H, Gotoh Y and Greenberg ME. Akt phosphorylation of BAD couples survival signals to the cell-intrinsic death machinery. *Cell* 91:231-241, 1997.

Davidson VL and Sittman DB. Biochemistry 3rd Edition. Harwal Publishing. Chapter 21: 370-373, 1994.

Davidoff AJ, Mason MM, Davidson MB, Carmody MW, Hintz KK, Wold LE, Podolin DA and Ren J. Sucrose-induced cardiomyocyte dysfunction is both preventable and reversible with clinically relevant treatments. *Am J Physiol Endocrin Metab.* 286(5): E718-724, 2004.

Davis TA, Klahr S, Tegtmeyer ED, Osborne DF, Howard TL and Karl IE. Glucose metabolism in epitrochlearis muscle of acutely exercise trained rats. *Am J Physiol.* 250(2 Pt 1): E137-143, 1986.

Dela F, Mikines KJ, von Linstow M, Secher NH and Galbo H. Effect of training on insulin-mediated glucose uptake in human muscle. *Am J Physiol.* 263: E1134-1143, 1992.

Del Pesto L, Gonzalez-Garcia M, Page C, Herrera R and Nunez G. Interleukin-3-induced phosphorylation of BAD through the protein kinase Akt. *Science.* 278: 687-689, 1997.

Delcommenne M, Tan C, Gray V, Rue L, Woodgett J and Dehar S. Phosphoinositide-3-OH kinase-dependent regulation of glycogen synthase kinase 3 and protein kinase B/AKT by the integrin-linked kinase. *Proc. Natl. Acad. Sci.* 95: 11211-11216, 1998.

De Luca JP, Garnache AK, Rulfs J and Miller Jnr TB. Wortmannin inhibits insulin-stimulated activation of protein phosphatase 1 in rat cardiomyocytes. *Am J Physiol.* 276 (*Heart Circ Physiol. 45*): H1520-H1526, 1999.

Depré C, Rider MH and Hue L. Mechanisms of control of heart glycolysis. *Eur J Biochem.* 258: 277-290, 1998.

Domin J, Dhand R and Waterfield MD. Binding to the platelet-derived growth factor receptor transiently activates the p85alpha-p110alpha phosphoinositide 3-kinase complex in vivo. *J Biol Chem.* 271: 21614-21621, 1996.

Domin J, Pages F, Volinia S, Rittenhouse SE, Zvelebil MJ, Stein RC and Watrfield MD. Cloning of a human phosphoinositide 3-kinase with a C2 domain that displays reduced sensitivity to the inhibitor wortmannin. *Biochem J.* 326: 139-147, 1997.

Douen AG, Ramlal T, Rastogi S, Bilan PJ, Cartee GD, Vranic M, Holloszy JO and Klip A. Exercise induces recruitment of the "insulin-responsive glucose transporter". *J Biol Chem.* 265(23): 13427-13430, 1990.

Douen AG, Ramlal T, Klip A, Young DA, Cartee GD and Holloszy JO. Exercise-induced increase in glucose transporters in plasma membranes of rat skeletal muscle. *Endocrinology.* 124: 449-454, 1989.

Duplain H, Burcelin R, Sartori C, Cook S, Egli M, Lepori M, Vollenweider P, Pedrazzini T, Nicod P, Thorens B, Scherrer U. Insulin resistance, hyperlipidemia, and hypertension in mice lacking endothelial nitric oxide synthase. *Circulation.* 104(3): 342-345, 2001.

Duronio V, Scheid MP and Ettinger S. Downstream signaling events regulated by phosphatidylinositol 3-kinase activity. *Cell Signal.* 10(4): 233-239, 1998.

Dyck JRB and Lopaschuk GD. Malonyl CoA Control of Fatty Acid Oxidation in the Ischemic Heart. *J Mol Cell Cardiol.* 34: 1099-1109, 2002.

Esfandiarei M, Luo H, Yanagawa B, Suarez A, Dabiri D, Zhang J and McManus BM. Protein kinase B/Akt regulates coxsackie virus B3 replication through a mechanism which is not caspase dependant. *J Virol* 78(8): 4289-4298, 2004.

Fischer Y, Thomas J, Sevilla L, Muñoz P, Becker C, Holman G, Kozka IJ, Palacin M, Testar X, Kammermeier H and Zorzano A. Insulin induced recruitment of glucose transporter 4 (GLUT4) and GLUT1 in isolated rat cardiac myocytes: evidence for the existence of different intracellular GLUT4 vesicle populations. *JBC Online*. 272(11): 7085-7092, 1997.

Fischer Y, Rose H and Kammermeier H. Highly insulin–responsive rat heart muscle cells yielded by a modified isolation method. *Life Sci.* 49: 1679-1688, 1991.

Fischer Y, Becker C and Loken C. Purinergic inhibition of glucose transport in cardiomyocytes. *J Biol Chem.* 274(2): 755-761, 1999.

Fisher JS, Gao J, Han DH, Holloszy JO and Nolte LA. Activation of AMP kinase enhances sensitivity of muscle glucose transport to insulin. *Am J Physiol.* 282: E18-E23, 2002.

Foster LJ and Klip A. Mechanism and regulation of GLUT-4 vesicle fusion in muscle and fat cells. *AJP-Cell Phys.* 279(4): C877-C890, 2000.

Fryer LGD, Hajduch E, Rencurel F, Salt IP, Harinder S, Hundal D, Hardie G and Carling D. Activation of Glucose transport by AMP-activated protein kinase via stimulation of nitric oxide synthase. *Diabetes* 49: 1978-1985, 2000.

Fujii N, Hayashi T, Hirshman MF, Smith JT, Habinowski SA, Kaijser L, Mu J, Ljungqvist O, Birnbaum MJ, Witters LA, Thorell A and Goodyear LJ. Exercise induces isoform-specific increase in 5'-AMP-activated protein kinase activity in human skeletal muscle. *Biochem Biophys Res Comm* 273: 1150-1155, 2000.

Funaki M, Randhawa P and Janmey PA. Separation of insulin signaling into distinct GLUT4 translocation and activation steps. *Mol Cell Biol.* 24(17): 7567-7577, 2004.

Furtado LM, Somwar R, Sweeney G, Niu W, Klip A. Activation of the glucose transporter GLUT4 by insulin. *Biochem Cell Biol.* 80(5): 569-78, 2002.

Fushiki T., Wells J.A., Tapscott E.B., and Dohm G.L. T. Fushiki, J. A. Wells, E. B. Tapscott, and G. L. Dohm. Changes in glucose transporters in muscle in response to exercise. *Am J Physiol Endocrinol Metab.* 256: E580-E587, 1989.

Hanada M, Feng J and Hemmings BA. Structure, regulation and function of PKB/AKT--a major therapeutic target. *Biochim Biophys Acta* 1697(1-2): 3-16, 2004.

Hardie DG and Carling D. The AMP-activated protein kinase – fuel gauge of the mammalian cell? *Eur J Biochem.* 246(2): 259-273, 1997.

Hardie DG, Carling D and Carlson M. The AMP-activated/SNF1 protein kinase subfamily: Metabolic sensors of the Eukaryotic cell? *Annu Rev Biochem.* 67: 821-855, 1998

Hardie DG and Hawley SA. AMP-activated protein kinase: the energy charge hypothesis revisited. *Bioessays.* 23(12): 1112-1119, 2001.

Hardie DG. The AMP-activated protein kinase cascade: the key sensor of cellular energy status. *Endocrinology.* 144(12): 5179-83, 2003.

Hawkins PT, Eguinoa A, Qiu R, Stokoe D, Cooke FT, Walters R, Wennstrom S, Claesson-Welch L, Evans T, Symons M and Stephens L. PDGF stimulates an increase in GTP-Rac via activation of phosphoinositide 3-kinase. *Curr Biol.* 5: 393-403, 1995.

Hawley SA, Davidson MD, Woods A, Davies, SP, Beri RK, Carling D and Hardie DG. Characterisation of the AMP-activated protein kinase kinase from rat liver, and identification of threonine-172 as the major site at which it phosphorylates and activates AMP-activated protein kinase. *J Biol Chem.* 271: 27879-27887, 1996.

Hawley SA, Boudeau J, Reid JL, Mustard KJ, Udd L, Makela TP, Alessi DR, Hardie DG. Complexes between the LKB1 tumor suppressor, STRAD alpha/beta and MO25 alpha/beta are upstream kinases in the AMP-activated protein kinase cascade. *J Biol.* 2(4): 28, 2003

Hayashi T, Hirshman MF, Kurth EJ, Winder WW, Goodyear LJ. Evidence for 5' AMP-activated protein kinase mediation of the effect of muscle contraction on glucose transport. *Diabetes* 47(8): 1369-73, 1998.

Hlobilkova A, Knillova J, Bartek J, Lukas J and Kolar Z. The mechanism of action of the tumour suppressor gene PTEN. *Biomed Pap Med Fac Univ Palacky Olomouc Czech Repub* 147(1): 19-25, 2003.

Holloszy JO. A forty–year memoir of research on the regulation of glucose transport into muscle. *Am J Physiol Endocrinol Metab.* 284: E453-E467, 2003.

Holman GD and Kasuga M. From receptor to transporter: insulin signaling to glucose transport. Review. *Diabetologia* 40(9): 991-1003, 1997.

Holmes BF, Kurth-Kraczek EJ, Winder WW. Chronic activation of 5'-AMP-activated protein kinase increases GLUT-4, hexokinase, and glycogen in muscle. *J Appl Physiol* 87(5): 1990-5, 1999.

Houmard JA, Shaw CD, Hickey MS and Tanner CJ. Effect of short term exercise training on insulin-stimulated PI3-kinase activity in human skeletal muscle. *Am J Physiol* 277:E1055-E1060, 1999.

Hudson ER, Pan DA, James J, Lucocq JM, Hawley SA, Green KA, Baba O, Terashima T and Hardie DG. A novel domain in AMP-activated protein kinase causes glycogen storage bodies similar to those seen in hereditary cardiac arrhythmias. *Current Biol.* 13:861-866, 2003.

Hue L, Maisin L, Rider MH. Palmitate inhibits liver glycolysis. Involvement of fructose 2,6-bisphosphate in the glucose/fatty acid cycle. Biochem J. 251(2): 541-5, 1988

Hughes VA, Fiatarone MA, Fielding RA, Kahn BB, Ferrara CM, Shepherd P, Fisher EC, Wolfe RR, Elahi D and Evans WJ. Exercise increases muscle GLUT4 levels and insulin action in subjects with impaired glucose tolerance. *Am J Physiol* 264:E855-862, 1993.

Jakobsen, SN, Hardie DG, Morrice N and Tornqvist HE. 5-AMP-activated protein kinase phosphorylates IRS-1 on Ser-789 in mouse C2C12 myotubules in response to 5-aminoimidazole-4-carboxamide riboside. *J Biol Chem* 276(50): 46912-46916, 2001.

Javaux F, Vincent MF, Wagner DR and van den Berghe G. Cell-type specificity of inhibition of glycolysis by 5-amino-4-imidazolecarboxamide riboside. Lack of

effect in rabbit cardiomyocytes and human erythrocytes, and inhibtion in FTO-2B rat hepatoma cells. *Biochem J* 305 (Pt 3): 913-919, 1995.

Jessen N, Pold R, Esben S. Buhl, ES. Jensen LS, Schmitz O and Lund S. Effects of AICAR and exercise on Insulin-stimulated glucose uptake, insulin signaling and GLUT4 content in rat skeletal muscles. *J Appl Physiol* 10: 1152, 2002.

Jones P.F. *et al.* Molecular cloning and identification of a serine/threonine protein kinase of the second messenger subfamily. *Proc Natl Acad Sci U.S.A.* 88:4174-4175, 1991.

Jones P.F. *et al.* Molecular cloning of a second isoform of *rac* protein kinase. *Cell Regul.* 2:1001-1009, 1991b.

Karlsson M, Thorn H, Parpal S, Stralfors P and Gustavsson J. Insulin induces translocation of the glucose transporter to plasma membrane caveolae in adipocytes. *FASEB J* 16:249-252, 2001.

Kaushik, Virendar K., Martin E.Young, David J.Dean, Thoedore G.Kurowski, Asish K.Saha, and Neil B.Ruderman. Regulation of fatty acid oxidation and glucose metabolism in rat soleus muscle: effects of AICAR. *AJP Endo Metab* 281(2)E335-E340, 2001.

Kemp BE, Mitchelhill KI, Stapleton D, Michell BJ, Chen Z-P and Witters LA. Dealing with energy demand: the AMP-activated protein kinase. *TIBS* 24: 22-25, 1999.

Kemppainen J, Fujimoto T, Kalliokoski KK, Viljanen T, Nuutila P and Knuuti J. Myocardial and skeletal muscle glucose uptake during exercise in humans. *J Physiol* 542(2): 403-412, 2002.

Kemppainen J, Hiroki T, Kira S, Karlsson H, Bjornholm M, Heinonen OJ, Nuutila P, Krook A, Knuuti J and Zierath JR. Insulin signaling and resistance in patients with chronic heart failure. *J Physiol* 550(1):305-315, 2003.

Kim F, Gallis B, Corson MA. TNF-alpha inhibits flow and insulin signaling leading to NO production in aortic endothelial cells. *Am J Physiol Cell Physiol.* 280(5): C1057-65, 2001.

Kim EC, Yun BS, Ryoo IJ, Min JK, Won MH, Lee KS, Kim YM, Yoo ID and Kwon YG. Complestatin prevents apoptotic cell death: inhibition of a mitochondrial pathway through AKT/PKB activation. *Biochem Biophys Res Commun* 313(1): 193-204, 2004.

King WG, Mattaliano MD, Chan TO, Tsichlis TN and JS Brugge. Phosphatidylinositol 3-kinase is required for integrin-stimulated AKT and Raf-1/mitogen-activated protein kinase pathway activation. *Mol Cell Biol* 17: 4406-4418, 1997.

Kirwin JP, Del Aguila IF, Hernandez JM, Williamson DL, O'Gorman DJ, Lewis R and Krishnan RK. Regular exercise enhances insulin activation of IRS-1-associated PI3-kinase in human skeletal muscle. *J Appl Physiol* 88: 797-803, 2000.

Klippel A, Reinhard C, Kavanaugh WM, Apell G, Escobedo MA and Williams LT. Membrane localization of phosphatidylinositol 3-kinase is sufficient to activate multiple signal-transducing kinase pathways *Mol Cell Biol* 16:4117-4127, 1996.

Klippel A, Kavanaugh WM, Pot D, and Williams LT. A specific product of phosphatidylinositol 3-kinase directly activates the protein kinase Akt through its pleckstrin homology domain. *Mol Cell Biol* 17: 338-344. 1997.

Kohn AD, Summers SA, Birnbaum MJ and Roth RR. Expression of a constitutively active Akt Ser/Thr kinase in 3T3-L1 adipocytes stimulates glucose uptake and glucose transporter 4 translocation. *J Biol Chem* 271(49): 31372-31378, 1996.

Koivisto VA, Soman VR, Defronzo R and Felig P. Effects of acute exercise and training on insulin binding to monocytes and insulin sensitivity in vivo. *Acta Paediatr Scand Suppl* 283: 70-78, 1980.

Konrad D, Somwar R, Sweeney G, Yaworsky K, Hayashi M, Ramlal T and Klip A. The Antihyperglycemic Drug α-Lipoic Acid Stimulates Glucose Uptake via

Both GLUT4 Translocation and GLUT4 Activation. Potential Role of p38 Mitogen-Activated Protein Kinase in GLUT4 Activation. *Diabetes* 50: 1464-1471, 2001.

Koval JA, Maezono K, Patti ME, Pendergrass M, DeFronzo RA and Mandarino LJ. Effects of exercise and insulin on insulin signaling proteins in human skeletal muscle. *Med Sci Sports Exerc* 31(7): 998-1004, July 1999.

Kudo N, Barr AJ, Barr RL, Desai S and Lopaschuk GD. High rates of fatty acid oxidation during repurfusion of ischemic hearts are associated with a decrease in malonyl CoA levels due to an increase in 5'-AMP-activated protein kinase inhibition of acetyl-CoA carboxylase. *J Biol Chem* 270: 17513-17520, 1995.

Lee J and Pilch PF. The insulin receptor: structure, function, and signaling *Am J Physiol* 266:C319-C334, 1994.

Lefebvre V, Mechin MC, Louckx MP, Rider MH and Hue L. Signaling pathway involved in the activation of heart 6-phosphofructo-2-kinase by insulin. *J Biol Chem* 271(37): 22289-22292, 1996.

Lemieux K, Konrad D, Klip A and Marette A. The AMP-activated protein kinase activator AICAR does not induce GLUT4 translocation to transverse tubules but stimulates glucose uptake and p38 mitogen-activated protein kinases alpha and beta in skeletal muscle. *FASEB J* 17(12): 1658-65, 2003.

Leslie NR, Bennet D, Lindsay YE, Stewart H, Gray A and Downes CP. Redox regulation of PI3-kinase signaling via inactivation of PTEN. *Embo J,* 22(20): 5501-5510, 2003.

Li J, Hu X, Selvakumar P, Russel RR III, Cushman SW, Holman GD and Young LH. Role of the nitric oxide pathway in AMPK-mediated glucose uptake and GLUT4 translocation in heart muscle. *Am J Physiol.* 287: E834-E841, 2004.

Lienhard GE, Slot JW, James DE and Muekler MM. How cells absorb glucose. *Sci Am* 266(1): 86-91, 1992.

Lochhead PA, Salt IP, Walker KS, Hardie DG and Sutherland C. 5-Aminoimidazole-4-carboxamide riboside mimics the effects of insulin on the expression of the 2 key enzymes. *Diabetes* 49(6): 896-903, 2000.

Longnus SL, Wambolt RB, Parsons HL, Brownsey RW and Allard MF. 5-Aminoimidazole-4-carboxamide 1-beta -D-ribofuranoside (AICAR) stimulates myocardial glycogenolysis by allosteric mechanisms. *Am J Physiol Regul Integr Comp Physiol.* 284(4): R936-R944, 2003.

Lopaschuk GD and Stanley WC. Manipulation of energy metabolism in the heart. *Sci & Med*: 42-50, 1997.

Lopez-Ilasaca M, Li WQ, Uren A, Yu JC, Kazlauskas A, Gutkind JS and Heidaran MA. Requirement of phosphatidylinositol-3 kinase for activation of JNK/SAPKs by PDGF. *Biochem Biophys Res Commun* 232: 273-277, 1997.

Lowry OH, Rosenbrough NJ, Farr AL and Randall RJ. Protein measurement with the Folin Phenol Reagent. *J Biol Chem* Nov 193(1): 265-275, 1951.

Luiken JJFP, Dyck DJ, Han XX, Tandon NN, Arumugam Y, Glatz JFC and Bonen A. Insulin induces the translocation of the fatty acid transporter FAT/CD36 to the plasma membrane. *Am J Physiol* 282: E491-E495, 2002.

Luiken JJFP, Coort SLM, Willems J, Coumans WA, Bonen A, van der Vusse GJ and Glatz JFC. Contration induced fatty acid translocase/ CD36 translocation in rat cardiomyocytes is mediated through AMP-activated protein kinase signaling. *Diabetes* 52:1627-1634, 2003.

Marks DB. Biochemistry, Board Review Series. Williams and Wilkins Pgs 125-127, 1990.

Marte BM and Downward J. PKB/Akt: connecting phosphoinositide 3-kinase to cell survival and beyond. *TIBS* 22: 355-358, 1997.

McDaniel HG, Jenkins RL, Digerness SB and Ong RL. Review: Myocardial fuel and energy balance, acute ischemia and diabetes. *Am J Med Sciences* 295(3): 207-211, 1988.

Merrill GF, Kurth EJ, Hardie DG and Winder WW. AICA riboside increases AMP-activated protein kinase, fatty acid oxidation, and glucose uptake in rat muscle. *Am J Physiol* 273(6 Pt 1):E1107-12, Dec 1997.

Meuckler M. Facilitative Glucose Transporters. *Eur J Biochem* 219: 713-725. 1994.

Meyers MG, Sun XJ and White MF. The IRS-1 signaling system. *Trends Biochem Sci* 19: 289-293, 1994.

Mirza AM, Kohn AD, Roth RA and McMahon M. Oncogenic Transportation of cells by a constitutively active form of the protein kinase Akt/PKB. *Cell Growth & Differen* 11: 279-292, 2000.

Mondon CE, Dolkas CB and Reaven GM. Site of enhanced insulin sensitivity in exercise-trained rats at rest. *Am J Physiol* 293(3): E169-177, 1980.

Morgan H, Henderson M, Regen D and Park C. Regulation of glucose uptake in skeletal muscle I. *J Biol Chem* 236: 253-261, 1961.

Moriya S, Kazlauskas A, Akimoto K, Hirai S, Mizuno K, Takenawa T, Fukui Y, Watanabe Y, Ozaki S and Ohno S. Platelet-derived growth factor activates protein kinase C epsilon through redundant and independent signaling pathways involving phospholipase C gamma or phosphatidylinositol 3-kinase. *Proc Natl Acad Sci U.S.A* 93: 151-155, 1996.

Musi N, Fujii N, Hirshman MF, Ekberg I, Froberg S, Ljunqvist O, Thorell A and Goodyear LJ. AMP-activated protein kinase (AMPK) is activated in muscle of subjects with type 2 diabetes during exercise. *Diabetes* 50: 921-927, 2001.

Musi N, Yu H, Goodyear LJ. AMP-activated protein kinase regulation and action in skeletal muscle during exercise. *Biochem Soc Trans.* 31(Pt 1): 191-195, 2003.

Myers MP, Pass I, Batty IH, Van der Kaay J, Stolarov JP, Hemmings BA, Wigler MH, Downes CP and Tonks NK. The lipid phosphatase activity of PTEN is critical for its tumour suppressor function. *Proc Natl Acad Sci U.S.A* 95:13513-13518, 1998.

Ng SS, Tsao MS, Nicklee T and Hedley DW. Wortmannin inhibits PKB/Akt phosphorylation and promotes gemcitabine antitumor activity in orthotopic human pancreatic cancer xenografts in immunodeficient mice. *Clin Cancer Res* 7(10):3269-75, 2001.

Ojuka EO, Nolte LA and Holloszy JO. Increased expression of GLUT4 and Hexokinase in rat epitrochlearis muscles exposed to AICAR in vitro. *J Appl Physiol* 88(3): 1072-1075, 2000.

Olson AL, Knight JB and Pessin JE. Syntaxin4, VAMP2 and/or VAMP3/cellubrevin are functional target membrane and vesicle SNAP receptors for insulin stimulated GLUT4 translocation in adipocytes. *Moll Cell Biol* 17:2425-2435, 1997.

Opie LH. The Heart: Physiology and Metabolism. 2nd Edition. Chapter 10, 208-246. Philadelpia, New York, Raven Press, 1991.

Opie LH. The Heart: Physiology, from Cell to Circuation. 3rd Edition. Chapter 11, Philadelphia, New York, Raven Press, 1998.

Opie LH. The Heart Physiology, form Cell to Circulation. 4th Edition. Pg 325. Philadelphia, New York , Raven Press, 2004.

Patrucco E, Notte A, Barberis L, Selvetella G, Maffei A, Brancaccio M, Marengo S, Russo G, Azzolino O, Rybalkin SD, Silengo L, Altruda F, Wetzker R, Wymann MP, Lembo G, Hirsch E. PI3Kgamma modulates the cardiac response to chronic pressure overload by distinct kinase-dependent and -independent effects. *Cell.* 118(3): 375-87, 2004.

Perrin C, Knauf C and Burcelin R. Intracerebroventricular infusion of glucose, insulin and the AMP-activated kinase activator AICAR controls muscle glycogen synthesis. *Endocrinology 145(9): 4025-4033,* 2004.

Pessin JE and Bell GI. Mammalian fascilitative glucose transporter family; structure and molecular regulation. *Ann Rev Physiol* 54: 911-930, 1992.

Pessin JE, Thurmond DC, Elmendorf JS, Coker KJ and Okada S. Molecular basis of insulin-stimulated GLUT4 vesicle trafficking. Location! Location! Location! *J Biol Chem* 274:2593-2596, 1999.

Philipson DK, Bers DM and Nishimoto AY. The role of phospholipids in the Ca^{2+} binding of isolated cardiac sarcolemma. *J Mol Cell Cardiol* 12:1159-1173, 1980.

Polekhina G, Gupta A, Michell BJ, van Denderen B, Murthy S, Feil SC, Jennings IG, Campbell DJ, Witters LA, Parker MW, Kemp BE and Stapleton D. AMPK β-subunit targets metabolic stress-sensing to glycogen. *Current Biol* 13:867-871, 2003.

Ponticos M, Lu QL, Morgan JE, Hardie GD, Partridge TA and Carling G. Dual regulation of the AMP-activated protein kinase provides a novel mechanism for the control of creatine kinase in skeletal muscle. *EMBO J* 17(6):1688-1699, 1998.

Powis G, Bonjouklian R, Berggren MM, Gallegos A, Abraham R, Ashendel C, Zalkow L, Matter WF, Dodge J, Grindley G and Vlahos CJ. Wortmannin, a potent and selective inhibitor of phosphatidylinisitol 3-kinase. *Cancer Res* 54: 2419-2423, 1994.

Randle PJ and Morgan HE. Regulation of glucose uptake by muscle. *Vitamins Horm* 20:199-249, 1962.

Randle PJ, Garland PB, Hales CN and Newsholme EA. The glucose-fatty acid cycle. Its role in insulin sensitivity and the metabolic disturbances of diabetes mellitus. *Lancet* 1:785-789, 1963.

Rauch B, Bode C, Piper HM, Hutter JF, Zimmermann R, Braunwell E, Hasselbach W and Kubler W. Palmitate uptake in calcium tolerant, adult rat myocardial single cells – evidence for an albumin mediated transport across sarcolemma. *J Mol Cell Cardiol* 19:159–166, 1987.

Rea S and James DE. Moving GLUT4: the biogenesis and trafficking of GLUT4 storage vesicles. *Diabetes* 46:1667-1677, 1997.

Ren J, Sowers JR, Walsh MF and Brown RA. Reduced contractile response to insulin and IGF-1 in ventricular myocytes from genetically obese Zucker rats. *Am J Physiol (Heart Circ. Physiol)* 279:H1708-H1714, 2000.

Richter EA, Derave W and Wojtaszewski JF. Glucose, exercise and insulin: emerging concepts. *J Physiol* 535.2:313-322, 2001.

Ribiere C, Jaubert AM, Sabourault D, Lacasa D and Giudicelli Y. Insulin stimulates nitric oxide production in rat adipocytes *Biochem Biophys Res Commun.* 291(2): 394-9, 2002.

Rogers MA, Yamamoto C, King DS, Hagberg JM, Ehsani AA and Holloszy JO. Improvement in glucose tolerance after 1 week of exercise training in patients with mild NIDDM. *Diabetes Care* 11:613-618, 1988.

Rowell LB. Human Circulation regulation during physical stress. pgs.96-256. Oxford University Press, New York, 1986.

Russel RR III, Bergeron R, Shulman G and Young LH. Translocation of myocardial GLUT4 and increased glucose uptake through activation of AMPK by AICAR. *Am J Physiol.* 277(2 Pt 2): H643-H649, 1999.

Sabina RL, Patterson D and Holmes EW. 5-Amino-4-imidazolecarboxamide riboside (Z-riboside) metabolism in eukaryotic cells. *J Biol Chem.* 260: 6107-6114, 1985.

Sable CL, Filippa N, Hemmings B and Van Obberghen E. cAMP stimulates protein kinase B in a wortmannin insensitive manner. *FEBS Lett* 409: 253-257, 1997.

Saha, Asish K., Alexandria J. Schwarsin, Raphael Roduit, Frederic Masse, Virendar Kaushik, Keith Tornheim, Marc Prentki, and Neil B. Ruderman. Activation of Malonyl-CoA decarboxylase in rat skeletal muscle by contraction and the AMP-activated protein kinase activator 5-aminoimidazole-4-carboxamide-1-β-D-ribofuranoside. *J. Biol. Chem.* 275(32):24279-24283, 2000.

Sakamoto J, Barr RL, Kavanagh KM and Lopaschuk GD. Contribution of malonyl-CoA decarboxylase to the high fatty acid oxidation rates seen in the diabetic heart. *Am J Physiol (Heart and Circ Physiol)* 278, 4: H1196-H1204, 2000.

Salt IP, Johnson G, Ashcroft SJ and Hardie DG. AMP-activated protein kinase is activated by low glucose in cell lines derived from pancreatic β cells, and may regulate insulin release. *Biochem J* 335: 533-539, 1998

Salt IP, Morrow VA, Brandie FM, Connell JM and Petrie JR. High glucose inhibits insulin-stimulated nitric oxide production without reducing endothelial nitric-oxide synthase Ser1177 phosphorylation in human aortic endothelial cells. *J Biol Chem* 278(21): 18791-18797, 2003.

Saltiel AR and Pessin JE. Insulin signaling in microdomains of the plasma membrane. *Traffic* 4:711-716, 2003.

Seals DR, Hagberg JM, Allen WK, Hurley BF, Dalsky GP, Ehsani AA and Holloszy JO. Glucose tolerance in younger and older athletes and sedentary men. *J Appl Physiol* 56:1521-1525, 1984.

Shaul PW and Anderson RGW. Role of plasmalemmal caveolae in signal transduction. *Am J Physiol* 275: L843-L851, 1998.

Shearer J, Fueger PT, Rottman JN, Bracy DP, Martin PH and Wasserman DH. AMPK stimulation inceases LCFA but not glucose clearance in cardiac muscle in vivo. *Am J Physiol.* 287: E871-E877, 2004.

Shepherd PR, Withers DJ and Siddle K. Phosphoinositide 3-kinase: the key switch mechanism in insulin signaling. *Biochem J* 333: 471-490, 1998.

Smart EJ, Graf GA, McNiven MA, Sessa WC, Engelman JA, Scherer PE, Okamoto T and Lisanti MP. Caveolins, liquid-ordered domains, and signal transduction. *Mol Cell Biol.* 19: 7289-7304, 1999.

Soman VR, Koivisto VA, Deibert D, Felig P and DeFronzo RA. Increased insulin sensitivity and insulin binding to monocytes after physical training. *N Engl J Med* 301(22): 1200-1204, 1979.

Somwar R, Kim DY, Sweeney G, Huang C, Niu W, Lador C, Ramlal T and Klip A. GLUT4 translocation precedes the stimulation of glucose uptake by insulin in muscle cells: potential activation of GLUT4 via p38 mitogen-activated protein kinase. *Biochem J* 359: 639-649, 2001.

Somwar R, Koterski S, Sweeney G, Sciotti R, Djuric S, Berg C, Trevillyan J, Scherer PE, Rondinone CM and Klip A. A dominant-negative p38 MAPK mutant and novel selective inhibitors of p38 MAPK reduce insulin-stimulated glucose uptake in 3T3-L1 adipocytes without affecting GLUT4 translocation. *J Biol Chem* 277(52):50386-95, 2002.

Song XM, Fiedler M, Galuska D, Ryder JW, Fernstrom M, Chibalin AV, Wallberg-Henriksson H and Zierath JR. 5-Aminoimidazole-4-carboxamide ribonucleoside treatment improves glucose homeostasis in insulin resistant (ob/ob) mice. *Diabetologia.* 45(1): 56-65, 2002.

Staal SP, Hartley JW and Rowe WP. Isolation of transforming murine viruses from mice with a high incidence of spontaneous lymphoma. *Proc Natl Acad Sci U.S.A.* 74:3065-3067, 1977.

Staal S.P. Molecular cloning and characterisation of the *akt* oncogene and its human homologues AKT1 and AKT2: amplification of AKT1 in primary human gastric adenocarcinomas. *Proc Natl Acad U.S.A.* 84:5034-5037, 1987.

Staal SP, and Hartley JW. Thymic lymphoma induction by the AKT8 murine retrovirus. *J Exp Med* 167:1259-1264, 1988.

Stanley WC, Lopaschuk GD and McCormack JG. Regulation of energy substrate metabolism in the diabetic heart. *Cardiovasc Res* 34:25-33, 1997.

Stapleton D, Mitchelhill KI, Gao G, Widmer J, Michell BJ, Teh T, House CM, Fernandez CS, Cox T, Witters LA and Kemp BE. Mammalian AMP-activated protein kinase subfamily. *J Biol Chem* 271:611-614, 1996.

Stein SC, Woods A, Jones NA, Davidson MD and Carling D. The regulation of AMP-activated protein kinase by phosphorylation. *Biochem J* 345: 437-443, 2000.

Stephens LR, Eguinoa A, Erdjument-Bromage H, Lui M, Cooke F, Coadwell J, Smrcka AS, Thelen M, Cadwallader K, Tempst P and Hawkins PT. The G beta gamma sensitivity of a PI3K is dependent upon a tightly associated adaptor, p101. *Cell* 89(1): 105-114, 1997.

Stephens TJ, Chen ZP, Canny BJ, Michell BJ, Kemp BE and McConell GK. Progressive increase in human skeletal muscle AMPKα2 activity and ACC

phosphorylation during exercise. *Am. J. Physiol. Endocrinol Metab* 282(3): E688-E694, 2002.

Stoyanova S, Bulgarelli-Leva G, Kirsch C, Hanck T, Klinger R, Wetzker R and Wymann MP. Lipid kinase and protein kinase activities of G-protein-coupled phosphoinositide 3-kinase gamma: structure-activity analysis and interactions with wortmannin. *Biochem J* 324:489-495, 1997.

Stremmel W, Pohl L, Ring A, Herrmann T. A new concept of cellular uptake and intracellular trafficking of long-chain fatty acids. Lipids.36(9): 981-989, 2001.

Sullivan JE, Carey F, Carling D and Beri RK. Characterisation of 5'-AMP-activated protein kinase in human liver using specific peptide substrates and the effects of 5'-AMP analogues on enzyme activity. *Biochem Biophys Res Commun* 200:1551-1556, 1994.

Sweeney G, Garg RR, Ceddia RB, Li D, Ishiki M, Somwar R, Foster LJ, Neilsen PO, Prestwich GD, Rudich A and Klip A. Intracellular delivery of phosphatidylinositol (3,4,5)-trisphosphate causes incorporation of glucose transporter 4 into the plasma membrane of muscle and fat cells without increasing glucose uptake. *J Biol Chem* 279(31): 32233-32242, 2004.

Takeuchi K, McGowan FX Jr, Glynn P, Moran AM, Rader CM, Cao-Danh H and del Nido PJ. Glucose transporter upregulation improves ischemic tolerance in hypertrophied failing heart. *Am Heart Ass, Inc* II-234 – II-239, 1998.

Tanti J-F, Grillo S, Grimeaux T, Coffer PJ, Van Obberghen E and Le Merchand-Brustel Y. Potential role of protein kinase B in glucose transporter 4 translocation in adipocytes. *Endocrinology* 138(5): 2005-2010, 1997.

Till M, Kolter T and Eckel J. Molecular mechanisms of contraction-induced translocation of GLUT4 in isolated cardiomyocytes. *Am J Cardiol* 80(3A):85A-89A, 1997.

Tilton B, Andjelkovic M, Didichenko AS, Hemmings BA and Thelen M. G-Protein coupled receptors and Fcγ-receptors mediate activation of Akt/ Protein kinase B in human phagocytes. *J Biol Chem* 272: 28096-28101, 1997.

Trovati M, Massucco P, Mattiello L, Costamagna C, Aldieri E, Cavalot F, Anfossi G, Bosia A and Ghigo D. Human vascular smooth muscle cells express a constitutive nitric oxide synthase that insulin rapidly activates, thus increasing guanosine 3':5'-cyclic monophosphate and adenosine 3':5'-cyclic monophosphate concentrations. *Diabetologia.* 42(7): 831-9, 1999.

Ueki K, Yamamoto-Honda R, Kaburagi Y, Yamauchi T, Tobe K, Burgering BM, Coffer PJ, Komuro I, Akanuma Y, Yazaki Y and Kadowaki T. Potential role of protein kinase B in insulin-induced glucose transport, glycogen synthesis, and protein synthesis. *J Biol Chem.* 273(9): 5315-5322, 1998.

Ui M, Okada T, Hazeki K and Hazeki O. Wortmannin as a unique probe for an intracellular signaling protein, phosphoinositide 3-kinase. *Trends Biol Sci* 20:303-307, 1995.

Vavvas D, Apazidis A, Saha AK, Gamble J, Patel A, Kemp BE, Witters LA and Ruderman NB. Contraction-induced changes in acetyl-CoA carboxylase and 5'-AMP-activated kinase in skeletal muscle. *J Biol Chem.* 272(20):13255-61, 1997.

Volchuk A, Wang Q, Ewart HS, Liu Z, He L, Bennett MK and Klip A. Syntaxin 4 in 3T3-L1 adipocytes. Regulation by insulin and participation in insulin-dependant glucose transport. *Mol Cell Biol* 7: 1075-1082, 1996.

Volinia S, Dhand R, Vanhaesebroeck B, MacDougall LK, Stein R, Zvelebil M, Domin J, Panareto C and Waterfield MD. A human phosphatidylinositol 3-kinase complex related to the yeast Vps34p-Vps15p protein sorting system. *EMBO J* 14(14):3339-3348, 1995.

Vona M, Rossi A, Capodaglio P, Rizzo S, Servi P, De Marchi M and Cobelli F. Impact of physical training and detraining on endothelium-dependent vasodilation in patients with recent acute myocardial infarction *Am Heart J.* 147(6):1039-46, 2004

Wahren J, Felig P, Ahlborg G and Jordfeldt L. Glucose metabolism during leg exercise in man. *J. Clin. Invest.* 50:2715-27725, 1971.

Walliman, T. Dissecting the role of creatine kinase. *Curr. Biol.* 4: 42-46, 1994.

Wang PH, Almahfouz A, Giorgino F, McCowen KC and Smith RJ. In Vivo insulin signaling in the myocardium of streptozotocin-diabetic rats: opposite effects of diabetes on insulin stimulation of glycogen synthase and c-Fos. *Endocrinology* 140(3): 1141-1150, 1999.

Wang Q, Somwar R, Bilan PJ, Liu Z, Jin J, Woodgett JR and Klip A. Protein kinase B participates in GLUT4 translocation by insulin in L6 myoblasts. *Mol Cell Biol* 19 (6): 4008-4018, 1999b.

Weber TM, Joost H-G, Simpson IA and Cushman SW. Methods for assessment of glucose transport activity and the number of glucose transporters in isolated rat adipose cells and membrane fractions. *Insulin Receptors, Part B: Clinical Assessment, Biological Responses, and Comparison to the IGF-I Receptor.* Liss, A.L., Inc., New York, 171-187, 1988.

Weekes J, Hawley SA, Corton J, Shugar D and Hardie DG. Activation of rat liver AMP-activated protein kinase by kinase kinase in a purified, reconstituted system. Effects of AMP and AMP analogues. *Eur J Biochem* 219:751-757, 1994.

White MF and Kahn CR. The insulin signaling system. *J Biol Chem* 269(1): 1-4, 1994.

Winder WW. AMP-activated protein kinase: possible target for treatment of type 2 diabetes. *Diabetes Technol Ther* 2(3):441-448, 2000.

Winder WW and Hardie DG. Inactivation of acetyl CoA carboxylase and activation of AMP-activated protein kinase in muscle during exercise. *Am J Physiol* 270: E299-E304, 1996.

Xi X, Han J and Zhang JZ. Stimulation of glucose transport by AMP-activated protein kinase via activation of p38 mitogen-activated protein kinase. *J Biol Chem* 276(44):41029-34, Nov 2, 2001.

Yano S, Tokumitsu H and Soderling TR. Calcium promotes cell survival through CaM-K kinase activation of the protein kinase B pathway. *Nature* 396:584-587, 1998.

Yatomi Y, Hazeki O, Kume S and Ui M. Suppression by wortmannin of platelet responses to stimuli due to inhibition of pleckstrin phosphorylation. *Biochem J* 285:745-751, 1992.

Zheng D, MacLean PS, Pohnert SC, Knight JB, Olson AL, Winder WW and Dohm GL. Regulation of muscle GLUT-4 transcription by AMP-activated protein kinase. *J Appl Physiol* 91(3): 1073-83, 2001.

Zierler K. Whole body glucose metabolism. *Am J Physiol Endocrinol Metab* 276(39*)*: E409-E426, 1999.

Zinda MJ, Johnson MA, Paul JD, Horn C, Konicek BW, Lu ZH, Sandusky G, Thomas JE, Neubauer BL, Lai MT and Graff JR. AKT-1, -2, and -3 are expressed in both normal and tumor tissues of the lung, breast, prostate, and colon. *Clin Cancer Res*. 7(8); 2475-2479, 2001.